Available online at www.sciencedirect.com
SCIENCE DIRECT®
Journal of African Earth Sciences 45 (2006) 279–317
Journal of African Earth Sciences
www.elsevier.com/locate/jafrearsci

Further Paleogene and Cretaceous sediment cores from the Kilwa area of coastal Tanzania: Tanzania Drilling Project Sites 6–10

Paul N. Pearson [a,*], Christopher J. Nicholas [b], Joyce M. Singano [c], Paul R. Bown [d], Helen K. Coxall [e], Bart E. van Dongen [f], Brian T. Huber [g], Amina Karega [c], Jackie A. Lees [d], Kenneth MacLeod [h], Ian K. McMillan [a], Richard D. Pancost [f], Marion Pearson [b], Emma Msaky [c]

[a] School of Earth, Ocean and Planetary Sciences, Cardiff University, Main Building, Park Place, Cardiff CF10 3YE, United Kingdom
[b] Department of Geology, Trinity College, Dublin 2, Ireland
[c] Tanzania Petroleum Development Corporation, P.O. Box 2774, Dar-es-Salaam, Tanzania
[d] Department of Earth Sciences, University College London, Gower Street, London WC1E 6BT, United Kingdom
[e] Graduate School of Oceanography, University of Rhode Island, Bay Campus, South Ferry Road, Narragansett, Rhode Island 02882, USA
[f] Organic Geochemistry Unit, Biogeochemistry Research Centre, School of Chemistry, Cantock's Close, Bristol University, Bristol BS8 1TS, United Kingdom
[g] Department of Paleobiology, MRC NHB-121, P.O. Box 37012, Smithsonian National Museum of Natural History, 10th and Constitution Avenue, Washington, DC 20012-7012, USA
[h] Department of Geology, University of Missouri-Columbia, Columbia, MO 65211, USA

Received 13 September 2005; received in revised form 16 December 2005; accepted 1 February 2006
Available online 15 May 2006

Abstract

Initial results from scientific drilling in southern coastal Tanzania are described. In a field season in 2003, a total of five sites was drilled (mostly using continuous coring) by the Tanzania Drilling Project for paleoclimate studies. The sediments are predominantly marine clays and claystones deposited in an outer shelf or slope environment and often contain excellently preserved microfossils suitable for geochemical analysis. The studies reported here include summaries of the lithostratigraphy, biostratigraphy (planktonic foraminifers, calcareous nannofossils, benthic foraminifers, and palynology) and organic geochemistry.

TDP Site 6 was drilled near Kilwa Masoko (UTM 37L 555752, 9014922), 350 m to the south-east of a previous site, TDP Site 1. The top 59.58 m, which was mostly drilled without coring, consists of an Oligocene clay formation belonging to nannofossil Zone NP23. The rest of the hole, to a total depth of 61.25 m, consists of a fault zone in which the Oligocene sediments are intermixed with middle Eocene clays of planktonic foraminifer Zone E9 and nannofossil Subzone NP15b.

TDP Site 7 consists of two holes (Hole TDP7A: UTM 37L 547126, 9030142; Hole TDP7B: UTM 37L 0547130, 9030140) drilled just 5 m apart at Kwamatola, a creek to the south of Kilwa Kivinje. Underneath approximately 20 m of unconsolidated sands and gravels, claystones and siltstones were recovered to a total depth of 128.00 m. The site spans lower Eocene planktonic foraminifer Zones E1, E2 and E3 and nannofossil Subzones NP 9b and NP10. The bottom of Hole TDP7B approaches the Paleocene–Eocene boundary but no unambiguously Paleocene sediments were recovered.

TDP Site 8 was drilled to the south-east of Singino Hill (UTM 37L 548033, 9025811). Below a covering of surface gravels, it yielded predominantly dark greenish-grey claystones to a total depth of 22.95 m. The sediments are from the lower Eocene and span the boundary between planktonic foraminifer Zones E3 and E4 and fall within nannofossil Zone NP10.

TDP Site 9 was drilled near Nangurukuru junction (UTM 37L 538987, 9027049). It yielded predominantly dark greenish-grey siltstones to a total depth of 88.80 m. Thin siliciclastic beds with trace fossils of the *Nereites* ichnofacies are common in the lower third of the site. These sediments span the Campanian–Maastrichtian stage boundary and are assigned to the *Globotruncanella havanensis* to *Gansserina gansseri* planktonic foraminifer zones and nannofossil Subzones UC15e^{TP} to UC17.

* Corresponding author.
E-mail address: PearsonP@cardiff.ac.uk (P.N. Pearson).

doi:10.1016/j.jafrearsci.2006.02.005

TDP Site 10 was drilled to the west of Singino Hill, adjacent to the main Kilwa road (UTM 37L 0541243, 9028791). Below a superficial covering of gravel, it yielded predominantly dark greenish-grey silty claystones to a total depth of 100.80 m. These sediments are assigned to Paleocene planktonic foraminifer Zone P4c–P5 and nannofossil Subzone NP9b.

Organic geochemical analyses from all the sites revealed biomarkers of predominantly terrestrial origin and collectively indicate an unusually low degree of thermal maturity for the area, suggesting shallow maximum burial depths. Traces of migrated hydrocarbons were found in TDP Sites 7 and 10.

Keywords: Cretaceous; Eocene; Oligocene; Foraminifers; Nannofossils; Geochemistry; Palynology

1. Introduction

The work presented here comprises initial results from geochemical, lithologic and biostratigraphic studies of sediment cores drilled in the Kilwa area of southern coastal Tanzania by the Tanzania Drilling Project (TDP). The TDP is an international partnership of investigators who are interested in using the thermally immature Tanzanian marine sediments of Cretaceous and Paleogene age for paleoclimate research. The area is well known for its excellently preserved microfossils (see Plate 1). Initial results from outcrop sampling were presented by Pearson et al. (2001) and Stewart et al. (2004) and results from the first season of drilling (2002; TDP Sites 1–5) were published by Pearson et al. (2004). The present contribution is a continuation of that work, dealing with TDP Sites 6–10 that were drilled in 2003. The purpose of this paper is to summarize the stratigraphy, biostratigraphy, geochemistry and environmental interpretation of the sites in question, which will be subject to more detailed specialist studies elsewhere. A location map of the drill sites in relation to TDP Sites 1–3, which were also drilled in the Kilwa area, is given in Fig. 1. See Pearson et al. (2004) for a summary of previous geological work in the area and description of the tectonic setting.

2. Methods

In this section we present a short summary of the methods used in the recovery, sampling and analysis of samples by the TDP. A more detailed description can be found in Pearson et al. (2004).

Sites were drilled using small rigs capable of wireline coring to about 150 m. Most of the sites were cored continuously, although some intervals were drilled without recovering cores. Core barrels of either 3 m or 1.6 m were used, with core diameters of 2 in. (~5 cm). A scientific team was on site at all times to photograph and describe the cores while they were fresh, and take samples for laboratory study. Cores are stored in the air-conditioned core repository at the Tanzania Petroleum Development Corporation (TPDC), Dar-es-Salaam. Requests for photographs, Visual Core Description (VCD) sheets and samples should be addressed to the corresponding author.

Sample identification numbers are modelled on the procedure used by the Integrated Ocean Drilling Program (IODP). Tables showing the depth of each core obtained are given in the relevant sections below. A typical sample identifier refers to the Site, Core number, Section number, and depth in cm from the top of that section. For example, Sample TDP6/7-2, 5–10 cm was taken from Tanzania Drilling Project Site 6, Core 7, Section 2, between 5 and 10 cm from the top of that 1 m section. The depth of the top of this sample can be calculated by adding 1 m for Section 1, plus 5 cm to the depth from the top of the core (58.28 m + 1.05 m = 59.33 m). The following code refers to the purpose of the samples; B = benthic (larger) foraminifers, L = lithostatigraphy, F = foraminifers, M = paleomagnetic analysis, N = nannoplankton, O = organic chemistry, T = TPDC (which were studied for palynology and smaller benthic foraminifers).

Procedures for lithologic description and drilling disturbance were based on IODP practise. Color variation was described using the Geological Society of America rock color chart (based on Munsell Soil colors). Lithologies were described in the field by Nicholas, M. Pearson, Huber and MacLeod. Microfossil assemblages were studied according to the procedures described in Pearson et al. (2004). Planktonic foraminifers were studied by P.N. Pearson and Coxall (Paleogene) and Huber (Cretaceous); nannofossils were studied by Bown (Paleogene) and Lees (Cretaceous); benthic foraminifers were studied by Karega, Singano and McMillan; palynomorphs were studied by Msaky.

The Cretaceous planktonic foraminifer biozonation used in this study combines zonal concepts used by Nederbragt (1991) for heterohelicids and Robaszynski and Caron (1995) for globotruncanids. Definitions of the middle Campanian through late Maastrichtian zones are as follows (from young to old):

Abathomphalus mayaroensis Partial Range Zone
Top: LO (last occurrence) of most late Cretaceous taxa.
Base: FO (first occurrence) of the nominate species, which has been correlated with the base of Chron C31n (Premoli Silva and Sliter, 1994).

Racemiguembelina fructicosa Interval Zone
Top: FO of *A. mayaroensis.*
Base: FO of *R. fructicosa.*

Gansserina gansseri Interval Zone
Top: FO of *R. fructicosa.*

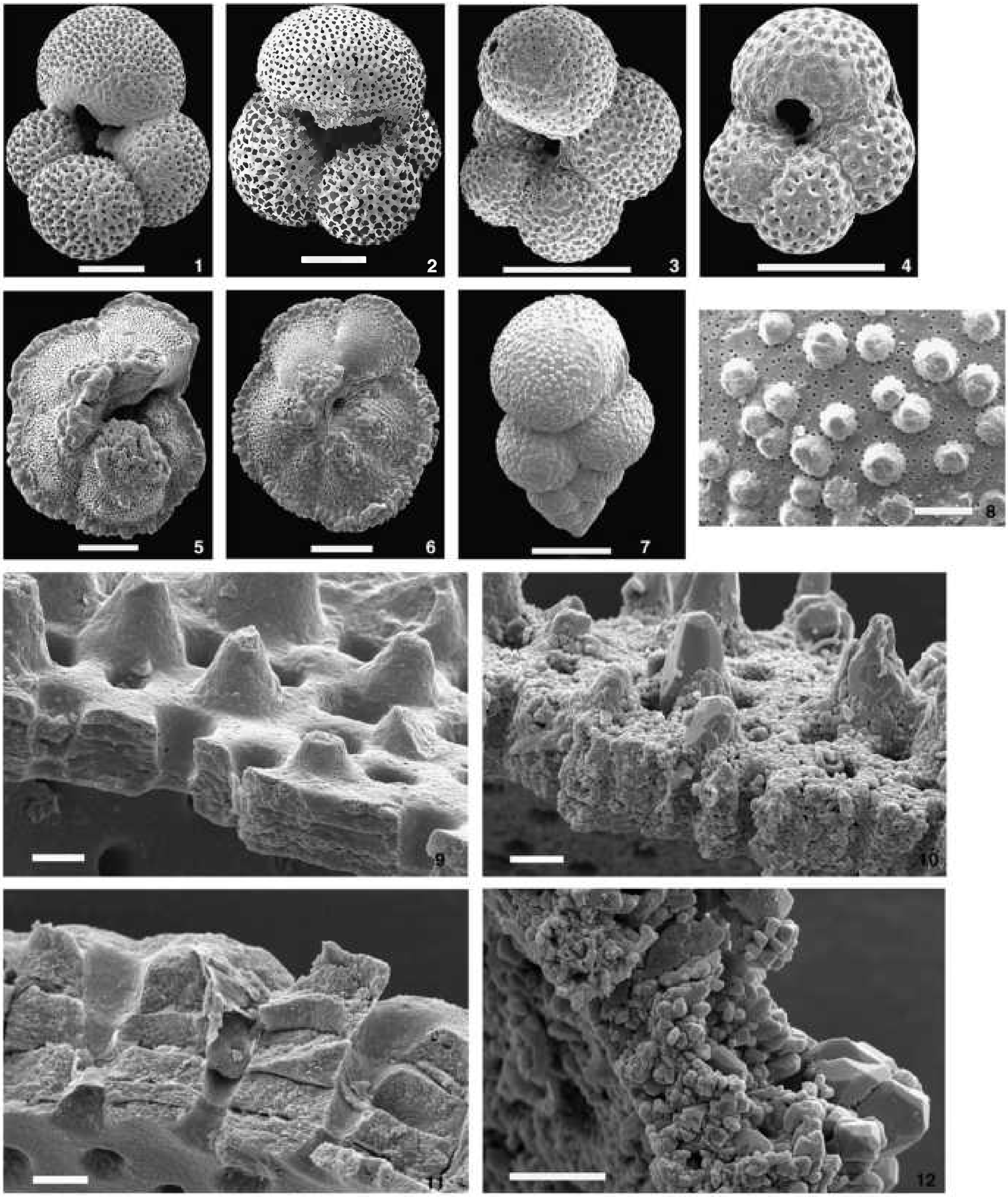

Plate 1. Selected planktonic foraminifers from TDP Sites 6 and 7 and comparison of ultrastructural preservation with ODP Site 865. (1) *Dentoglobigerina globularis*, Sample TDP6/5-1, 158–166 cm; (2) *Dentoglobigerina galavisi*, Sample TDP6/5-1, 158–166 cm; (3) *Globigerina* cf. *ciperoensis*, Sample TDP6/5-1, 158–166 cm; (4) *Globoturborotalita* sp., Sample TDP6/5-1, 158–166 cm; (5) *Morozovella velascoensis*, Sample TDP7B/50/1, 50–55 cm; (6) *Morozovella occlusa*, Sample TDP7B/50/1, 50–55 cm; (7) *Chiloguembelina crinita*, Sample TDP7A/65/2, 71–86 cm including (8) detail of wall texture; (9) detail of deliberately broken wall of *Morozovella subbotinae*, Sample TDP7A/64/1, 50–65 cm. Note micrograular texture and smooth wall surface; (10) detail of deliberately broken wall of *Morozovella subbotinae*, Sample ODP865C/12 H/5, 100–113 cm. Note micron scale diagenetic crystals throughout wall and almost complete replacement of muricae by large single crystals; (11) detail of delibrately broken wall of *Subbotina velascoensis*, Sample TDP7A/64/1, 50–65 cm. Note well-preserved layered wall and remains of organic pore linings; (12) detail of delibrately broken wall of *Subbotina velascoensis*, Sample ODP865C/12 H/5, 100–113 cm. Note pervasive recrystallization and partial overgrowth.

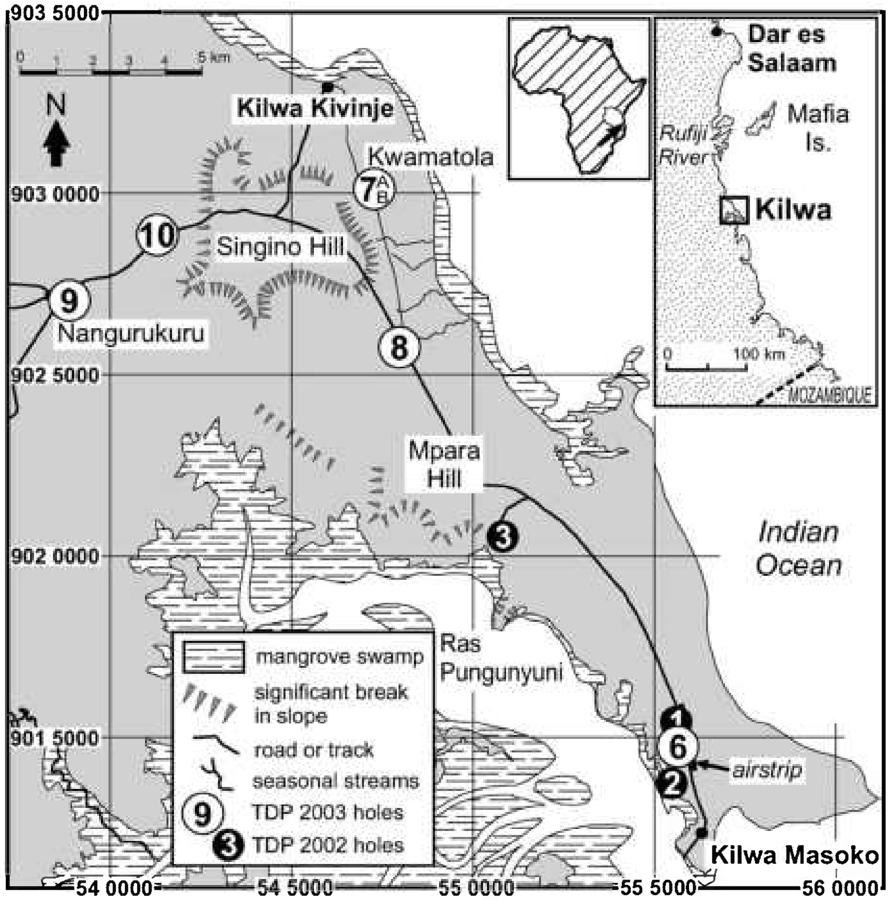

Fig. 1. Map of the Kilwa study area on the southern Tanzanian coast, showing the drill sites discussed in this paper (white numbered circles) in relation to earlier TDP drill sites discussed in Pearson et al. (2004) (black numbered circles). The map is overlain by a 5 km UTM grid.

Base: FO of nominate species, which has been correlated with upper Chron 32n2n (Premoli Silva and Sliter, 1994).

Globotruncana aegyptiaca Interval Zone
Top: FO of *G. gansseri*.
Base: FO of the nominate species, which has been correlated with the first quarter of Chron C32r 2r (Premoli Silva and Sliter, 1994).

Globotruncanella havanensis Partial Range Zone
Top: FO of *G. aegyptiaca*.
Base: LO of *R. calcarata*.

Radotruncana calcarata Total Range Zone
Top: LO of the nominate species.
Base: FO of the nominate species.

For Paleogene planktonic foraminifer biostratigraphy we have used the recently published (sub)tropical zonation of Berggren and Pearson (2005, 'P', 'E', and 'O' zones) but also provide translation to the previous standard zonation of Berggren et al. (1995, 'P' zones) to facilitate comparison with our previously published data. We apply the taxonomy of the recently published *Atlas of Eocene Planktonic Foraminifera* (Pearson et al., in press). Note that some specimens from the cores described here have been illustrated in that work. Similarly, detailed taxonomic studies of the Paleogene nannofossils from these and other TDP sites have already been published by Bown (2005), including the description of many new species, as referred to in the appropriate sections below.

Nannofossil smear slides were prepared following the technique described in Bown and Young (1998). The nannofossil biozonations applied are those of Burnett (1998, UC zones of the Upper Cretaceous) and Martini (1971, NP zones of the Paleogene). The UC biozonation replaces the cosmopolitan CC zones of Sissingh (1977) as modified by Perch-Nielsen (1985).

For organic geochemistry, sediments from selected depths at each of the sites were freeze-dried and crushed. Nine sediments were chosen for biomarker analyses according to the scheme depicted in Fig. 2. The Soxhlet extraction, removal of elemental sulfur, addition of standards, separation, derivatization, gas chromatography (GC) and gas chromatography/mass spectrometry (GC/MS) were performed as described previously (Pearson et al., 2004.). The analyses were conducted in the Organic Geochemistry Unit at the Bristol University by van Dongen and Pancost. Table 1 summarizes the relative abundance of biomarker classes

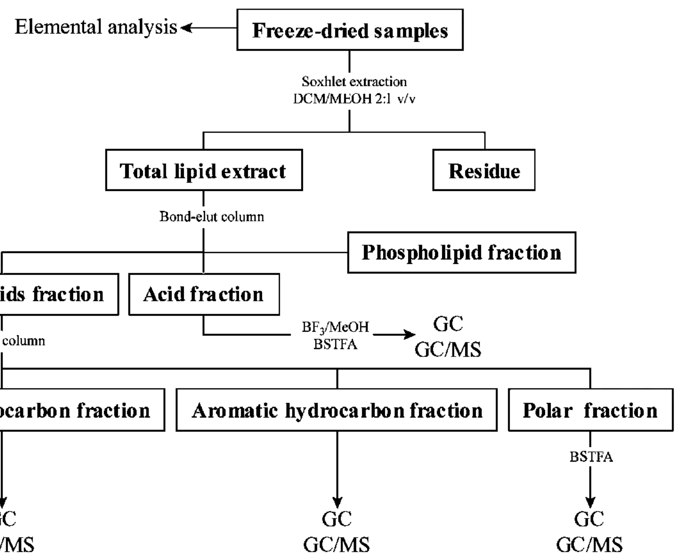

Fig. 2. Extraction and isolation scheme for organic geochemistry.

Table 1
Relative abundance of biomarker classes found in the analysed sediments (++ = Abundant, + = present, +/− = trace and − = absent)

Compound classes	Sample from Section TDP/								
	6/4-1	7A/46-1	7A/54-1	7A/64-1	7B/50-1	8/11-1	9/28-3	10/13-2	10/26-1/2
n-Alkanes	++	++	++	++	++	++	++	++	++
n-Alkanoic acids	++	++	++	++	++	++	++	++	++
n-Alkanols	++	+	+	++	+	+/−	++	+	+
Aromatic des-*A*-triterpenes	++	+/−	+/−	+/−	−	+/−	+/−	+/−	+/−
Aromatic pentacyclic triterpenoids	+	+/−	−	−	−	−	−	−	+/−
Archaeol	+	−	−	−	−	−	−	−	−
Des-*A*-triterpenes	+	+/−	−	−	−	+/−	−	+/−	+/−
Des-*E*-hopenes	+	+/−	−	−	−	+/−	−	+/−	+/−
C_{15}/C_{15} diether	+	−	−	−	−	−	−	−	−
ω-Hydroxy alkanoic acids	+	++	+	+	+	+	+	+	+
Hopanes	+	+	+	+	+	+	+	+	+
Hopanoic acids	+	+	+	+	+	++	++	++	+
Hopanoids	+/−	++	++	++	+	+	+	+	+
Hopenes	++	+	+	+	+	+	+/−	+	+
Midchain ketones	−	−	+/−	+/−	+/−	+/−	+/−	−	−
Steranes	+	+/−	+/−	+/−	+/−	+	+/−	+/−	+/−
Steroids	+/−	+/−	+/−	+/−	+/−	+/−	+/−	+/−	+/−
Triterpenoids	++	+	++	+	++	+	+/−	++	++
Triterpenoic acids	++	+/−	+	+/−	+/−	+	+/−	+	+/−

found in the analysed sediments. Structures of the most important biomarkers are given in Fig. 3 and the results of a typical analysis are given in Fig. 4.

3. TDP Site 6: Kilwa Masoko

3.1. Site selection

TDP Site 6 was drilled in a field adjacent to the main Kilwa Masoko approach road, about 3 km north of the town center on the opposite side of the road from the air-strip (UTM 37L 555752, 9014922). It was located 350 m to the south-east of TDP Site 1 (see Pearson et al., 2004). The objective of the drilling was to find the base of the Oligocene clay formation that had unexpectedly been discovered at TDP Site 1, hence the first 50 m was mostly drilled without coring, except for occasional spot cores. Continuous coring began at 54.89 m. Coring was terminated when it became apparent that the hole had penetrated a fault zone with middle Eocene clays below.

An integrated summary of the litho- and biostratigraphy of this site, in relation to TDP Site 1, is given in Fig. 5. A list of the cores and their depths is given in Table 2.

3.2. Lithostratigraphy

TDP Site 6 was spudded-in on unconsolidated sands and non-core drilling was continued for the first 26 m. A thin, benthic foraminiferal limestone was encountered close to the bottom of this drilled interval, as inferred from a

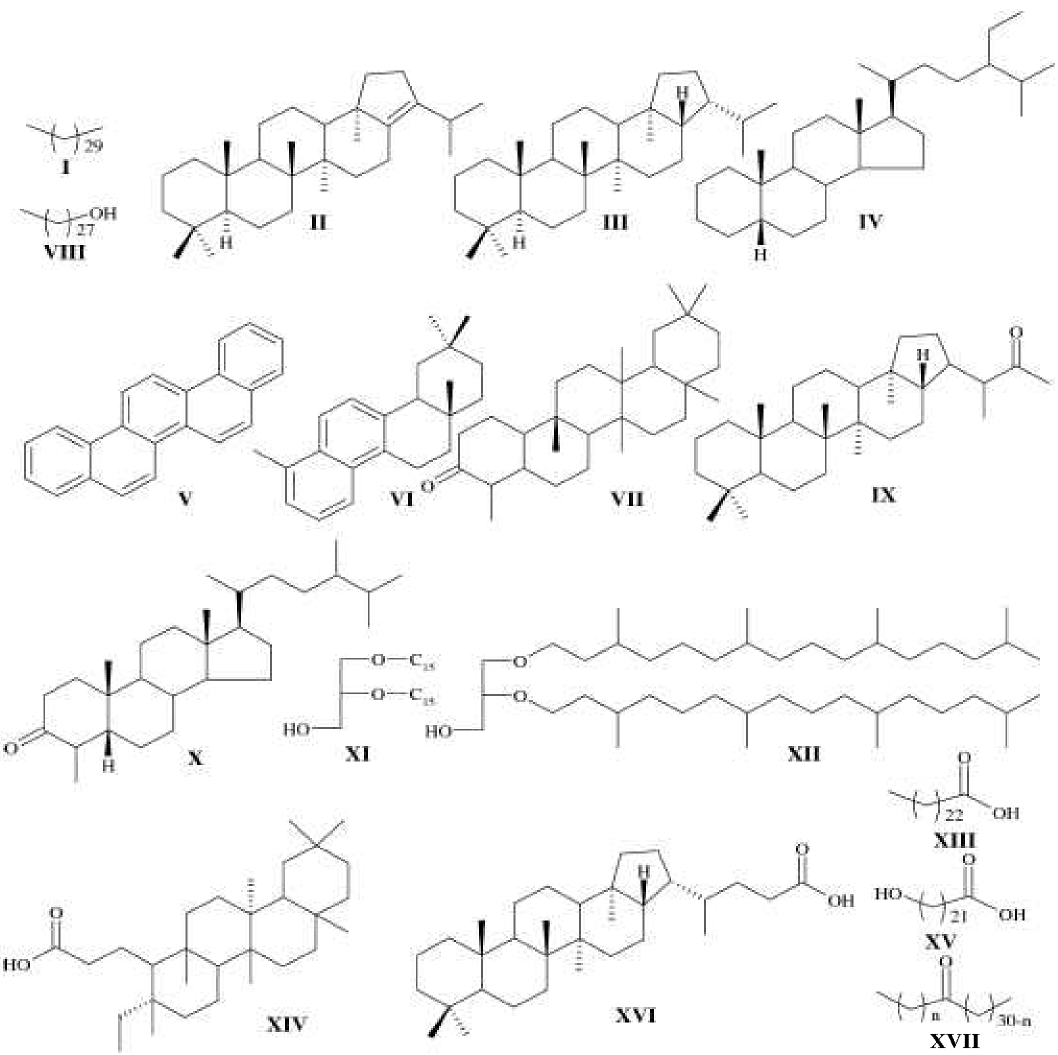

Fig. 3. Structures of the principal biomarkers recorded in this study: (I) C_{31} *n*-alkane, (II) C_{30} hop-17(21)-ene, (III) 17β(H),21β hopane, (IV) ethylcholestane, (V) picene, (VI) des-*A*-26,27 dinorlupa-5,7,9,11,13-pantaene, (VII) friedelan-3-one, (VIII) C_{28} *n*-alkanol, (IX) homohopane-29-one, (X) 4,24-dimethylcholestan-3-one, (XI) glycerol dipentadecyl diether, (XII) archaeol, (XIII) C_{24} *n*-alkanoic acid, (XIV) 3,4-seco-friedelan-3-oic acid, (XV) C_{22} ω-hydroxy alkanoic acid, (XVI) 17β (H), 21β (H)-bishomohopanoic acid and (XVII) C_{33} midchain ketone.

change in formation hardness and the presence of limestone chippings in the drilling slurry. This limestone has its basal bedding surface at about 24.4 m. It probably correlates with the first limestone encountered down-hole in TDP Site 1 at 29 m, suggesting a very gentle dip to the west or north-west in the beds (Fig. 5).

At 26 m, it was decided to take a test core to confirm the physical properties of the clays that were showing in the cuttings slurry. Core TDP6/1 consists of dark greenish-grey to greenish-black clays (5G 4/1 to 5G 2/1), with a slightly muddy content. Within these clays, occasional thin sandy partings that consist of fine, angular quartz grains are present. Disseminated carbonate cement grains are developed within these partings, giving them a characteristic 'sugary' texture. Traces of thin laminations are visible within the clays and rare burrows were also observed. Based on the depth to the first limestone horizon, the slightly muddy nature of the clays and the sugary texture in the sandy partings, it is most likely that this core correlates with the base of Core TDP1/9 or the top of Core TDP1/10. The transition to more muddy clays, similar to those observed in Core TDP6/1 occurred at ~33.4 m in TDP Site 1, and this again suggests that there is a gentle westerly or north-westerly dip in the beds between these two sites.

Drilling recommenced at 27.05 m and continued until the top of a second limestone horizon was encountered at 36.25 m. About 12 cm of this limestone was drilled before it was decided to use a short core barrel to retrieve the limestone. The limestone in Core TDP6/2 has a matrix of subangular, fine carbonate sand mixed with rounded quartz grains. These quartz grains increase in abundance towards the base of the bed and give an overall impression of crude normal grading. Clay is also present in the matrix, and the mixture of this with the more dominant carbonate and quartz grains gives the bed an olive grey coloration (5Y 5/2). Set within this matrix, relatively large blocks, up to 10 cm in size, of yellowish-grey micritic limestone are present between 36.55 and 36.71 m. These contain bored coral

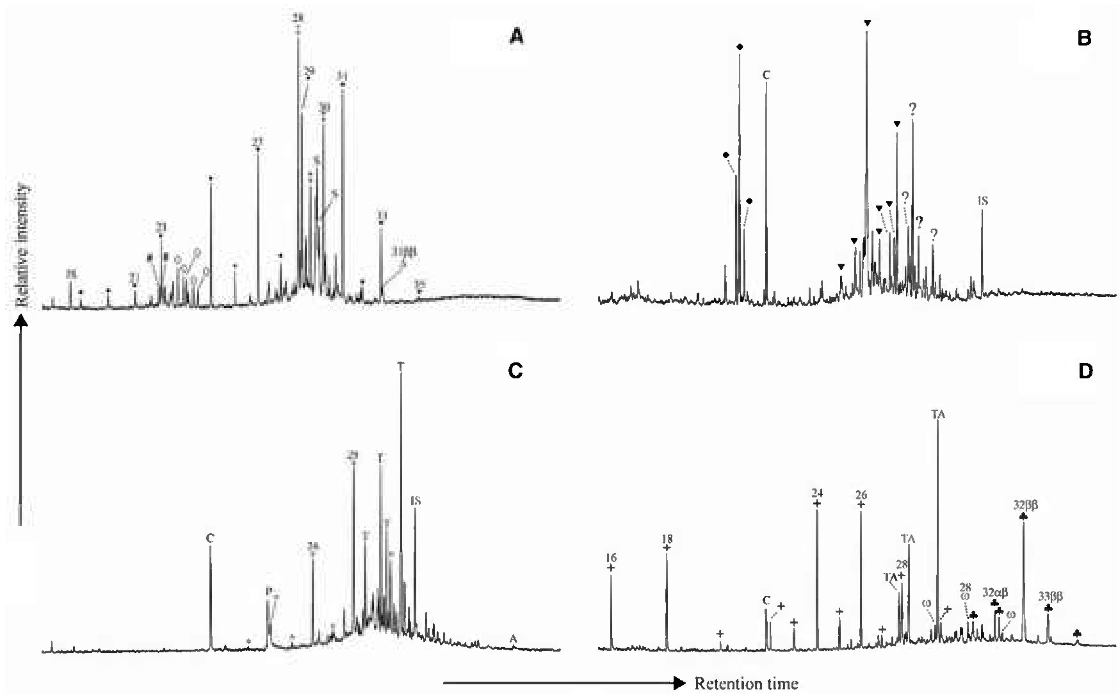

Fig. 4. Total ion currents of (A) the saturated hydrocarbon fraction, (B) the aromatic hydrocarbon fraction, (C) the polar fraction and (D) the acid fraction of Sample TDP6/4-1, 50–60 cm. (●) *n*-alkanes, (#) des-*E*-hopenes, (◇) des-*A*-triterpenes, (‡) hopenes, (△) hopanes, (S) steranes, (◆) aromatic des-*A*-triterpenes, (▼) aromatic pentacyclic triterpenoids, (?) unknown, (*) *n*-alkanols, (P) polycyclic aromatic hydrocarbons (PAH), (T) triterpenoids, (A) archaeol, (+) *n*-alkanoic acids, (ω) ω-hydroxy alkanoic acids, (♣) hopanoic acids, (TA) triterpenoic acids, (IS) internal standard and (C) contaminant. Numbers indicate carbon chain length and αβ or ββ indicates stereochemistry.

and sponge fragments. Below these blocks, numerous bivalve and small coral fragments and large benthic foraminifers are mixed with rip-up clasts of greenish-grey clay. The bivalves and rip-up clasts are generally at high-angle orientations and many of the shelly fragments show borings. Cross-laminations are developed at the top of the limestone unit. The size of the micritic blocks within this bed suggests that the central portion at least was essentially a laminar debris flow, but the normal grading below, and the cross-bedding on top, indicate that the finer sediment was transported and deposited from turbulent flow currents. This bed suggests destabilization of unlithified or partly lithified sediment on the shelf and may be due to storm activity or fault movement. It is likely that this limestone correlates with a similar unit encountered in Core TDP1/16 at a depth of 53.1 m.

Non-core drilling re-commenced at 36.94 m, until continuous coring began at 53.58 m. From the top of Core TDP6/3 (at 53.58 m), the dominant lithology is a greenish-black to dark greenish-grey, slightly muddy clay (5G 2/1 to 5G 4/1). Pervasive throughout this clay are thin, fine angular quartz sand partings with disseminated carbonate cement grains. Burrows are rare to uncommon. Laminations are occasionally preserved undisturbed by coring and these consistently showed a gentle dip from ~14° to 20° down to about 56 m, but gradually increased in angle down-hole, reaching 39° at 59.58 m.

A lithologically complex interval, which is interpreted as a fault zone, was cored in Cores TDP6/8 and TDP6/9 between 59.58 m and 61.25 m. The steepening of dip in the overlying beds down-hole towards this zone suggests a drag fold on the hanging wall of the fault. The supposed fault zone interval consists of angular clasts of greenish-black clay floating in a matrix of pale olive clays with streaks of dusky yellow clay. The lighter, mottled color of the clays in this interval indicates oxidation by groundwaters moving along the fault. From 60.85 m to 60.92 m, a sliver of greenish-black to dark greenish-grey clay is present. Below this, these darker clays are intimately mixed and inter-fingered with dark greenish-grey clays, with some partly cemented horizons containing abundant large benthic foraminifers. The slightly lighter-colored clays were found to contain middle Eocene microfossils (see below). The disparity in age between the clays separated by the oxidized interval is further evidence of a faulted contact between the middle Eocene and overlying lower Oligocene clays in TDP Site 6. The nature of the complex intermixing of the two lithologies and the angular, matrix-supported clays argue against an unconformity. Based on this evidence, it was decided to abandon TDP Site 6 after Core TDP6/9, giving it a total depth (TD) of 61.25 m.

3.3. Planktonic foraminifers

As noted above, drilling at TDP Site 6 recovered lower Oligocene strata, which were intermittently cored, overlying middle Eocene sediments, with a fault zone in between. Microfossil assemblages from Cores TDP6/1 to TDP6/5

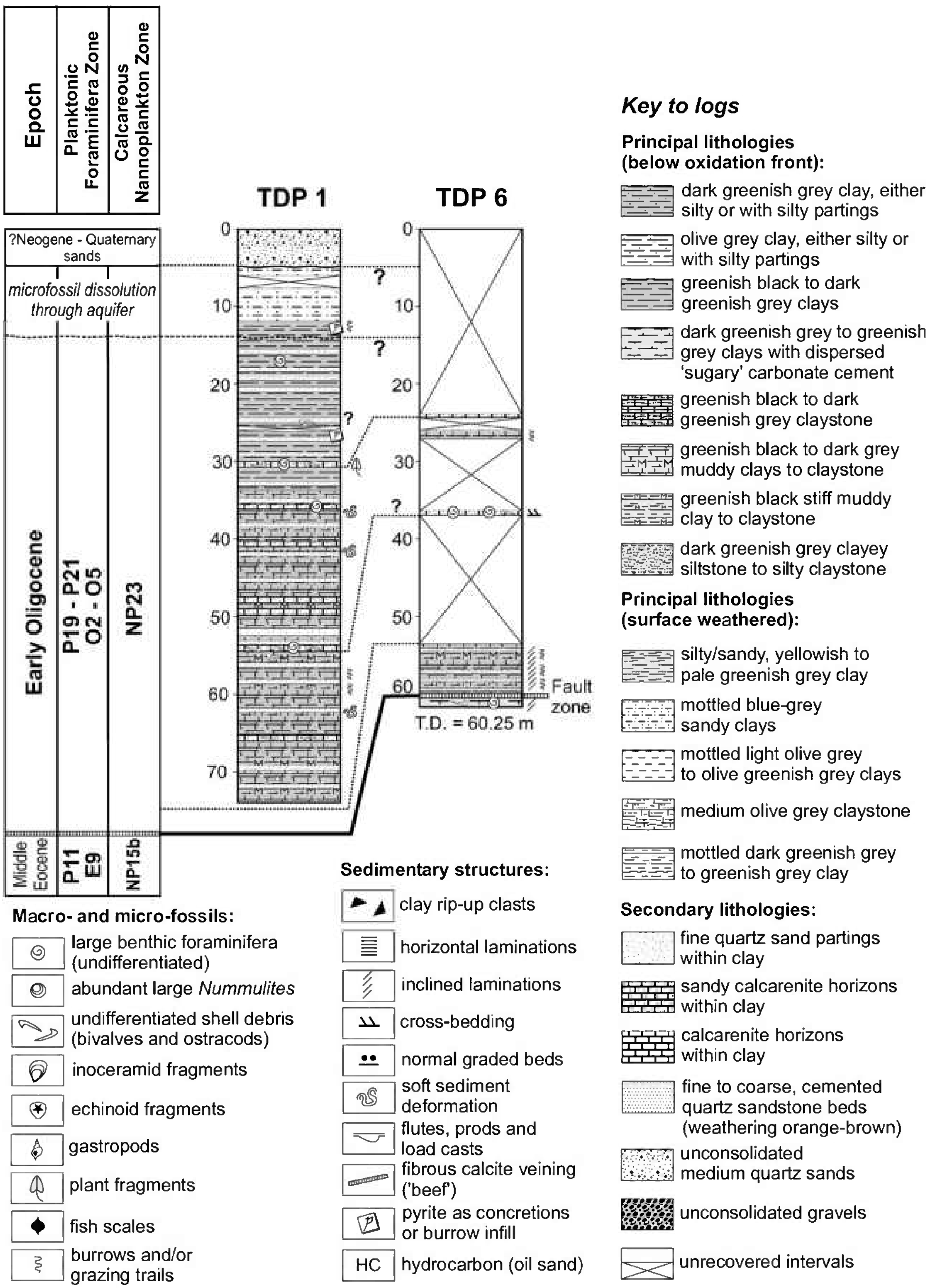

Fig. 5. Integrated litho- and biostratigraphy for TDP Site 6 in comparison to TDP Site 1 as described by Pearson et al. (2004) with inferred correlations.

Table 2
Intervals drilled and cored in TDP Site 6 (Kilwa Masoko, UTM 37L 555752, 9014922)

Site	Core	Top (m)	Bottom (m)	Drilled	Recovered	Recovery (%)	Comment
TDP6/		0.00	26.00	26.00	0.00	0	Interval drilled
	1	26.00	27.05	1.05	1.19	113	Spot core; 1.5 m core barrel
		27.05	36.37	9.32	0.00	0	Interval drilled
	2	36.37	36.94	0.57	0.79	138	Spot core; includes 12 cm of collapse
		36.94	53.38	16.44	0.00	0	Interval drilled
	3	53.58	54.90	1.52	1.55	102	
	4	54.90	55.78	0.88	0.88	100	Short core
	5	55.78	57.20	1.42	1.66	117	
	6	57.20	58.28	1.08	0.22	20	Short core
	7	58.28	59.58	1.30	1.65	127	
	8	59.58	60.12	0.54	0.65	120	
	9	60.12	61.25	1.13	1.18	104	
Total drilled: 61.25 m			Total recovered: 9.41 m			Recovery: 15.4%	

are dominated by benthic foraminifers and micro-gastropod shells indicating a shallow-water, nearshore environment. Planktonic foraminifers from this interval are extremely rare but excellently preserved, exhibiting glassy walls and no infilling. Assemblages are low in diversity and individuals are unusually small. The morphotypes found were assigned to *Chiloguembelina cubenisis*, *Tenuitella gemma*, *Globoturborotalita* sp. (Plate 1(4)), *Dentoglobigerina galavisi*, *D. globularis* (Plate 1(1), *D. pseudovenezuelana* (Plate 1(2)), *Globigerina officinalis*, *G.* cf. *ciperoensis* (a possibly ancestral form) (Plate 1(3)) and *Globorotaloides* sp. These species have limited biostratigraphic utility, but the co-occurrence of *Globigerina* cf. *ciperoensis* and *T. gemma* is consistent with the middle early Oligocene age indicated by nannofossils (see below). The assemblages are closely comparable to those found in TDP Site 1 (Pearson et al., 2004); however, slightly higher yields of planktonic foraminifers towards the lower part of the Oligocene interval in Core TDP6/5 may indicate slightly deeper water conditions than were interpreted from TDP Site 1. This may indicate that Core TDP6/5 is from a slightly lower stratigraphic level than was drilled at the bottom of TDP Site 1.

Samples from Core TDP6/8 and TDP6/9 show variable microfossil preservation, although both samples are clearly middle Eocene clays from the supposed fault zone. Samples TDP6/8-1, 64–65 cm and TDP6/9-1, 82–85 cm contain diverse planktonic foraminifer assemblages showing moderate to good preservation, whereas most specimens from Sample TDP6/9-1, 41–52 cm are infilled by diagenetic calcite. Sample TDP6/8-1, 64–65 cm shows the best preservation, and contains the most diverse assemblage. Age diagnostic species include: *Acarinina bullbrooki*, *A. pseudotopilensis*, *A. rohri*, *Morozovelloides lehneri*, *M. crassata*, *Morozovella aragonensis*, *Parasubbotina inaequispira*, *Hantkenina mexicana*, *H. liebusi*, *Guembelitrioides nuttalli*, *G. kugleri*, *Turborotalia frontosa* and *T. pomeroli*. Based on the co-occurrence of these species, the samples are assigned to Biozone E9 (=P11). The assemblage is indistinguishable from that encountered at the top of TDP Site 2 (Pearson et al., 2004).

3.4. Calcareous nannofossils

Seven samples were studied from TDP Site 6 for nannofossils, of which three were barren, except that all samples studied yielded rare, reworked Cretaceous nannofossils of mid- to late-Cretaceous age. Nannofossil abundance is very low in samples from Sections TDP6/5-1 and TDP6/8-2, and high in the samples from Sections TDP6/8-2 and TDP6/9-1. The nannofossil assemblages are relatively diverse, and preservation is moderate to good or good. Samples from Sections TDP6/8-1 and TDP6/9-1 yielded particularly abundant and diverse assemblages, which are notably rich in rhabdoliths, holococcoliths, pontosphaerids and pentaliths.

The co-occurrence of *Lanternithus minutus*, *Helicosphaera ethologa* and *H. perch-nielseniae* (Plate 2(3)) in Sample TDP6/5-1, 157 cm indicates Zone NP23 (Martini, 1971) (Lower Oligocene) (Perch-Nielsen, 1985; de Kaenel and Villa, 1996). The absence of age diagnostic sphenoliths such as *Sphenolithus distentus* and *S. ciperoensis*, suggests the lower part of Zone NP23 (equivalent to the shorter Zone CP17 of Okada and Bukry, 1980). This biostratigraphic interval was not recorded in neighbouring TDP Site 1, hence these samples may come from a level from below the base of that site.

Samples from Cores TDP6/6 and TDP6/7 are barren apart from rare reworked Cretaceous specimens. The presence of *Chiasmolithus gigas* (Plate 2(22)) in samples from Sections TDP6/8-1 and 6/9-1 indicates the presence of Subzone NP15b (middle Eocene). Other figured species from this site are *H. lophota* (Fig. 2(2)) and *Zygrhablithus bijugatus* (Plate 2(35)). One species, *Blackites globosus*, was described for the first time from this site (Bown, 2005, p. 35).

3.5. Benthic foraminifers

Nine samples from TDP Site 6 were investigated for benthic foraminifers. Preservation varies from moderate to excellent. Fifty-seven genera were identified in this borehole. Large benthic foraminifers predominate in Cores

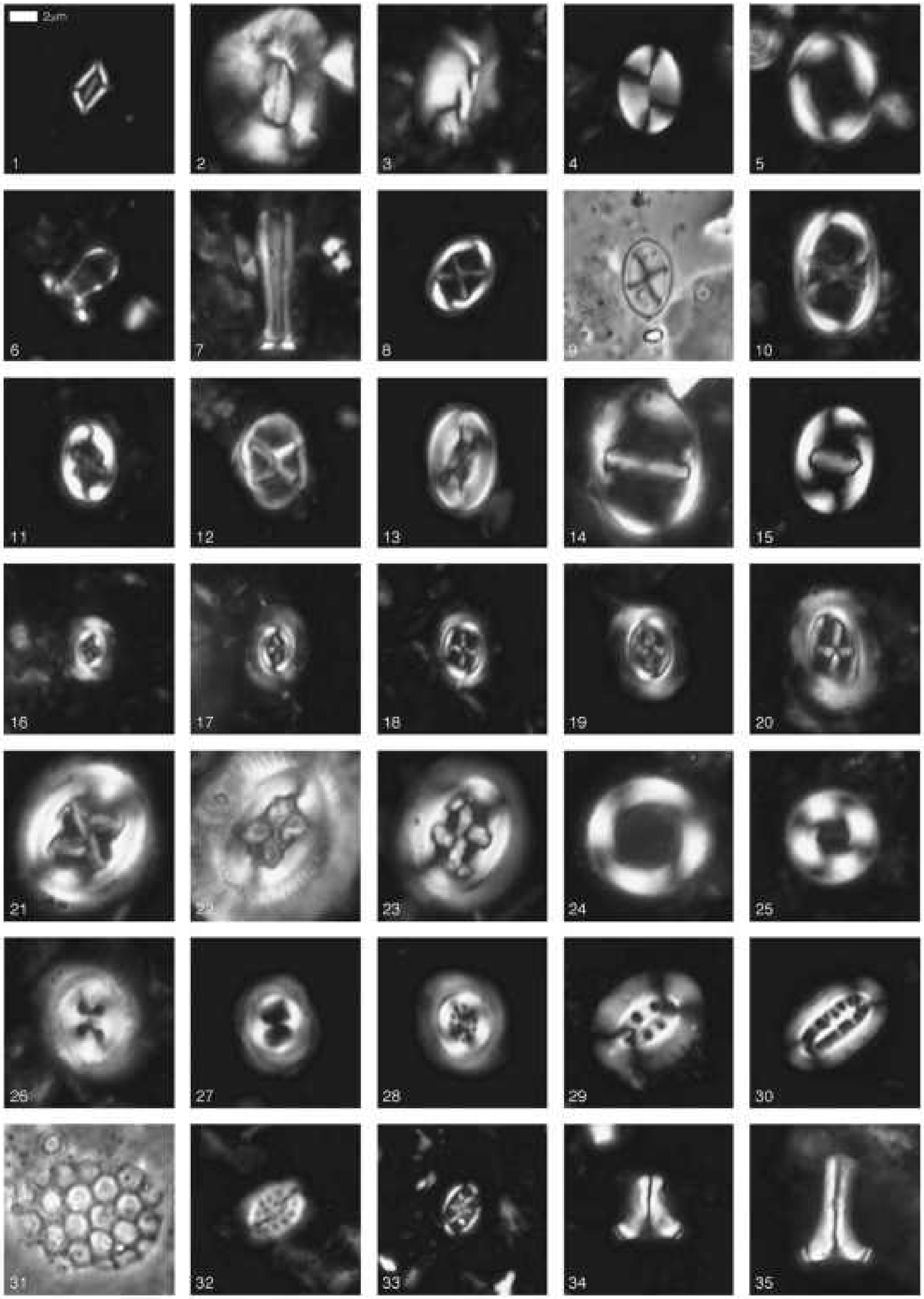

Plate 2. Selected calcareous nannofossils from TDP Sites 6–10. (1) *Calciosolenia aperta*, Sample TDP10/8-1, 100 cm; (2) *Helicosphaera lophota*, Sample TDP6/8-1, 15 cm; (3) *Helicosphaera perch-nielseniae*, Sample TDP6/5-1, 157 cm; (4) *Pontosphaera plana*, Sample TDP10/14-1, 50 cm; (5) *Pontosphaera rimosa*, Sample TDP10/19/3, 40 cm; (6) *Blackites moronium*, Sample TDP8/1/1, 30 cm; (7) *Blackites herculesii*, Sample TDP7B/43/3, 35 cm; (8) *Neochiastozygus rosenkrantzii*, Sample TDP10/14-1, 50 cm; (9) *Neochiastozygus imbriei*, Sample TDP7B/45/2, 20 cm; (10) *Neochiastozygus junctus*, Sample TDP8/1/1, 30 cm; (11) *Neochiastozygus rosenkrantzii*, Sample TDP7A/2-1, 10 cm; (12) *Neococcolithes protenus*, Sample TDP7B/50/2, 45 cm; (13) *Neochiastozygus distentus*, Sample TDP7B/36/1, 20 cm; (14) *Lophodolithus nascens*, Sample TDP10/9-2, 82 cm; (15) *Zygodiscus plectopons*, Sample TDP10/37-2, 68 cm; (16–20) *Campylosphaera dela*, Samples TDP7A/2-1, 10 cm; TDP10/40-1, 85 cm; TDP10/35-3, 58 cm; TDP7A/56-1, 18 cm; TDP6/9-1, 85 cm; (21) *Chiasmolithus bidens*, Sample TDP8/1-1, 30 cm; (22) *Chiasmolithus gigas*, Sample TDP6/9/1, 85 cm; (23) *Cruciplacolithus frequens*, Sample TDP10/40/3, 68 cm; (24) *Ericsonia robusta*, Sample TDP10/14/1, 50 cm; (25) *Ericsonia subpertusa*, Sample TDP10/28-1, 72 cm; (26) *Toweius eminens*, Sample TDP10/2/1, 45 cm; (27) *Toweius occultatus*, Sample TDP7B/47/1, 20 cm; (28) *Toweius serotinus*, Sample TDP7B/47/1, 20 cm; (29) *Ellipsolithus bollii*, Sample TDP7A/35/1, 77 cm; (30) *Ellipsolithus distichus*, Sample TDP10/37/2, 68 cm; (31) *Clathrolithus ellipticus*, Sample TDP7B/42-3, 40 cm; (32) *Holodiscolithus macroporus*, Sample TDP7A/2-1, 10 cm; (33) *Holodiscolithus solidus*, Sample TDP7B/46-2, 40 cm; (34–35) *Zygrhablithus bijugatus*, Samples TDP10/37-2, 68 cm; Sample TDP6/5/1, 157 cm.

TDP6/1 through TDP6/7 (the Oligocene part of the hole) and smaller benthics predominate in the Eocene part.

Both long- and short-ranging benthic foraminifers are present in cores TDP6/1 through TDP6/7 (the Oligocene part). Long-ranging forms include *Lepidocyclina* sp., *Quinqueloculina contorta*, *Asterigerina* sp., *A.* sp. aff. *subacuta* (Plate 4(24)), *Pararotalia* sp., *Reticulophragmium* sp. (Plate 4(21)), *Toddinella* sp. (Plate 4(9)), *Oridorsalis* sp. (Plate 4(13)), *Ammonia beccarii*, *Heterostegina* sp., *Elphidium* sp., *Amphistegina* sp., *Globocassidulina subglobosa*, *Cassidulina* sp., *Lenticulina* sp., *Spiroloculina* sp., *S. canaliculata*, *Reusella* sp. (Plate 4(3)), *Patellina*, *Marginulinopsis longiforma*, *Fursenkoina schreibersiana* (Plate 4(4)), *Bolivina* sp., *Nonion* sp. (Plate 4(7)), *Gyroidinoides girardanus*, *Bulimina impedens*, *Uvigerina mexicana*, *U.* cf. *havanensis* (Plate 4(6)), *U. eocaena*, *Truncatulina costata*, *Cibicidoides eocaenus*, *C. mexicanus*, *Glomospira charoides*, *Nodosaria torsicostata*, *Fissurina trinitatensis*, *F. scarenaensis*, *Guttulina communis, Bathysiphon eocaenus*, *Vaginulinopsis* sp. (Plate 4(5)) and *Triloculina austriaca* (Plate 4(2)).

Samples recovered from Sections TDP6/1-1 through TDP6/7-2 were assigned to the lower Oligocene due to the presence of short-ranging species of *Pararotalia canui*, *Srvatkina perlata*, *Rectuvigerina elegans*, *Vaginulinopsis sulzensis*, *G. subglobosa*, *Stilostomella subspinosa*, *Nummulites intermedius*, *Cycloforina gracilis* (Plate 4(1)), *Nonion gulincki* (Plate 4(8)) and *P. mexicana* (Plate 4(12); reported by Carbonnel et al., 1996, from the lower Oligocene of Benin, West Africa).

Species having their highest occurrences in the lower Oligocene include *G. ovata*, *N. leave*, *Ammodiscus cretacea*, *B. semicostata* and *Hanzawaia isidroensis* (Plate 4(10)). Species with lowest occurrences in the lower Oligocene are *Nodosaria soluta*, *Planulina mexicana*, *Anomalinoides alazanensis*, *Operculina complanata*, *Chrysalogonium longicostatum*, *M. subulata*, *Lenticulina inornata*, *L. caltrata*, *L. curvisepta*, *L. peregrina*, *Sphaeroidinella bulloides*, *Planulina mexicana*, *Neoeponides campester* and *Melonis pompilioides*. The concurrent occurrences of these benthic foraminifers, and the presence of some species restricted to the lower Oligocene, supports the age-dating suggested by calcareous nannofossils.

Planktonic:benthic ratios in the Eocene part of the hole, in Cores TDP6/8 and TDP6/9 are higher than in the Oligocene part above, with planktonic foraminifers generally being as abundant as benthics. Benthic species present include *Cibicidoides eocaenus*, *C. havanensis*, *H. ammophila*, *B. callahani*, *B. trinitatensis*, *Nuttallides truempyi*, *C. grimsdalei*, *M. fragaria*, *N. latejugata*, *V. decorata*, *N. karsteni*, *U. eocaena*, *M. affinae*, *Rectuvigerina mexicana*, *N. longiscata*, and *Aragonia aragonensis*. Large, and other small benthic foraminifers are abundant, such as *Nummulites*, *Lepidocyclina*, *Operculina*, *Asterocyclina*, *Cibicidoides*, *G. girardanus* and *Neoeponides* sp.

Species with their first or last occurrences in the middle Eocene are present, as well as some that are restricted to the middle Eocene. These species include *B. callahani*, *N. karsteni*, *U. eocaena*, *M. affinae*, *Rectuvigerina mexicana*, *N. longiscata* and *A. aragonensis*.

3.6. Palynology

Seven samples from TDP Site 6 were studied for organic walled dinoflagellate cysts (dinocysts) and miospores. Preservation varies from poor to fairly good and dinocysts are generally rare, with abundant plant debris in the samples, especially in the Oligocene part of the site. Samples TDP6/1-1, 42 cm and TDP6/3-1, 32 cm yielded a few non-diagnostic species. Sample TDP6/7-1, 74 cm was found to be barren of palynomorphs. Samples TDP6/5-1, 40 cm, TDP6/6-1, 50 cm and TDP6/7-2, 50 cm yielded a few diagnostic palynomorphs that are consistent with the Oligocene age indicated by calcareous microfossils reported above. These include the dinocyst species *Thalassiphora reticulata* Plate 6(19)) and *Lejeunecysta fallax*. The Oligocene pollen species *Magnatostriatus howadii* was documented from Sample TDP6/8-1, 30 cm. In contrast, Sample TDP6/9-1, 68 cm, yielded a few middle Eocene dinocyst species, including *Homotryblium oceanica*, *Operculodinium ornamentum* and *Areoligera tauloma*. The palynological assemblages suggest a shallow marine, possibly deltaic, environment for the Oligocene part of the site and a deeper marine setting for the middle Eocene.

3.7. Organic geochemistry

A single sample (Sample TDP6/4-1, 50–60 cm) was selected from TDP Site 6 for detailed organic geochemical analysis using GC and GC/MS. This sample, from the Oligocene part of the site, had total organic carbon (TOC), carbonate and total sulfur contents of 1.6%, 3.7% and 0.5%, respectively. Analyses of the saturated hydrocarbon fraction reveal predominantly C_{18}–C_{33} *n*-alkanes (Fig. 3a, Table 1) with C_{31} *n*-alkane (**I**; Fig. 2) being the most abundant component, and an odd-over-even carbon-number predominance indicating a terrestrial origin (Eglinton and Hamilton, 1963, 1967). In addition, hopenes, predominantly C_{28} and C_{30} hop-17(21)-enes (**II**; Fig. 2), hop-18(13)-enes and hopanes, predominantly 17β(H),21β homohopane and 17β(H),21β hopane (**III**; Fig. 2), all of bacterial origin (Ourisson et al., 1979), are abundant. Also present are des-*A*-triterpenes, originating from higher plant triterpenoids (Wolff et al., 1989; Trendel et al., 1989; Freeman et al., 1994), and des-*E*-hopenes and steranes, predominantly ethylcholestane (**IV**; Fig. 2). The presence of these des-*A*-triterpenes and des-*E*-hopenes is evidence for microbial degradation processes within the sediment (Hauke et al., 1993). The aromatic hydrocarbon fraction (Fig. 3b, Table 1) is dominated by a series of aromatic pentacyclic triterpenoids, ranging from A-ring monoaromatics to the fully aromatic picene derivatives (**V**; Fig. 2). These most likely originate from microbially mediated aromatization of higher plant triterpenoids (Greiner et al., 1976; Freeman et al., 1994). Also present are substantial amounts of aromatic des-*A*-triterpenes, such as des-*A*-26,27-dinorlupa-5,7,9,11,13-pentaene (**VI**; Fig. 2), also originating from aromatization of higher plant triterpenoids (Wolff et al., 1989; Trendel et al., 1989). In addition, a number of unidentified compounds, most likely having a triterpenoic origin, are also present.

The polar fraction is also dominated by triterpenoids, especially friedelan-3-one (**VII**; Fig. 2) and α- and β-amyrin, important constituents of higher plants (Pant and Rastogi, 1979; ten Haven et al., 1992). Besides the triterpenoids, substantial amounts of C_{16}–C_{32} *n*-alkanols (Fig. 3c, Table 1) are present, with C_{28} *n*-alkanol (**VII**; Fig. 2) being the most abundant component, and an even-over-odd carbon-number distribution, consistent with a terrestrial origin (Eglinton and Hamilton, 1963, 1967). In addition, bacterial hopanoids, predominantly homohopan-29-one (**IX**; Fig. 2) and bishomohopan-31-one, are present. Steroids, especially 4,24-dimethylcholestan-3-one (**X**; Fig. 2) and 23,24-dimethyl-5α-cholestan-3-one or 24-ethyl-5α-cholestan-3-one, are also present but only in trace amounts. The last two can originate from multiple sources (Volkman, 1986) but in these sediments they probably derive from higher plant material. In contrast, 4-methyl steroids, such as 4,24-dimethylcholestan-3-one (**X**; Fig. 2), are though to originate from dinoflagellates (Withers et al., 1978; Volkman et al., 1990, 1999), although a contribution from diatoms (Volkman et al., 1993) is also possible. Glycerol dipentadecyl diether (C_{15}–C_{15} diether; **XI**; Fig. 2) and archaeol (**XII**; Fig. 2) are also present, although in low amounts comparable to the steroids. The former compound is thought to derive from sulfate-reducing bacteria (Pancost et al., 2001), while archaeol is diagnostic for archaea (Kates et al., 1993; Koga et al., 1993).

The acid fraction is generally dominated by C_{16}–C_{34} *n*-alkanoic acids (Fig. 3d, Table 2), with C_{24} *n*-alkanoic acid (**XIII**; Fig. 2) being the most abundant component and an even-over-odd carbon-number predominance consistent with a terrestrial origin (Eglinton and Hamilton, 1963, 1967), and higher plant triterpenoic acids, especially 3,4-seco-friedelan-3-oic acid (**XIV**; Fig. 2). Substantial amounts of C_{22}–C_{32} ω-hydroxy alkanoic acids are also present, dominated by C_{22} ω-hydroxy alkanoic acid (**XV**; Fig. 2) and characterized by an even-over-odd predominance, again indicating a terrestrial origin (Eglinton and Hamilton, 1967; Holloway, 1982). In addition, bacterial hopanoic acids, predominantly 17β(H),21β(H)-bishomohopanoic acid (**XVI**; Fig. 2), are also abundant.

3.8. Summary

Apart from a short interval of unconsolidated gravel cover, sediments from TDP Site 6 belong to two different formations, of early Oligocene and middle Eocene age, respectively. The upper part of the site, down to about 60 m, consists of predominantly dark greenish-grey to greenish-black clays of early Oligocene age that are interpreted as having been deposited in a shallow marine environment with anoxic bottom-waters. Plant debris is abundant in the palynological preparations and the organic geochemistry is dominated by terrestrial biomarkers derived from higher plants, but some marine biomarkers are also present. Planktonic foraminifers are either absent or rare and benthic foraminifer communities are dominated by shallow-water species. Many of the larger foraminifers are interpreted as allochthonous, having either been carried by submarine gravity flows with other shallow-water debris to form the occasional limestone bands, or possibly introduced individually by down-slope movement.

The most accurate age-dating is provided by the calcareous nannofossils, which indicate an assignment to Zone NP23 in the scheme of Martini (1971), with the site straddling the CP17/CP18 boundary in the zonation of Okada and Bukry (1980). This indicates an age of about 31.6 Ma (the middle part of the early Oligocene, or Rupelian stage) according to the timescale of Berggren et al. (1995). Reworked middle and upper Cretaceous nannofossils throughout suggest that some of the clay was derived from the older Cretaceous formations in the area. Organic geochemistry indicates a very low level of thermal maturity.

Very similar clays were recovered in neighbouring TDP Site 1 (Pearson et al., 2004). Plausible bed-to-bed correlations between the sites can be made using some of the harder limestone bands. These suggest that TDP Site 6 may have spudded in on a level slightly below the top of TDP Site 1 and also penetrated to a stratigraphically lower level. The presence of a slightly lower nannofossil zone in TDP Site 6 than occur at TDP Site 1 and more abundant planktonic foraminifers at the same depth both support this interpretation.

The middle Eocene clays from the fault zone and below in Cores TDP6/8 and TDP6/9 are very similar to those recovered from the upper levels of TDP Site 2, which was also drilled in the vicinity (Fig. 1). The boundary between the two formations is interpreted as a fault rather than an unconformity because of the complex intermixing of the formations, in what is interpreted as a fault gouge. Surface outcrop mapping in the area suggests that this is probably a major fault separating the north-east and south-west parts of the Kilwa peninsula (Nicholas et al., in press).

Unfortunately, the presence of the fault means that we are unable to define the stratigraphic base of the Oligocene clay formation; further drilling to the north-east might accomplish this in the future.

4. TDP Site 7 (Holes TDP7A and TDP7B): Kwamatola

4.1. Site selection

TDP Site 7 and the other remaining sites (TDP Sites 8, 9 and 10) were all drilled around the flanks of Singino Hill, a broad, flat-topped prominence at the north end of the Kilwa peninsula (see Fig. 1). This hill is capped by red conglomerates and gravels of supposed Plio-Pleistocene age (Moore et al., 1963), but older formations are exposed on the sides of the hill in gullies and along road cuttings. Extensive collection from roadside outcrops, along stream beds and by the coast indicates the presence of Paleocene and lower Eocene sediments in the area, with upper Cretaceous formations to the west (Moore et al., 1963; Nicholas et al., in press).

Two holes were drilled at TDP Site 7. Site selection was partially constrained by access, which is along the old German road south of Kilwa Kivinje. This road is currently impassable by truck south of TDP Site 7 because of collapsed bridges. Hole TDP7A (UTM 37L 547126, 9030142) was drilled in order to obtain lower Eocene sediments that had not yet been cored by us but had been collected from outcrop in the neighbouring creek (which is locally called Kwamatola). A second hole (TDP7B; UTM 37L 0547130, 9030140) was drilled when it became apparent that the stratigraphic level at the base of Hole TDP7A was very close to penetrating the Paleocene–Eocene boundary, an interval of significant interest in paleoceanography.

The two holes are just 5 m apart and very similar lithologic sequences were obtained, as summarized in Fig. 6. A list of cores and their depths is provided in Table 3. The best recovery was in Hole TDP7B, and it is therefore on samples from this hole that most subsequent studies will be based.

4.2. Lithostratigraphy

4.2.1. Hole TDP7A

Unconsolidated sands were drilled for the first 2.2 m before coring commenced. Core TDP7A/1 was retrieved between 2.2 m and 2.52 m and consists of dark yellowish-orange to light olive-brown (10YR 6/6 to 5Y 5/6) clayey quartz sand. The rounded clasts vary in size from medium sand to gravel. The lithology is identical to superficial river terrace deposits in the area. Drilling re-commenced until a more clay-rich lithology began to show in the cuttings slurry. Coring began again at 21.64 m with the recovery of Core TDP7A/2. This core is dominantly composed of a dark greenish-grey (5G 4/1) claystone with a minor muddy component. The color indicates that it is from below the oxidation front in the clays. It is soft and friable and reacts with 10% HCl throughout suggesting a significant carbonate component subordinate to the clays.

In Core TDP7A/3, between 22.99 m and 24.6 m, similar muddy claystones also contain carbonate grains and small shelly fragments in ripple cross-bedded partings. This produces a slightly lighter color (5GY 4/1). When clear laminations are preserved they are inclined, typically at about 11°. In Core TDP7A/4 (between 24.6 m and 25.5 m), the claystones display a more inclined planar foliation and the presence of thin (up to 1 cm) fibrous calcite veining, or 'beef'. Indeed, this beef is a common feature of the claystones throughout the hole. At the base of Core TDP7A/4 the claystones are drag-folded and brecciated beneath a minor reverse fault along one such beef horizon.

Similar muddy claystones were cored continuously down to 44.4 m. Throughout this interval, when cores were prepared fresh and prior to desiccation, the claystones possess a characteristic waxy lustre and texture accompanied by a delicate friability upon peeling. This differentiates these claystones in the field from the more clay-rich and carbonate-poor middle Eocene clays encountered previously in TDP Sites 2 and 4.

Core TDP7A/15 (between 40.0 m and 41.5 m) displays an interesting change in angle of lamination. At the top of the core, the lamination dip is ~50°. This increases down over the next 30 cm to about 52° and then gradually decreases to 0° at the base of the core. No planar foliations associated with faulting were observed, and this change in the lamination dip suggests that a slump fold was cored in the claystones. At 41.5 m, a 40 cm-thick, partly carbonate-cemented horizon was encountered, containing abundant allochthonous large benthic foraminifers and small bivalve fragments.

From 44.4 m, for an interval of 2.98 m, the mud component increases to the extent that the sediments are more correctly termed clayey mudstones rather than muddy claystones. The color remains dark greenish-grey. When they are allowed to desiccate and are then sprayed down with water to rehydrate, these mudstones develop and then disintegrate along shaly partings.

Between, 47.38 m and 53.1 m, there is again an interval of the dark greenish-grey, waxy-lustred crumbly claystones. This is punctuated in Core TDP7A/24 between 49.26 m and 50.46 m by a zone of oxidized light olive brown (5Y 5/6) clay interswirled with the claystones and angular claystone fragments. As in TDP Site 6 (see above), the presence of a sharp-bounded oxidation zone containing angular fragments suggests a fault zone with associated fluid flow, although this may be a more minor example.

Between 53.1 m and 54.4 m (Core TDP7A/27), the clayey mudstones briefly return before passing down into a dark greenish-grey to greenish-grey (5GY 4/1 to 5GY 6/1) clayey and muddy siltstone, which varies to occasionally very fine sandstone in patches. This siltstone remains the dominant lithology for the remainder of the hole, from 54.4 m to its base at 107.8 m. It is punctuated by two thin intervals of dark greenish-grey clayey mudstones from 58.05 m to 65.05 m and 80.1 m and 81.3 m. The clayey siltstones differ subtly, in terms of facies, from the claystones which dominate the upper half of the hole. Bioturbation is far more prevalent throughout the siltstones than in the claystones and this also seems to be linked to the development of more pyrite nodules. Macroscopic bioclastic fragments are also dispersed intermittently in the siltstones, including plant fragments, echinoid plates and spines, gastropods and fish scales. The siltstones may indicate a shallower depositional environment or a change in the local sediment supply.

At 97.15 m, a 40 cm-thick interval of mottled greyish-olive to dark yellowish-orange (10Y 4/2 to 10YR 6/6) clay was noted to have a strong smell of oil. The mottled light color of the clays in this thin interval again suggests a fault with some oxidizing fluid movement along it. This fault probably also acted as a conduit for migrating oil.

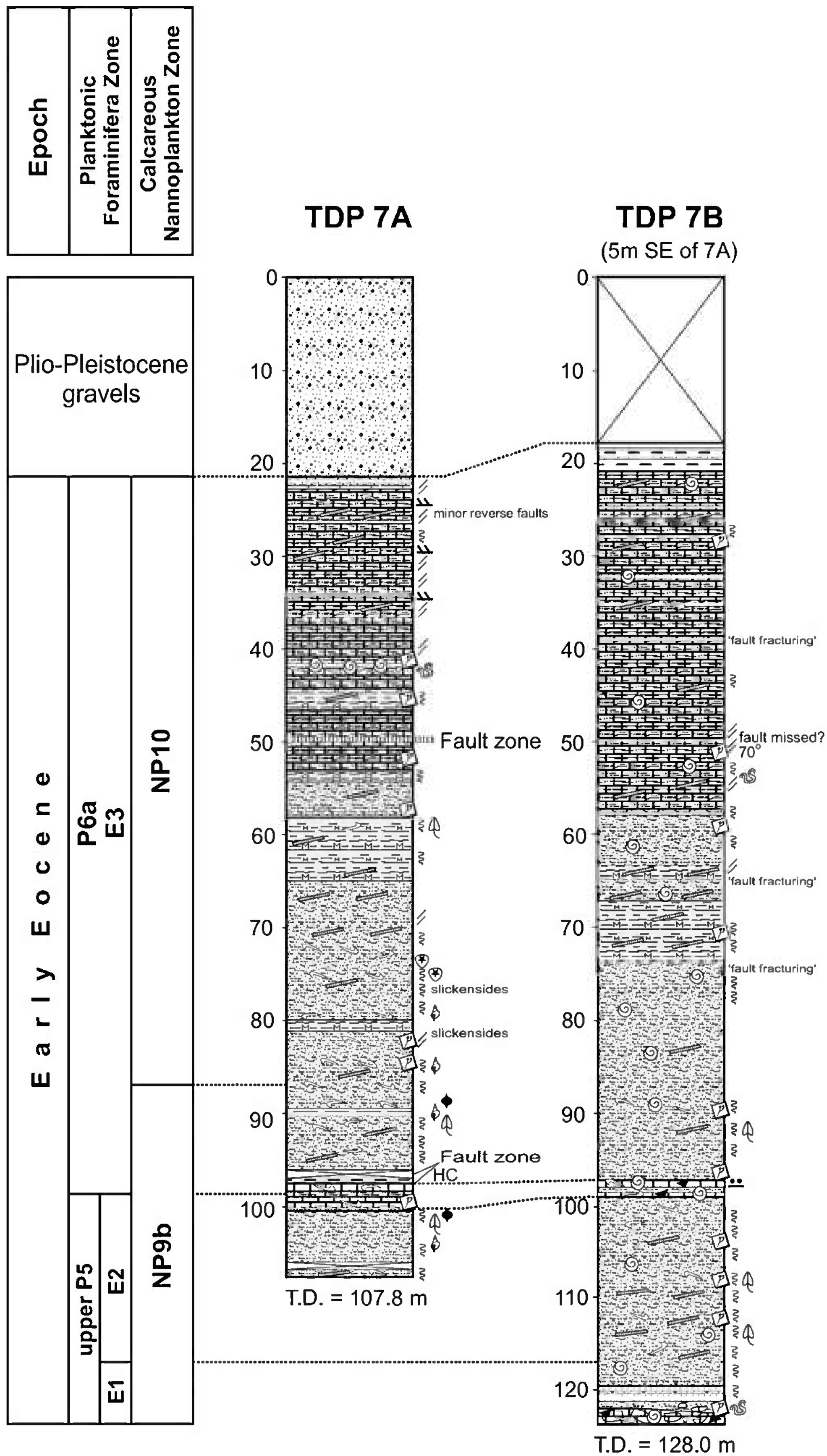

Fig. 6. Integrated litho- and biostratigraphy for Holes TDP7A and TDP7B with inferred correlations. Symbols as given in Fig. 5.

Table 3
Intervals drilled and cored in Holes TDP7A (UTM 37L 547125, 9030142) and TDP7B (UTM 37L 0547130, 9030140)

Hole	Core	Top (m)	Bottom (m)	Drilled	Recovered	Recovery (%)	Comment
TDP7A/		0.00	2.20	0.00	0.00	0	Interval drilled
	1	2.20	2.52	0.32	0.80	250	Includes surface collapse
		2.52	21.64	19.12	0.00	0	Interval drilled
	2	21.64	22.99	1.35	0.52	39	1.6 m core barrel shipped
	3	22.99	24.60	1.61	1.84	114	
	4	24.60	25.50	0.90	0.81	90	
	5	25.50	27.00	1.50	1.57	105	
	6	27.00	28.40	1.40	1.07	76	
	7	28.40	30.00	1.60	1.54	96	
	8	30.00	31.10	1.10	0.90	82	
	9	31.20	32.70	1.50	1.48	99	
	10	32.70	34.20	1.50	1.50	100	
	11	34.50	35.60	1.60	1.11	69	
	12	35.60	37.20	1.60	1.57	98	
	13	37.20	38.70	1.50	1.56	104	
	14	38.70	40.00	1.30	1.24	95	
	15	40.00	41.50	1.50	1.36	91	
	16	41.50	41.80	0.30	0.47	157	Short core
	17	41.80	42.90	1.10	1.00	91	
	18	42.90	44.40	1.10	1.39	126	
	19	44.40	45.60	1.10	1.13	102	
	20	45.60	46.75	1.15	1.08	94	
	21	46.75	47.38	0.63	0.00	0	Lost core; core catcher failed
	22	47.38	48.00	1.62	0.56	0.35	
	23	48.36	49.26	0.90	0.74	82	
	24	49.26	50.46	1.20	0.49	41	Poor recovery
	25	50.46	51.60	1.14	1.23	108	
	26	51.60	53.10	1.50	1.62	108	
	27	53.10	54.40	1.30	1.13	87	
	28	54.40	55.40	1.00	0.31	31	Poor recovery
	29	55.40	57.00	1.60	1.69	106	
	30	57.00	58.05	1.05	0.99	94	
	31	58.05	59.65	1.60	1.41	88	
	32	59.65	60.35	0.80	0.84	105	
	33	60.35	61.95	1.60	1.59	99	
	34	61.95	63.45	1.50	1.60	107	
	35	63.45	65.05	1.60	1.78	111	
	36	65.05	66.65	1.60	1.29	80	
	37	66.65	67.65	1.00	1.11	111	
	38	67.65	69.25	1.60	1.61	101	
	39	69.25	70.45	1.20	1.29	107	
	40	70.45	71.85	1.40	1.45	104	
	41	71.95	73.45	1.50	1.60	107	
	42	73.45	74.95	1.50	1.46	97	
	43	74.95	76.55	1.60	1.60	100	
	44	76.55	77.60	1.05	1.14	109	
	45	77.60	79.20	1.60	1.68	105	
	46	79.20	80.80	1.60	1.65	103	
	47	80.80	82.40	1.60	1.90	119	
	48	82.40	83.90	1.50	0.65	43	Poor recovery
	49	83.90	85.15	1.25	1.65	132	Includes part of previous interval
	50	85.15	86.65	1.50	1.47	98	
	51	86.65	88.15	1.50	1.08	72	
	52	88.15	88.85	0.70	1.29	184	
	53	88.85	90.35	1.50	1.50	100	
	54	90.35	91.35	1.00	0.97	97	
	55	91.35	92.85	1.50	1.10	73	
	56	92.85	93.15	0.30	0.31	103	Short core
	57	93.15	94.35	1.20	0.98	82	
	58	94.35	95.95	1.60	0.48	30	Poor recovery
	59	95.95	96.25	0.30	1.06	353	Includes part of previous interval
	60	96.25	97.15	0.90	0.00	0	Lost core
	61	97.15	97.35	0.20	0.62	310	Includes part of previous interval

(*continued on next page*)

Table 3 (*continued*)

Hole	Core	Top (m)	Bottom (m)	Drilled	Recovered	Recovery (%)	Comment
	62	97.35	97.65	0.30	0.47	157	
	63	97.65	100.45	2.80	0.52	18	3 m core barrel deployed
	64	100.45	103.15	2.70	2.05	77	
	65	103.15	106.15	3.00	2.98	99	
	66	106.15	107.00	0.85	0.00	0	Core lost
	67	107.00	107.80	0.80	0.25	0.31	Poor recovery
Total drilled: 107.80 m			Total recovered: 78.13 m			Recovery: 72.5%	
TDP7B/		0.00	17.95	17.95	0.00	0	Interval drilled
	1	17.95	20.95	3.00	3.25	108	3 m core barrel deployed
	2	20.95	23.95	3.00	3.45	115	
	3	23.95	25.80	1.85	2.07	112	1.6 m core barrel deployed
	4	25.80	27.80	2.00	1.87	93	
	5	27.80	28.80	1.00	1.03	103	
	6	28.80	31.80	3.00	3.15	105	3 m core barrel deployed
	7	31.80	34.80	3.00	0.84	28	Poor recovery
	8	34.80	36.30	1.50	1.38	92	
	9	36.30	37.80	1.56	1.48	104	
	10	37.80	40.80	3.00	2.84	95	
	11	40.80	43.70	2.90	2.38	82	
	12	43.70	45.50	1.80	1.43	79	
	13	45.50	46.80	1.30	0.70	54	
	14	46.80	48.80	2.00	1.56	78	
	15	48.80	49.80	1.00	0.93	93	
	16	49.80	52.80	3.00	2.96	99	
	17	52.80	55.10	2.30	1.96	85	
	18	55.10	55.80	0.70	0.78	111	
	19	55.80	57.40	1.60	1.48	92	
	20	57.40	58.80	1.40	1.07	76	
	21	58.80	61.70	2.90	2.56	88	
	22	61.70	63.70	2.00	1.70	85	
	23	63.70	64.80	1.10	1.07	97	
	24	64.80	65.20	0.40	0.40	100	Short core
	25	65.20	66.40	1.20	0.84	70	
	26	66.40	67.80	1.40	1.32	94	
	27	67.80	69.00	1.40	0.54	38	Poor recovery
	28	69.00	70.80	1.80	1.80	100	
	29	70.80	73.80	3.00	2.90	97	
	30	73.80	76.80	3.00	2.85	95	
	31	76.80	78.10	1.30	1.25	96	
	32	78.10	79.80	1.70	0.90	53	
	33	79.80	82.30	2.50	3.17	127	
	34	82.30	82.80	0.50	0.44	88	Short core
	35	82.80	85.80	3.00	2.30	77	
	36	85.80	88.80	3.00	1.45	48.3	Poor recovery
	37	88.80	91.50	2.70	3.10	115	
	38	91.50	91.80	0.30	0.20	67	Short core
	39	91.80	93.90	2.10	2.10	100	
	40	93.90	95.65	1.75	0.98	56	
	41	95.65	97.80	2.15	2.90	135	
	42	97.80	100.80	3.00	2.89	96	
	43	100.80	103.80	3.00	2.52	84	
	44	103.80	106.40	2.60	3.30	127	
	45	106.40	108.30	1.90	1.52	80	
	46	108.30	109.80	1.50	1.72	115	
	47	109.80	112.80	3.00	2.92	97	
	48	112.80	115.80	3.00	3.00	100	
	49	115.80	118.80	3.00	2.79	93	
	50	118.80	121.80	3.00	3.18	106	
	51	121.80	123.80	2.00	1.65	82	
	52	123.80	126.20	2.40	1.35	56	
	53	126.20	128.00	1.80	0.95	53	
Total drilled: 128.00 m			Total recovered: 99.17 m			Recovery: 77%	

Similar evidence for oil, confirmed by geochemical analysis, was previously found in the lower Eocene claystones at TDP Site 3 (Pearson et al., 2004, p. 50). Organic geochemical analysis confirms these traces as oil coming from outside the formation (see Section 4.7, below).

Directly beneath this probable fault, at 97.7 m, Core TDP7A/63 contains a 3.05 m-thick, light greenish-grey to white (5GY 7/1 to N7) bioclastic grainstone, with centimeter-sized clay rip-up clasts and large benthic foraminifers.

Table 4 includes geochemical results of 11 samples from TDP Hole 7A. The calcium carbonate content is generally low (<10%) but one sample contained 34.6% $CaCO_3$, probably indicating extensive diagenetic cement at that level (near the top of the hole, in Core TDP7A/3). The sulfur content ranges from 0.04% to 0.5% and TOC from 0.1% to 0.9%.

4.2.2. Hole TDP7B

Unconsolidated sands and gravels were drilled for the first 17.95 m before coring commenced in this hole. Core TDP7B/1, from 17.95 m to 20.9 5 m, recovered a mottled light olive grey to greenish-grey claystone (5Y 6/1 to 5GY 6/1) with beef. The claystones possess a much deeper color at the top of Core TDP7B/2 at 20.95 m (dark greenish-grey; 5GY 4/1), suggesting that the weathering oxidation front lies between these first two cores. The physical characteristics of the dark greenish-grey claystones are identical to those at the equivalent level in Hole TDP7A, in that they have a subordinate carbonate component throughout which causes them to react with weak hydrochloric acid. They also contain a muddy fraction and upon desiccation–rehydration they develop and then disintegrate along a shaly parting.

Similar claystones were cored continuously from 20.95 m to a depth of 57.4 m. At 32.2 m, a 15 cm-thick, fine quartz sand horizon is present. Large benthic foraminifers are dispersed throughout the claystones and burrows are rare to uncommon. In Core TDP7B/10, between 37.8 m and 40.8 m, an interval containing a second sandy parting in amongst a series of planar fractures with angles of inclination between 50° and 70° was recovered. Drilling disturbance in this core is only moderate throughout and these fractures appear to be tectonic features.

A similar set of fractures is present in Core TDP7B/16 (between 49.8 m and 52.8 m). Within this interval, there is also another fine quartz sand parting, which has a dip of 70°. A probable fault zone was recorded at an equivalent depth in Hole TDP7A, 5 m to the north-west. One explanation might be that the fracturing and dip in Hole TDP7B is a result of fault drag and folding against a high-angle fault plane that passes through Hole TDP7A at this depth. There is also some deformation just below this interval, at 55.1 m, which may also be a result of tectonic rather than syn-sedimentary deformation.

From 57.4 m to 119.7 m, the principal lithology is a dark greenish-grey (5G 4/1 to 5GY 4/1) silty claystone to clayey siltstone. This subtle change from the overlying claystones reflects a pervasive increase in visible siliciclastic content throughout this unit. As in Hole TDP7A at this depth, there are intervals where this siliciclastic component is dominated by mud-sized rather than silt-sized grains. This finer, muddy claystone, was cored at two intervals, from 63.7 m to 64.8 m and between 67.8 m and 73.8 m. The interval between 57.4 m and 119.7 m is also characterized by uncommon to common bioturbation, particularly below about 90 m depth. This subtle increase in bioturbation down-hole was also recorded in Hole TDP7A and suggests that there was a change in relative water depth or sediment

Table 4
Results of geochemical analyses of sediments from TDP Site 7 (Holes TDP7A and TDP7B)

Sample	Depth (m)	$CaCO_3$ (%)	Sulfur (%)	TOC (%)
TDP 7A/3-1, 21–31 cm	23.20–23.30	34.6	0.4	0.8
TDP 7A/9-1, 23–33 cm	31.43–31.53	6.2	0.1	0.1
TDP 7A/15-1, 91–100 cm	40.91–41.00	0.4	0.1	0.2
TDP 7A/19-1, 45–54 cm	44.85–44.94	5.9	0.1	0.3
TDP 7A/23-1, 8–16 cm	48.44–48.52	4.5	0.2	0.3
TDP 7A/35-1, 67–77 cm	64.12–64.22	7.4	0.04	0.3
TDP 7A/39-1, 56–67 cm	69.81–69.91	7.0	0.1	0.3
TDP 7A/46-1, 30–40 cm*	79.50–79.60	8.2	0.2	0.5
TDP 7A/52-1, 85–95 cm	89.70–89.80	3.6	0.5	0.7
TDP 7A/54-1, 26–36 cm*	90.61–90.71	5.9	0.1	0.9
TDP 7A/64-1, 68–82 cm*	101.13–101.27	10.2	0.1	0.5
TDP 7B/35-1, 55–62 cm	83.32–83.39	3.2	0.2	0.4
TDP 7B/37-1, 55–62 cm	89.35–89.42	4.4	0.3	0.9
TDP 7B/39-1, 55–62 cm	92.35–92.42	3.2	0.1	0.5
TDP 7B/41-2, 55–62 cm	97.20–97.27	3.4	0.1	0.6
TDP 7B/42-2, 55–62 cm	99.35–99.42	4.6	0.1	1.3
TDP 7B/43-2, 55–62 cm	102.35–102.42	4.0	0.1	0.5
TDP 7B/44-3, 65–72 cm	106.45–106.52	21.2	0.1	1.0
TDP 7B/46-2, 65–72 cm	109.95–110.02	28.8	0.1	1.0
TDP 7B/48-1, 55–62 cm	113.35–113.42	2.2	0.1	0.4
TDP 7B/49-2, 55–62 cm	117.35–117.42	2.1	0.2	0.2
TDP 7B/50-1, 55–62 cm*	119.35–119.42	15.2	0.7	0.5

Sediments highlighted with an asterisk were selected for biomarker study (see Table 1).

surface oxygenation during deposition of this unit. In addition, pyrite infills to burrows are also more abundant in these clayey siltstones than in the claystones above. Again, as observed in Hole TDP7A within this interval, macrofossils such as bivalves and plant fragments and large benthic foraminifers are occasionally dispersed throughout.

Further evidence that Holes TDP7A and 7B are almost directly correlatable is the presence of the same bioclastic grainstone marker horizon in both. The top of this bed is at 97.7 m in Hole TDP7A, and 97.45 m in Core TDP7B/41. In Hole TDP7B, this marker is a 1.4 m-thick, light greenish-grey to white (5GY 7/1 to N7) bioclastic grainstone, with centimeter-sized clay rip-up clasts and large benthic foraminifers. Crude normal grading occurs towards its top. However, in Hole TDP7A, an oxidized clay zone with a strong smell of oil was recorded directly overlying this marker bed, whereas in Hole TDP7B, no such evidence was encountered. As with higher in the hole, this might suggest that the faulting is at a high angle and the fault zone passing through Hole TDP7A at this depth does not extend across to Hole TDP7B.

The clayey siltstones present near the bottom of Hole TDP7A (107.8 m) were found to continue down to 119.7 m, in core TDP7B/50. From 119.7 m to 122.0 m, the principal lithology is a clayey, light grey (N7) carbonate cemented fine quartz sandstone. There is abundant bioturbation of the sands and they pass down, at 122.0 m in Core TDP7B/51 into the top of a slump breccia horizon, which comprises the remainder of the hole to a final depth of 128 m. This breccia interval is composed of a matrix of olive grey to dark greenish-grey (5Y 4/1 to 5GY 4/1) silty claystone to occasionally fine quartz sandy claystone. These claystones react with weak hydrochloric acid throughout and contain dispersed large benthic foraminifers. The clasts are matrix supported and consist of light grey to medium light grey (N7–N6) benthic foraminiferal and shelly limestone fragments, ranging in size from 1 to 5 cm. Although outlines are present, little of the original cement and fossil texture is preserved in the later sparry calcite. Increased drilling disturbance towards the base of the hole eventually caused it to be abandoned. Thus the apparent successive layering of breccia and claystone horizons within this interval may have been a product of this disturbance rather than original sedimentary deposition.

Table 4 includes geochemical results from 11 samples from TDP Hole 7B. The calcium carbonate content is generally low (<10%) but three high values, up to 28.8%, probably indicate pervasive diagenetic cements at certain levels. The sulfur content ranges from 0.1% to 0.7% and the TOC from 0.2% to 1.3%.

4.3. *Planktonic foraminifers*

4.3.1. *Hole TDP7A*

The two holes drilled at TDP Site 7 recovered a thick basal Eocene sequence that can be assigned to biozones E2 (=uppermost P5) to E3 (=P6a). Planktonic foraminifers are a common component of the washed clay residues, and assemblages are generally diverse. In Hole TDP7A, little change in species composition was noted between Cores TDP7A/1 and TDP7A/62. Shell preservation is variable, ranging from excellent, where specimens are unfilled and have glassy shell walls (Plate 1(9, 11)), to poor (with common calcite and pyrite infilling, but with the walls still unrecrystallized). These planktonic foraminifer assemblages are characterized by common acarininids, morozovellids, subbotinids and globanomalinid species typical of the lower Eocene. Common taxa include: *A. coalingensis*, *A. soldadoensis*, *A. wilcoxensis*, *C. crinita* (Plate 1 (7–8)), *C. wilcoxensis*, *M. aequa*, *M. marginodentata*, *M. subbotinae*, and *Subbotina patagonica*. Less frequent but consistent constituents include *M. gracilis*, *M. edgari*, *S. hornibrooki*, *S. velascoensis*, *Pseudohastigerina wilcoxensis* and *Parasubbotina varianta*. Based on the absence of *M. velascoensis* and *M. formosa* these samples are assigned to Biozone E3 (=P6a).

Samples TDP7A/64-1, 50–65 cm and TDP7A/65-2, 71–86 cm contain similar assemblages to the cores above but, in addition, contain few to common specimens of *M. velascoensis*, *M. occlusa*, *M. pasionensis* and *M. acuta*. Based on the co-occurrence of the latter species with *P. wilcoxensis* the stratigraphically lowest samples are assigned to lower Eocene Zone E2 (=uppermost P5).

4.3.2. *Hole TDP7B*

Hole TDP7B contains a similar set of planktonic foraminifer assemblages to Hole TDP7A, as would be expected. The extinction of the *Morozovella velascoensis* group of species (which includes *M. velascoensis* itself (Plate 1(5) and *M. occlusa* (Plate 1(6))) is very marked. This, the boundary between Zones E3 (=P6a) and E2 (=topmost P5) lies between Samples TDP7B/41/3, 60–65 cm and TDP7B/42/1, 50–55 cm. The former of these samples was taken from a cored interval of just 30 cm between two limestone beds. The limestone above is approximately 70 cm thick and the one below, which spans the core break between Cores TDP7B/41 and TDP7B/42, is 40 cm thick. More detailed sampling might reveal whether the zone boundary lies above or below the lower limestone. The shell preservation is excellent in this part of the hole, suggesting that it may be useful for investigating the cause of this selective extinction.

This hole penetrates to about 20 m deeper than Hole TDP7A and questionably enters Zone E1 towards the bottom. Zone E1 is differentiated from Zone E2 by the lack of *P. wilcoxensis*. This species is a rare component of all samples examined down to Sample TDP7B/49/1, 50–55 cm. It is absent from Sample TDP7B/49/2, 50–55 cm and below. However the zone boundary is very difficult to locate precisely in this material because both *P. wilcoxensis* and its ancestral form, *G. luxorensis*, are generally rare, and their differentiation is subtle (see Speijer and Samir, 1997; Olsson and Hemleben, in press). Another difficulty is that rare forms resembling *P. wilcoxensis* have been recorded as low as Zone P4c in TDP Site 10 (see below).

Despite seemingly penetrating Zone E1 (a very short zone, equivalent to a time interval of about 100 kyr duration after the onset of the Paleocene–Eocene thermal maximum; see Berggren and Pearson, 2005), no specimens of the Paleocene–Eocene boundary 'excursion taxa' *A. sibaiyaensis*, *A. africana* and *M. allisonensis* were found in the hole and no unambiguously Paleocene sediments were recovered.

4.4. Calcareous nannofossils

4.4.1. Hole TDP7A

Twenty-five samples were studied from Hole TDP7A, and all yielded rare to common, diverse nannofossil assemblages of good or moderate to good preservation. The assemblages are notably rich in rhabdoliths, holococcoliths (especially *Zygrhablithus bijugatus*), pontosphaerids and pentaliths, all considered to be indicators of shelf environments (Perch-Nielsen, 1985; Aubry, 1999), but yield only rare discoasters.

The presence of *Rhomboaster cuspis* throughout, and *Rhomboaster bramlettei* in all but the uppermost cores, indicates a biostratigraphic assignment to Zone NP10. *Rhomboaster* specimens are very rare: cubic morphologies are classified as *R. cuspis*, and morphologies with two, symmetrically superimposed triradiate cycles are called *R. bramlettei* (see Plates 2 and 3). The absence of younger members of the *Rhomboaster–Tribrachiatus* lineage, e.g. *Tribrachiatus contortus* or *T. digitalis*, suggests the level is within the lower part of the zone. The lowermost core included *Fasciculithus* and *Discoaster mahmoudii*, taxa that are consistently present in Hole TDP7B (see below).

Taxa figured from this hole are *Neochiastozygus rosenkrantzii* (Plate 2(11)), *Campylosphaera dela* (Plate 2(16)), *Ellipsolithus bollii* (Plate 2(29)), *Holodiscus macroporus* (Plate 2(32)), and *D. binodosus* (Plate 3(16)). Seven new species were named from this hole by Bown (2005). These are *Coccolithus minimus* (Bown, 2005, p. 27), *C. foraminis* (Bown, 2005, p. 27), *Cruciplacolithus cassus* (Bown, 2005, p. 28), *Calcidiscus parvicrucis* (Bown, 2005, p. 29), *B. clavus* (Bown, 2005, p. 236), *Semihololithus kanungoi* (Bown, 2005, p. 41) and *Discoaster acutus* (Bown, 2005, p. 44).

4.4.2. Hole TDP7B

Twenty-nine samples were studied from Hole TDP7B, and all but one yielded rare to common, diverse nannofossil assemblages of good or moderate to good preservation. The general nature of the assemblages is identical to that of the adjacent Hole TDP7A. The lowermost cores (Cores TDP7B/53 and TDP7B/52) yielded very sparse assemblages, but these include *C. dela*, indicating a biostratigraphic level no lower than Zone NP9 (or Subzone CP8a). *R. cuspis* (Plate 3(24–25)) has a first occurrence in Section TDP7B/51-1 and *R. bramlettei* (Plate 3(21–23)) in Section TDP7B/44-2. Applying the NP zonation strictly, the FO of *R. bramlettei* marks the base of NP10, but the presence of *R. cuspis* from Section TDP7B/51-1 suggests the base of the section is in the uppermost part of Zone NP9. However, the sparsity of assemblages in the lowermost cores undermines confidence in the occurrence data for this interval, and particularly the putative first occurrences. The FO of *D. diastypus* was recorded in Section TDP7B/50-2, suggesting a lower position for the base of NP10, but the reliability of this marker has been questioned (Aubry, 1995). *Fasciculithus* spp. (Plate 3(16–17)) are rare in the lowermost cores (Cores TDP7B/50-53), very rare in Cores TDP7B/49-45, and absent above this level. Other notable occurrences include the common to frequent presence of *Z. bijugatus* from Section TDP7B/51-1, the presence of *Lophodolithus nascens* throughout, and the rare to frequent presence of *D. mahmoudii* (Plate 3(11–13)) from Sections TDP7B/51-1 to TDP7B/44-2. The 'excursion' discoaster, *D. araneus*, was not observed.

Although the chronology of high-resolution nannofossil events through the Paleocene/Eocene boundary interval is still rather poorly constrained, the nannofossil data from Hole TDP7B suggests a correlation corresponding to uppermost Zone NP9 (CP8a) through Subzone NP10a, and possible incorporating, or lying just above, the Paleocene/Eocene thermal maximum and associated carbon isotope excursion interval (see e.g. Angori and Monechi, 1995; Aubry, 1995; Bralower and Mutterlose, 1995; Aubry et al., 1996; Schmitz et al., 1997).

Additional species figured from this hole are *B. herculesii* (Plate 2(7)), *N. imbriei* (Plate 2(9)), *Neococcolithes protenus* (Plate 2(12)), *N. bukryi* (Plate 2(13)), *C. dela* (Plate 2(19)), *Toweius occultatus* (Plate 2(27)), *T. serotinus* (Plate 2(28)), *Clarolithus ellipticus* (Plate 2(31)), *H. solidus* (Plate 2(33)), *Braarudosphaera bigelowii* (Plate 3(1)), *Micrantholithus attenuatus* (Plate 3(3)), *M. flos* (Plate 3(4)), *M. bramlettei* (Plate 3(5)), *D. falcatus* (Plate 3(9)), *D. lenticularis* (Plate 3(10)), *D. mediosus* (Plate 3(14)), *D. multiradiatus* (Plate 3(55)), *Fasciculithus schaubii* (Plate 3(16)), *F. tonii* (Plate 3(17)) and *Sphenolithus anarrhopus* (Plate 3(19–20)). Three new species were described from this hole by Bown (2005); *B. turritus* (Bown, 2005, p. 36), *H. serus* (Bown, 2005, p. 38) and *Neocrepidolithus grandiculus* (Bown, 2005, p. 70).

4.5. Benthic foraminifers

Fifty-six samples were examined for benthic foraminifers from TDP Site 7. Generally the benthic foraminifers are not as abundant as the planktonic foraminifers. Most of the benthics are indicative of upper slope, rather dysoxic sea-floor conditions. Preservation varies from moderate to good, while occasional samples contain excellently preserved, glassy specimens. However, calcite infilling occurs at a number of horizons, notably in Cores 22, 34 and 42.

The benthic foraminifer assemblages contain a mixture of transported near-shore species and in situ deep-water species. Those derived from shallow-water include species of *Pararotalia*, *Quinqueloculina*, *Nummulites*, *Operculina* and *Heterostegina*, and these occur in fluctuating numbers through the succession. They reflect an intertidal to inner

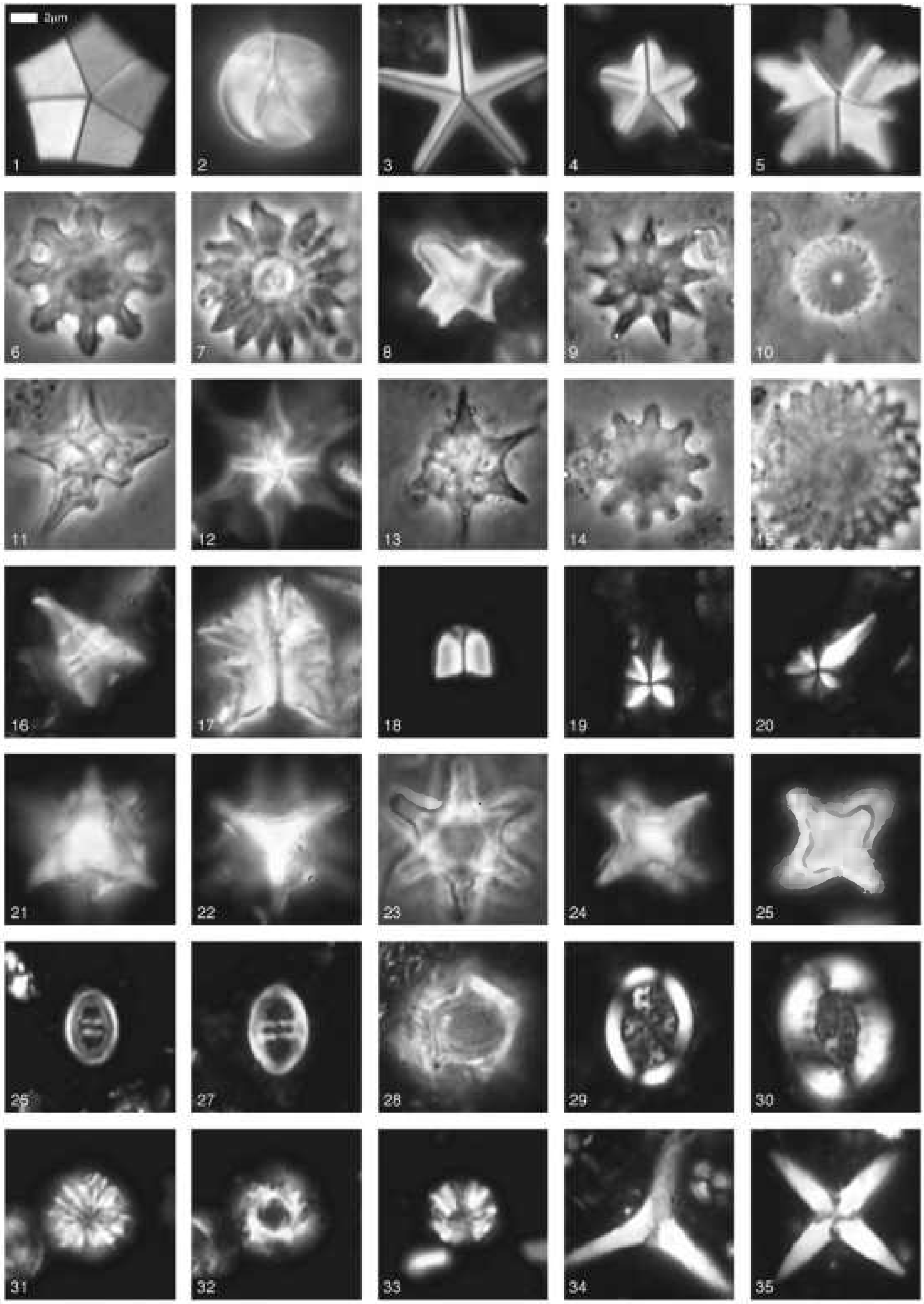

Plate 3. Selected calcareous nannofossils from TDP Sites 6–10. (1) *Braarudosphaera bigelowii*, Sample TDP7B/46-2, 40 cm; (2) *Micrantholithus disculus*, TDP10/35-3, 58 cm; (3) *Micrantholithus attenuatus*, Sample TDP7B/49-2, 40 cm; (4) *Micrantholithus breviradiatus*, TDP7B/47/1, 20 cm; (5) *Micrantholithus bramlettei*, Sample TDP7B/43/3, 35 cm; (6) *Discoaster binodosus*, Sample TDP7A/17/1, 83 cm; (7) *Discoaster diastypus*, Sample TDP8/11/2, 20 cm; (8) *Discoaster diastypus* side view, Sample TDP8/12-1, 50 cm; (9) *Discoaster falcatus*, Sample TDP7B/39/1, 20 cm; (10) *Discoaster lenticularis*, Sample TDP7B/41/3, 15 cm; (11–13) *Discoaster mahmoudii*, Samples TDP7B/50/2, 45 cm; TDP7B/44/2, 40 cm; TDP7B/51/1, 20 cm; (14) *Discoaster mediosus*, Sample TDP7A/56/1, 18 cm; (15) *Discoaster multiradiatus*, Sample TDP7B/51/1, 20 cm; (16) *Fasciculithus schaubii*, Sample TDP7B/52-2, 23 cm; (17) *Fasciculithus tonii*, Sample TDP7B/51/2, 23 cm; (18) *Fasciculithus tympaniformis*, Sample TDP10/40-1, 85 cm; (19, 20) *Sphenolithus anarrhopus*, Sample TDP7B/33-1, 20 cm; (21–23) *Rhomboaster bramlettei*, Sample TDP7B/43/3, 35 cm; (24, 25) *Rhomboaster cuspis*, Samples TDP7B/44/2, 40 cm; TDP7B/41/3, 15 cm; (26) *Zeugrhabdotus bicrescenticus*, Sample TDP9/11/1, 37 cm; (27) *Tranolithus orionatus*, Sample TDP9/11/1, 37 cm; (28) *Cribrosphaerella ehrenbergii* coccosphere, Sample TDP9/49/2, 62 cm; (29) *Arkhangelskiella cymbiformis*, Sample TDP9/49/2, 62 cm; (30) *Broinsonia parca constricta*, Sample TDP9/49/2, 62 cm; (31, 32) *Cribrocoronia*? *echinus*, Sample TDP9/11/1, 37 cm; (33) *Cribrocoronia*? *echinus* side view, Sample TDP9/11/1, 37 cm; (34) *Uniplanarius trifidus*, Sample TDP9/11/1, 37 cm; (35) *Uniplanarius sissinghii*, Sample TDP9/11/1, 37 cm.

shelf environment, a highly oxygenated and wave-influenced substrate, with the numbers of miliolids indicating some hypersalinity in the coastal water column, which is to be expected in tropical waters.

In contrast, the species indicative of upper slope conditions reflect quiet-water, dysoxic conditions with rapid fine-grained clay sedimentation: these include species of the calcareous genera *Chilostomella*, *Stilostomella* and *Nodogenerina*, *Melonis*, *Saracenaria*, *Lenticulina*, *Dorothia* (Plate 5(13)), *Oridorsalis*, *Spiroplectinella*, *Nonionella*, *Anomalinoides* (Plate 5(19, 20)), *Gyroidinoides*, *Gavelinella*, *Nuttallides*, *Nodosaria* (Plate 5(28)) and *Neoflabellina*. Also evident in the in situ assemblage are small numbers of deep-water agglutinated species, of which *Rzehakina epigona* is commonest. Upper slope environments of deposition (estimated water depths between 250 and 500 m) appear to have prevailed throughout the succession drilled at TDP Site 7.

4.6. Palynology

Eleven samples from Hole TDP7A were studied for dinocysts and miospores. No samples from TDP Hole 7B were studied. Sample TDP7A/2-1, 11–15 cm is barren of palynomorphs. Samples TDP7A/10-1, 62–66 cm, TDP7A/23-1, 7–8 cm, TDP7A/35-1, 63–67 cm, TDP7A/49-1, 40–50 cm, TDP7A/59-1, 85–95 cm and TDP7A/62-1, 20–30 cm are poor in palynomorphs; however, a few lower Eocene dinocyst species were documented from these samples (e.g., *Phthanoperidium crenulatum*; Plate 6(5)). Sample TDP7A/53-1, 40–50 cm contains common dinocysts which are consistent with a stratigraphic assignment to the lower Eocene. The sample was found to be rare in miospores. The stratigraphically significant taxa that are typical of the lower Eocene include *Fibrocysta bipolaris*, *Glaphyrocysta delicata*, *Charlesdownlea insolens* and *Corrudinium obscurum*.

Sample TDP7A/64/1, 89–98 cm is fairly rich in palynomorphs, with common dinocysts and rare miospores. These include some additional stratigraphically important dinocysts typical of the upper Paleocene to lower Eocene such as *Apectodinium parvum* (Plate 6(6)), *A. homomorphum* (Plate 6(7)) and *A. quinquelatum* (Plate 6(8)). Other stratigraphically important dinocyst species documented from this sample include: *Hafniasphaera septata*, *Adnatosphaeridium robustum*? (Plate 6(3,9)), *Dracodinium waipawaense*, *C. edwardsii*, *Muratodinium fimbriatum* (Plate 6(4)) and *Alisocysta margarita*. These indicate an early Eocene age.

Sample TDP7A/65/3, 10–17 cm has a contrasting assemblage to those examined from higher levels in the core. It contains rare miospores but fairly common dinocysts. The dinocyst species *M. fimbriatum*, *Manumiella rotunda*, *Fibradinium annetorpense* and *H. septata* co-occur. Other genera documented from this sample include *Homotryblium*, *Polysphaeridium*, *Alisocysta*, *Spinidinium*, *Cordosphaeridium* and *Deflandrea*.

4.7. Organic geochemistry

Three samples from TDP Hole 7A and one from TDP Hole 7B (indicated by asterisks in Table 4) were selected for organic geochemical analysis.

4.7.1. TDP Hole 7A

Fractions of the three samples chosen from Hole TDP7A for biomarker analyses are predominantly *n*-alkanes (Table 1), with the C_{29} *n*-alkane being the most abundant. Substantial amounts of hopanes and hopenes and lesser amounts of steranes are also present in all the samples. In addition, the saturated hydrocarbon fraction of Sample TDP7A/46-1, 30–40 cm contains traces of des-*A*-triterpenes and des-*E*-hopenes. The aromatic hydrocarbon fractions from the three samples contain only relatively small amounts of aromatic des-*A*-triterpenes (Table 1) and only the aromatic hydrocarbon fraction from Sample TDP7A/46-1, 30–40 cm was found to contain aromatic pentacyclic triterpenoids, and only then in low abundances. However, the fractions of the other two samples from this hole contain small amounts of midchain ketones, with C_{33} midchain ketone (**XVII**; Fig. 2) being the most abundant homologue.

The polar fractions are dominated by hopanoids and *n*-alkanols (Table 1), with C_{28} *n*-alkanol being the most abundant *n*-alkanol present, and in the case of Sample TDP7A/54-1, 26–36 cm, triterpenoids. In the other two samples triterpenoids are present but in substantially smaller amounts. In addition, the samples contain only trace amounts of steroids, and neither the C_{15}/C_{15} diether nor archaeol is present.

The dominant acids in the three samples are *n*-alkanoic acids, with C_{28} *n*-alkanoic acid being most abundant in Sample TDP7A/54-1, 26–36 cm and C_{24} *n*-alkanoic acid being most abundant in the other two. In the case of Sample TDP7A/46-1, 30–40 cm, the ω-hydroxy alkanoic acids, especially C_{22} ω-hydroxy alkanoic acid, are also abundant. In the other samples, the ω-hydroxy alkanoic acids are present, but less abundant. In addition, all three samples contain substantial amounts of hopanoic acids and substantial to trace amounts of triterpenoic acids.

An additional sediment sample, Sample TDP7A/61-1, 65–79 cm, was analysed because it emitted a faint petroleum odour during recovery. The saturated hydrocarbon fraction of this sample has a very different composition compared to all the other saturated hydrocarbon fractions analysed from this site. It contains a relatively large Unresolved Complex Mixture (UCM; "hump"), typical of heavily biodegraded organic material, including petroleum (Magoon and Claypool, 1985; Gough and Rowland, 1990, 1991; Gough et al., 1992; van Dongen et al., 2003). In addition, the hopanes/hopenes and steranes have a thermally mature distribution distinct from the other samples analysed. This indicates the presence of biodegraded petroleum, which must have migrated from greater depths. The apolar fraction also contains substantial amounts of *n*-alkanes with an odd-over-even predominance, although this is less obvious than in other samples from the site. This indicates that besides the biodegraded petroleum, immature organic matter, probably associated with the original sediment deposition, is also present and abundant.

4.7.2. TDP Hole 7B

From this hole, only one sample (Sample TDP7B/50-1, 55–62 cm) was analysed. The saturated hydrocarbon fraction contains predominantly *n*-alkanes (with C_{29} *n*-alkane being the most abundant component), hopenes and hopanes and lesser amounts of steranes. However, the saturated hydrocarbon fraction contains neither des-*A*-triterpenes nor des-*E*-hopenes. The aromatic hydrocarbon fraction contains only small amounts of midchain ketones and no aromatic des-*A*-triterpenes or aromatic pentacyclic triterpenoids. The polar fraction contains predominantly triterpenoids (Table 1). In addition, the sample contains substantial amounts of *n*-alkanols (with the C_{28} *n*-alkanol being the most abundant), hopanoids and lesser amounts of steroids, but neither the C_{15}/C_{15} diether nor archaeol was detected. The acid fraction is generally dominated by *n*-alkanoic acids, with the C_{28} *n*-alkanoic acid being the most abundant *n*-alkanoic acid (Table 1). In addition, the sample contains substantial amounts of hopanoic acids, ω-hydroxy alkanoic acids (with C_{22} ω-hydroxy alkanoic acid being the most abundant) and lesser amounts of triterpenoic acids. The sample is similar to those studied from TDP Hole 7A.

4.8. Summary

The two holes at TDP Site 7 were drilled just 5 m apart and contain very similar sequences. Approximately the top 20 m consists of unconsolidated sands and gravels of probable Recent age, which overlies about 100 m of lowermost Eocene claystones and siltstones. The benthic and planktonic foraminifers from these claystones and siltstones indicate an open ocean environment in relatively deep water; the nannoplankton assemblages are typical of the outer shelf. The organic geochemistry is dominated by the remains of terrestrial vegetation, with subsidiary marine influences, and indicates a very low degree of thermal maturity. There are occasional subsidiary limestones horizons, which are interpreted as debris flow deposits, which introduced shelly debris from the inner shelf. The facies is very similar to that recovered in TDP Sites 3 (Pearson et al., 2004), 8 and 10 (see below).

The age assignment comes mainly from planktonic foraminifers and calcareous nannofossils, and is supported by benthic foraminifers and palynology. The bottom of TDP Hole 7B is evidently very close to the Paleocene/Eocene boundary but no unequivocally Paleocene sediments were recovered.

A single sample from a small fault zone that emitted an oily smell was confirmed as containing traces of thermally mature oil, which must have migrated from depth. Similar evidence for oil was found further down the Kilwa peninsula at TDP Site 3 (Pearson et al., 2004) and at TDP Site 10 (see below), underlining the hydrocarbon exploration potential of the area.

5. TDP Site 8: South-east of Singino hill

5.1. Site selection

TDP Site 8 was drilled in a field on the south-west side of the Nangurukuru–Kilwa Masoko road, about 5 km from the summit of Singino Hill (UTM 37L 548033, 9025811). The site was chosen because a small outcrop of lower Eocene sediments occurs in the drainage ditches beside the main road nearby. Only a short hole was drilled to obtain material from below the surface oxidation front and confirm the age of the sediment, thereby constraining the geological structure in the vicinity of Singino Hill. A summary stratigraphy is given in Fig. 7 and a table of core depths is given in Table 5.

5.2. Lithostratigraphy

This hole spudded-in on unconsolidated gravels, which were drilled to a depth of 4.95 m, at which point coring began. Core TDP8/1 consists of olive grey clay with streaks and mottles of light olive brown clay (5Y 4/1 to 5Y 5/6), containing a dispersed carbonate content throughout. This causes the clays to effervesce gently with weak hydrochloric acid. A thin fibrous calcite veining, or beef, also occurs in places. This lithology persists down to 8.2 m, where it changes color abruptly, losing the olive brown streaks. This level represents the oxidation front caused by recent subaerial weathering.

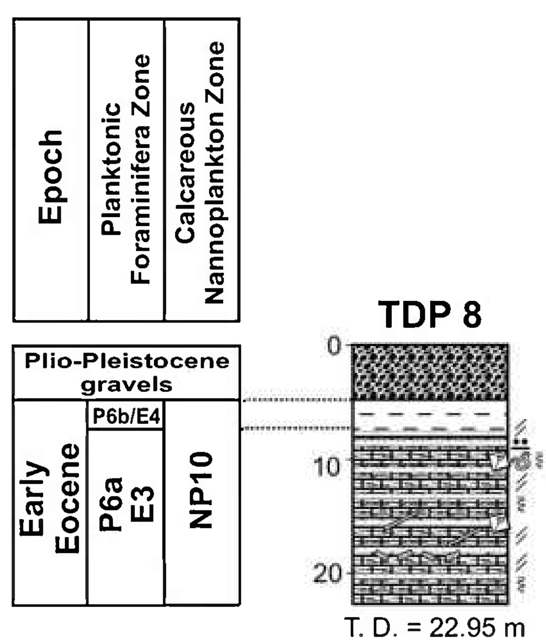

Fig. 7. Integrated litho- and biostratigraphy for TDP Site 8. Symbols as given in Fig. 5.

Table 5
Intervals drilled and cored in TDP Site 8 (south-east of Singino hill, UTM 37L 548033, 9025811)

Site	Core	Top (m)	Bottom (m)	Drilled	Recovered	Recovery (%)	Comment
TDP8/		0.00	4.95	4.95	0.00	0	Interval drilled
	1	4.95	6.45	1.50	0.63	42	1.5 m core barrel deployed
	2	6.45	7.95	1.50	1.97	131	Includes part of previous core
	3	7.95	9.45	1.50	1.45	97	
	4	9.45	10.95	1.50	1.57	105	
	5	10.95	12.45	1.50	1.29	86	
	6	12.45	13.95	1.50	1.70	113	
	7	13.95	15.45	1.50	1.05	70	
	8	15.45	16.95	1.50	1.63	109	
	9	16.95	18.45	1.50	1.47	98	
	10	18.45	19.95	1.50	1.55	103	
	11	19.95	21.45	1.50	1.33	89	
	12	21.45	22.95	1.50	1.23	82	
Total drilled: 22.95 m			Total recovered: 16.87 m			Recovery: 74%	

Table 6
Results of geochemical analyses of sediments from TDP Site 8

Sediments	Depth (m)	$CaCO_3$ (%)	Sulfur (%)	TOC (%)
TDP 8/2-1, 67–77 cm	7.12–7.22	0.7	0.1	0.2
TDP 8/5-1, 30–40 cm	11.25–11.35	1.5	0.3	0.3
TDP 8/9-1, 10–20 cm	17.05–17.15	11.7	0.1	0.7
TDP 8/11-1, 24–34 cm*	20.19–20.29	11.4	0.1	0.7

Sediment highlighted with an asterisk was selected for biomarker study (see Table 1).

Below this level, and for the remainder of the hole to its total depth of 22.95 m, the principal lithology is that of a dark greenish-grey (5GY 4/1) muddy claystone. As with the claystones in the upper third of Holes TDP7A and −7B, the carbonate component is subordinate to the clay and both are mixed to some degree with mud-sized particles. Thus, in these three holes, the principal lithology seems broadly similar. However, in TDP Site 8, the claystones also contain repetitive partings of dark greenish-grey (5G 4/1), very fine to fine quartz sand in clay throughout. These partings are only occasionally dispersed in the claystones at TDP Site 7. In core TDP8/3, two of these sand partings were observed to be normally graded and inclined at an angle of 18°. Soft sediment deformation was observed in the claystones at 10.05 m and 10.25 m. Bioturbation is reasonably common throughout the hole, in association with some pyrite infilling. Fragmented beef at a depth of 17.05 m in an interval of only mild drilling disturbance may indicate some fault movement in the claystones.

Geochemical results from four samples from this site are given in Table 6. Levels of $CaCO_3$ range from 0.7% to 11.7%, probably as a result of varying diagenetic cementation. Sulfur varies from 0.1% to 0.3% and TOC from 0.2% to 0.7%.

5.3. Planktonic foraminifers

Planktonic foraminifers are common throughout, but preservation varies widely between samples. Samples from Cores TDP8/1 and TDP8/2 (above the oxidation front) contain assemblages that have been influenced by meteoric water, and iron oxide coatings are common. Specimens from Cores TDP8/3-12 have suffered extensive infilling and pyritization. In several samples, the shells have been completely dissolved, leaving only a sparry calcite or micro-pyrite cast. Occasionally, however, preservation is good with high quality glassy preservation of shell calcite and no infilling.

Samples TDP8/1-1, 20–30 cm and TDP8/2-1, 77–86 cm contain the most diverse planktonic formainiferal assemblages. The calcite wall of many specimens in these samples have been slightly dissolved; however, gross shell morphologies are well preserved. These samples contain numerous morozovellids belonging to the *M. subbotinae* group, which are characteristic of lower Eocene pelagic, tropical environments. Most have four or five chambers in the final whorl (*M. aequa*, *M. subbotinae*, *M. marginodentata*, *M. gracilis*, with occasional specimens of *M. edgari*). Rare specimens with six chambers in the final whorl were recorded as *M. formosa*, indicating Biozone E4 (=P6b). Other age-diagnostic species present include *S. patagonica*, *S. hornibrooki*, *S.* cf. *patagonica*, *A. wilcoxensis*, *A. angulosa*, *Igorina lodoensis* and *Pseudohastigerina wilcoxensis*. Several biserial morphotypes are also present and are tentatively assigned to *Chiloguembelina crinita*, *C. wilcoxensis* and *C. trinitatensis*. In addition, the small sediment size fraction (65–150 μm) contains a few *G. chapmani* and possible *G. australiformis*.

Sample TDP8/3-1, 40–50 cm is composed of similar species to those found in Cores TDP8/1 and TDP8/2 but lacks *M. formosa*. All specimens are infilled with sparry calcite and many are represented only as solid calcitic casts. Morozovellids of the *M. subbotinae* group dominate in Cores TDP8/4 down to TDP8/12 and five-chambered *M. gracilis* are scarce. These samples are assigned to Biozone E3 (=P6a) in the absence of *M. formosa*. All samples are strongly affected by calcite infilling and pyrite formation except Sample TDP8-4-1, 30–40 cm, which contains excellently preserved specimens that are not infilled. However, the assemblage in this sample is low in diversity and individuals are smaller.

5.4. Calcareous nannofossils

Nine samples were studied from TDP Site 8 for nannofossils, and all but two yielded rare to common, diverse assemblages of good or moderate to good preservation. The assemblages are rich in rhabdoliths, holococcoliths (especially *Zygrhablithus*), pontosphaerids and pentaliths.

The presence of *C. dela*, *D. diastypus* (Plate 3(7–8)) together with *R. cuspis* and *R. bramlettei*, indicate Zone NP10. The absence of *Tribrachiatus* spp. indicates a level within the lower part of the zone. The assemblages are similar to those of TDP Site 7, but represent a slightly higher stratigraphical interval, as indicated by the absence of *Fasciculithus* spp. and *D. falcatus*, and the consistent presence of *D. binodosus*. In addition, *Zeugrhabdotus sigmoides*, *S. anarrhopus* and *Ellipsolithus distichus* are found in the lowermost samples only, and *D. mahmoudii* is absent. Interestingly, the 'background' *Toweius* assemblage also differs between the two sites; both have frequent to common *T. pertusus* but TDP Site 8 also has consistent, frequent to common *T. callosus*, but lacks *T. eminens* and *T. occultatus*. The stratigraphic level is apparently lower than that drilled at TDP Site 3, which yielded *T. orthostylus* (Pearson et al., 2004).

The following additonal taxa from this site are illustrated: *Blackites morionum* (Plate 2(6)), *N. junctus* (Plate 2(10)) and *C. bidens* (Plate 2(21)). Two new species have been described from this hole, namely *Umbilicosphaera jordanii* (Bown, 2005, p. 29) and *Micrantholithus breviradiatus* (Bown, 2005, pp. 42–43).

5.5. Benthic foraminifers

Thirteen core samples were analysed from this borehole for benthic foraminifers. Most samples were only moderately to poorly preserved but preservation was found to be good in Cores TDP8/10 through TDP8/12. However, even at these depths, some of the specimens exhibit pyrite or calcite infilling. Microgastropods, ostracods and mica are also present.

Forty-one genera of benthic foraminifers have been identified. These include long- as well as short-ranging species of *B. semicostata*, *C. eocaenus*, *B. callahani*, *Loxostomoides applinae*, *B. trinitatensis*, *Vaginulinopsis decorata*, *N. latejugata*, *Quinqueloculina contorta*, *Dentalina communis*, *R. epigona*, *Hoeglundina elegans*, *Clavulinoides subparisiensis* and *Stilostomella nuttalli*. Other specimens were identified to genus level including *Chilostomella* sp., *Dentalina* sp., *Melonis* sp., *Bulimina* sp., *Lenticulina* sp., *Saracenaria* sp., *Planulina* sp., *Trochammina* sp., *Clavulinopsis* sp., *Ammobaculites* sp., *Astacolus* sp., *Pleurostomella* sp., *Lagena* sp., *Nonion* sp., *Anomalinoides* sp., *Dorothia* sp., *Marginulinopsis* sp., *Eponides* sp., *Gyroidina* sp., *Clavulinoides* sp., *Pararotalia* sp., *Lagenaglandulina* sp., *Rectuvigerina* sp., *Cibicidoides* sp., and *Pseudonodosaria* sp.

Species with last appearances in the early Eocene, and others that are locally restricted to that interval, include *Textularia plummerae*, *Stilostomella midwayensis*, *Osangularia plummerae*, *Uvigerina batjesi*, *H. ammophila*, *Alabamina obtusa*, *Anomalinoides aragonensis*, *M. wetherellii*, *Pullenia quinqueloba*, *Glandulina laevigata*, *G. inaequalis* and *H. producta*.

5.6. Palynology

Seven samples from TDP Site 8 were studied for dinocysts and miospores. Samples are rich in undiagnostic organic particles, which include plant tissues, cuticles and armophous organic matter, except for Sample TDP8/2-1, 86–89 cm, which contains fairly abundant and well-preserved palynomorphs. In this sample, miospores are common while dinocysts are rare.

Lower Eocene dinocyst species documented from this site include *Dracodinium condylos, Polysphaeridium subtile* (Plate 6(12)), *Homotryblium tenuispinosum*, *Deflandrea truncata* (Plate 6(11)), *D. robusta*, *D. convexa* and *F. bipolaris*.

5.7. Organic geochemistry

Sample TDP8/11-1, 24–34 cm was selected for organic geochemical analysis. It was found that the saturated hydrocarbon fraction contains predominantly *n*-alkanes (with C_{29} *n*-alkane being the most abundant component), hopenes and hopanes and lesser amounts of steranes. However, the saturated hydrocarbon fraction contains only trace abundances of des-*A*-triterpenes and des-*E*-hopenes. The aromatic hydrocarbon fraction contains relatively small amounts of aromatic des-*A*-triterpenes and midchain ketones and no aromatic pentacyclic triterpenoids. The polar fraction contains predominantly hopanoids and triterpenoids (Table 1). In addition, the samples contain minor amounts of *n*-alkanols (with the C_{28} *n*-alkanol being the most abundant) but neither the C_{15}/C_{15} diether nor archaeol was detected. The acid distribution revealed predominantly hopanoic acids (with 7β(H),21β(H)-bishomohopanoic acid (**XVI**; Fig. 2) being the most abundant) and *n*-alkanoic acids (with C_{24} *n*-alkanoic acid being the most abundant; Table 1). In addition, the sample contains substantial amounts of ω-hydroxy alkanoic acids (with C_{22} ω-hydroxy alkanoic acid being the most abundant) and triterpenoic acids.

5.8. Summary

This site belongs to the same Paleocene–lower Eocene claystone formation drilled in TDP Sites 3 (Pearson et al., 2004), 7 (see above) and 10 (see below). Despite the fact that the microfossil preservation is generally not as good as in the other sites, it is useful in establishing their respective stratigraphic positions.

The topmost part of the claystones is from a higher stratigraphic level than any drilled at TDP Site 7, because it is assigned to planktonic foraminifer Zone E4; however the majority of the site, which is assigned to planktonic foraminifer Zone E3 and nannofossil Zone NP10, may overlap stratigraphically with the upper claystones drilled at TDP Site 7. The claystones at TDP Site 8 are, however, slightly older than those drilled at TDP Site 3, as indicated by the nannofossil biostratigraphy. The presence of the planktonic foraminifer Zone E3/4 (=P6a/b) subzone boundary in this site, falling as expected (Berggren et al., 1995) within nannofossil Zone NP10, indicates that the tentative assignment of some of the sediments at TDP Site 3 to planktonic foraminifer Subzone P6a (Pearson et al., 2004, p. 51) was probably an error because of poor preservation.

The sedimentary facies and benthic foraminiferal assemblages indicate a similar depositional environment to that inferred for TDP Sites 3, 7 and 10, namely a deep water outer shelf to slope setting.

6. TDP Site 9: Nangurukuru

6.1. Site selection

A patch of level ground near the road junction at Nangurukuru (UTM 32L 538987 9027049) afforded a good opportunity to recover some of the locally exposed Maastrichtian clay formation from below the level of surface oxidation, assess it for foraminifer preservation, and investigate its stratigraphic thickness. The ground surface at the drill site is littered with the broken shells of inoceramid bivalves, which form an interesting marker horizon within the Maastrichtian in the area (Kent et al., 1971). The upper Cretaceous sediments in the Kilwa area were described from roadside outcrop investigations by Ernst and Zander (1993) and Schlüter (1997), but had not previously been obtained in cores. A summary stratigraphy is given in Fig. 8 and a list of core depths in Table 7.

6.2. Lithostratigraphy

Unconsolidated sands and gravels were drilled until coring began at 4.6 m. From 4.6 m to 9.45 m, the principal lithology is a light olive grey to olive grey (5Y 6/1 to 5Y 4/1) carbonate-rich clay. This is streaked and mottled with light brown to dark yellowish-orange (5YR 5/6 to 10YR 6/6) clay. Fibrous calcite veining (beef) was also observed. However, some of the fibrous calcite appeared to be broken into fragments within this interval. During our previous field surveys in the vicinity of this site, large inoceramids had been found weathering out at the surface and it is highly likely that these upper few meters of TDP Site 9 contain a mixture of both inoceramids and beef. The light color and yellowish-orange mottling is a universal feature of oxidized, weathered surfaces of the claystones in this area.

From 9.45 m to the base of the hole at 88.8 m, the principal lithology is a dark greenish-grey (5G 4/1 to 5GY 4/1) silty claystone to clayey siltstone, similar to that recorded in

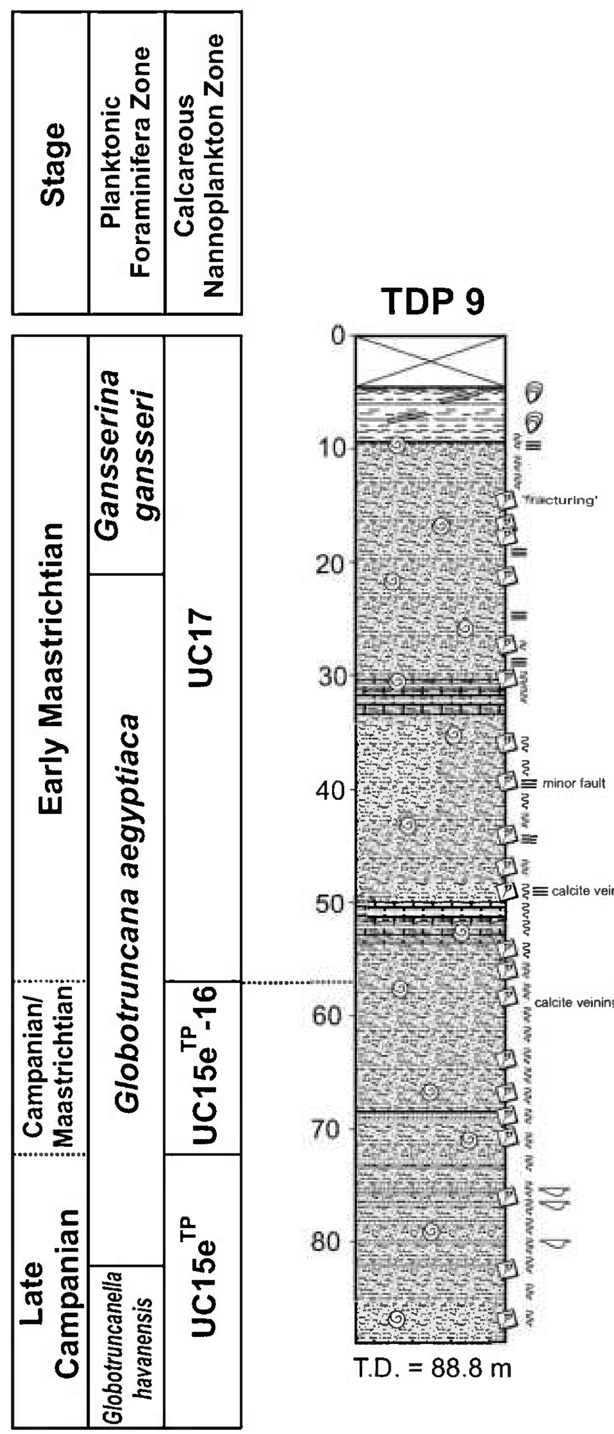

Fig. 8. Integrated litho- and biostratigraphy for TDP Site 9. Symbols as given in Fig. 5.

Table 7
Intervals drilled and cored in TDP Site 9 (Nangurukuru, UTM 37L 538987, 9027049)

Site	Core	Top (m)	Bottom (m)	Drilled	Recovered	Recovery (%)	Comment
TDP9/		0.00	4.60	4.60	0.00	0	Interval drilled
	1	4.60	4.95	0.35	0.35	100	1.5 m core barrel; short core
	2	4.95	6.45	1.50	0.90	60	Poor recovery
	3	6.45	7.95	1.50	1.82	121	Includes part of previous core
	4	7.95	9.45	1.50	1.50	100	
	5	9.45	10.95	1.50	1.24	83	
	6	10.95	12.45	1.50	1.59	106	
	7	12.45	13.95	1.50	1.46	97	
	8	13.95	15.45	1.50	1.72	115	
	9	15.45	16.95	1.50	1.72	115	
	10	16.95	18.45	1.50	1.38	92	
	11	18.45	19.95	1.50	1.80	120	
	12	19.95	22.95	3.00	3.12	104	3 m core barrel deployed
	13	22.95	25.95	3.00	2.07	69	
	14	25.95	27.45	1.50	1.36	91	1.5 m core barrel deployed
	15	27.45	28.95	1.50	1.43	95	
	16	28.95	30.45	1.50	1.57	105	
	17	30.45	31.95	1.50	1.60	107	
	18	31.95	33.45	1.50	1.39	93	
	19	33.45	34.95	1.50	0.94	63	
	20	34.95	36.45	1.50	2.17	145	Includes part of previous core
	21	36.45	37.95	1.50	1.48	99	
	22	37.95	39.45	1.50	1.52	101	
	23	39.45	40.95	1.50	1.43	95	
	24	40.95	44.45	3.50	3.25	93	3 m core barrel deployed
	25	44.45	45.45	1.00	1.25	125	1.5 m core barrel deployed
	26	45.45	46.95	1.50	0.95	63	
	27	46.95	48.05	1.10	0.74	67	
	28	48.05	49.95	1.90	2.47	130	3 m core barrel deployed
	29	49.95	51.95	2.00	0.97	48	Poor recovery
	30	51.95	52.95	1.00	1.15	115	
	31	52.95	55.25	2.30	2.09	91	
	32	55.25	55.95	0.70	1.07	153	Includes part of previous core
	33	55.95	57.00	1.05	0.83	79	
	34	57.00	57.50	0.50	0.50	100	Short core
	35	57.50	58.80	1.30	1.33	102	
	36	58.80	60.60	1.80	1.85	103	
	37	60.60	61.80	1.20	1.28	107	
	38	61.80	64.40	2.60	2.61	100	
	39	64.40	66.30	1.90	1.88	99	
	40	66.30	67.80	1.50	1.67	111	
	41	67.80	70.80	3.00	2.47	82	
	42	70.80	72.70	1.90	2.46	129	Includes part of previous core
	43	72.70	73.80	1.10	0.62	56	
	44	73.80	75.80	2.00	1.40	70	
	45	75.80	76.80	1.00	1.96	196	Includes part of previous cores
	46	76.80	79.80	3.00	2.98	99	
	47	79.80	82.80	3.00	2.91	97	
	48	82.80	85.80	3.00	2.91	97	
	49	85.80	88.80	3.00	2.22	74	
Total drilled: 88.80 m			Total recovered: 82.66 m			Recovery: 93%	

the lower two-thirds of TDP Site 7. This dominant lithology is punctuated from 30.9 m to 33.9 m and between 50.0 m and 52.95 m by a waxy-lustred, friable, dark greenish-grey (5GY 4/1) claystone, similar to that which comprises most of TDP Site 8 and the upper third of TDP Site 7.

Bioturbation is common throughout TDP Site 9. However, it becomes common to abundant in the clayey siltstones below about 30 m and there is a corresponding increase in the amount of pyrite observed infilling these burrows.

Whilst the dominant lithology is relatively uniform in TDP Site 9 between 9.45 m and the base of the hole at 88.8 m, there is an important change in secondary lithologies which occurs below 68.5 m (from Core TDP9/41 downwards). In this basal 20.3 m, there is a series of thin (typically 5–20 cm thick), fine to very fine, carbonate-cemented quartz sandstone beds. In previous TDP holes, the presence of coarser, sandy sediment was always present as partings or horizons with indistinct upper and basal sur-

Table 8
Results of geochemical analyses of sediments from TDP Site 9

Sediments	Depth (m)	$CaCO_3$ (%)	Sulfur (%)	TOC (%)
TDP 9/3-1, 99 cm to TDP 9/3-2, 10 cm	7.44–7.55	5.9	0.1	0.4
TDP 9/6-1, 6–15 cm	11.01–11.10	10.4	0.1	0.7
TDP 9/9-1, 32–44 cm	15.77–15.87	13.1	0.04	0.9
TDP 9/15-1, 31–41 cm	27.76–27.86	21.7	0.1	0.7
TDP 9/18-1, 20–30 cm	32.15–32.25	9.2	0.1	0.4
TDP 9/24-1, 53–62 cm	41.48–41.57	18.5	0.04	0.2
TDP 9/28-3, 10–20 cm*	50.15–50.25	11.4	0.1	0.6
TDP 9/31-1, 52–62 cm	53.47–53.57	9.8	0.1	0.8
TDP 9/40-1, 46–60 cm	66.76–66.90	9.9	0.1	0.7
TDP 9/44-1, 15–30 cm	73.95–74.10	4.8	0.1	0.7
TDP 9/49-2, 62–78 cm	87.42–87.58	9.1	0.03	1.1

Sediment highlighted with an asterisk was selected for biomarker study (see Table 1).

faces. However, the sandstone beds present in Core TDP9/41 and below are characteristic in having sharp bounding surfaces, often irregular and uneven. These sandstones are highly bioturbated, which appears to be the cause of the uneven bedding planes. Bioturbation takes the form of both grazing trails and vertical burrows and can be assigned to the *Nereites* ichnofacies described in roadside exposures nearby by Gierlowski-Kordesch and Ernst (1987) and Ernst and Zander (1993). The lower bedding surfaces of these sands also frequently bare flutes, prod marks and load casts. These are particularly well developed in Cores TDP9/45 to TDP9/47 (from 75.8 m to 82.8 m). No normal grading or characteristic Bouma sequences were observed in these beds, possibly due to subsequent disturbance from bioturbation. However, it is likely that these sandstones were deposited from repetitive, pulsing turbulent currents, either storm induced or from syn-depositional slumping.

Geochemical results from eleven samples from TDP Site 9 are presented in Table 8. The $CaCO_3$ content varies from 4.8% to 21.7%, possibly as a result of differing degrees of diagenetic cementation. Sulfur contents are all low (0.1% or less), which seems to differentiate this site from all other TDP sites drilled to date (including TDP Site 5, from near Lindi, which is of a similar age), which commonly have values up to and exceeding 0.5%. TOC values range from 0.2% to 1.1%.

6.3. Planktonic foraminifers

TDP Site 9 contains Late Cretaceous age sediments that can be assigned to the upper Campanian–middle Maastrichtian based on planktonic foraminifer indicator species. Foraminifers are common to abundant, and preservation is moderate in all samples studied, with test infilling and shell recrystallization found in most calcareous specimens. The assemblages are dominated by benthic foraminifers in most upper Campanian samples, with some samples containing as many as 90% benthic specimens. Planktonic foraminifers dominate most Maastrichtian samples, with planktonic percentages reaching up to 75%. In counts of agglutinated versus calcareous benthic foraminifer populations, agglutinated species dominate most of the Campanian samples, with some samples containing up to 76% agglutinated specimens, but most Maastrichtian samples contain 50% or fewer agglutinated specimens.

The planktonic foraminifer assemblages are diverse and typical of tropical/subtropical open ocean settings. Throughout the Upper Cretaceous sequence, they are characterized by abundant globotruncanids, including *G. arca*, *G. austinensis*, *G. bulloides*, *G. esnehensis*, *G. linneiana*, *G. stuartiformis*, *G. ventricosa*, *Contusotruncana patelliformis*, *Rugoglobigerina rugosa*, and *R. subpennyi*. Heterohelicids include common to abundant *Heterohelix globulosa*, *H. rajagopalani*, *Laeviheterohelix dentata*, *P. costulata*, *P. elegans*, and *P. nuttalli*.

Three planktonic foraminifer zones are identified in the Cretaceous sequence. Samples TDP9/2/1, 5–25 cm and Sample TDP9/11-1, 37–59 cm both contain *G. gansseri*, the nominate species of the *G. gansseri* Zone, and thus are assigned to that zone. Samples below this, down to Sample TDP9/47-2, 30–45 cm lack *G. gansseri* and mostly contain *G. aegyptiaca*, the nominate species of the *G. aegyptiaca* Zone, and hence are assigned to that zone. The next sample examined was Sample TDP9/49/2, 31–47 cm, which assigned to the *G. havanensis* biozone on the absence of *G. aegyptiaca*. Note however that the nominate species for these zones are rare and sporadic in their stratigraphic occurrence, and thus placement of the zonal boundaries is not based on a high degree of certainty. The FOs of *P. excolata* and *Planomalina multicamerata* in the lower *G. aegyptiaca* Zone are consistent with their distribution at other open ocean sites (e.g., Nederbragt, 1991). Absence of *R. fructicosa*, *C. contusa*, and *A. mayaroensis* from the uppermost cores of the sequence indicates that the middle and upper Maastrichtian are absent at this site. Occurrence of abundant inoceramid bivalves on the sediment surface at the drill site also indicates that the sediments must predate the middle Maastrichtian, as the extinction of this group has been recorded between 68.6 and 70 Ma (MacLeod et al., 1996; Frank et al., 2005).

6.4. Calcareous nannofossils

There is a discrepancy between Burnett (1998) and Gardin et al. (2001), concerning the positioning of the

Campanian/Maastrichtian stage boundary with respect to nannofossil events; in the summary figure (Fig. 8) the boundary according to Burnett (1998) is shown. As in TDP Site 5 (Pearson et al., 2004), TDP Site 9 ranges from lower Maastrichtian to upper Campanian (UC17-15e^{TP}), although at this site, Zone UC17 is more expanded.

Sixty-one samples were analysed through the core, all of which were productive. Nannofossil preservation was generally moderate to moderate–good throughout, with the nannofossils showing only slight etching. The abundance of nannofossils to background sediment was moderate to moderate–high, nannofossils being one of the major components of the sediments.

The presence at the top of the site (Sample TDP9/1-1, 19 cm) of *Tranolithus orionatus* (Plate 3(27)) and *Cribrocorona echinus* (Plate 3(31–33)) indicates an age assignment no younger than Zone UC17 (uppermost Campanian–lower Maastrichtian, according to Burnett, 1998). This biozone is confirmed by the FO of *C. echinus* in Sample TDP9/19-1, 30 cm and the LO of *Uniplanarius trifidus* (Plate 3(34)) in Sample TDP9/29-1, 99 cm. Note that the range of *C. echinus* has recently been constrained by Lees and Bown (2005) in sediments of similar age from the Shatsky Rise (NW Pacific Ocean).

Identification of the bases of UC17 and UC16 is problematic. The base of UC17 has herein been estimated as lying at or around Sample TDP9/34-1, 25 cm. The marker-taxon, *Broinsonia parca constricta* (Plate 3(30)), appears to range above this level, but there is a possibility that these are reworked specimens; some of them have lost their central plates and the rims appear paler (thinner) than usually observed, which might be consistent with them having been exposed for longer to mechanical and/or chemical depositional effects. Also, *B. parca constricta* was not found in the three samples above this level (Samples TDP9/33-1, 56 cm, 32-1, 74 cm and 31-2, 62 cm, equivalent to about 3 m), and the LO of *B. parca parca* (the ancestral form of *B. parca constricta*, which commonly has its LO immediately below the LO of *B. parca constricta*), lies in the sample below (Sample TDP9/35-1, 65 cm). The LO of *U. trifidus* also somewhat constrains the positioning of the base of UC17. The base of UC16 is marked by the LO of *E. eximius*, but this species does not seem to occur in this region (as previously remarked on in Pearson et al., 2004).

The basal sample (Sample TDP9/49-2, 62 cm) contains *E. parallelus* (and *U. trifidus*), thus falls into UC15e^{TP} (upper Campanian). The FO of *Cylindralithus*? *nieliae* in Sample TDP9/42-1, 65 cm confirms that biozone.

Other species figured from this site are *Zeugrhabdotus bicrescenticus* (Plate 3(26)), *Cribrosphaerella ehrenbergii* (Plate 3(28)), *Arkhangelskiella cymbiformis* (Plate 3(29)) and *Uniplanarius sissinghii* (Plate 3(35)). New species, among others, of *Ceratolithoides*, *Chiastozygus*, *Cylindralithus*, *Gartnerago*, *Prediscosphaera*, *Rhagodiscus*, along with one new nannolith genus and three <3 μm-long coccoliths of indeterminate genus, have been identified in TDP Site 9, and will form the basis of a future taxonomic and extended biostratigraphic paper.

6.5. Benthic foraminifers

Forty samples were examined for benthic foraminifers from TDP Site 9. In the Campanian succession, benthic foraminifers are generally more common than planktonic foraminifers although the reverse is true for most of the Maastrichtian. Preservation of foraminifer tests is generally moderate to good, but calcite infilling is common. All of the benthic assemblages are indicative of upper slope, dysoxic, quiet water, fine-grained clay sedimentation. There are no benthic species which can be interpreted as having derived from the shoreline or shelf top.

Benthic assemblages are dominated by a few agglutinated species of *Bathysiphon* and *Ammodiscus* (including *A. cretaceus*; Plate 5(12)), occurring in large numbers, with small numbers of *Tritaxia* (Plate 5(26, 27)), *Glomospira*, *Hormosina* including *H. excelsa* (Plate 5(6)) and *H. velascoensis* (Plate 5(7)), *Ammobaculites*, *Hyperammina* (Plate 5(30)) and *Haplophragmoides*. In addition, the less common calcareous benthic species include *Bolivinoides draco draco* (Plate 5(2)), *B. draco miliaris* (Plate 5(3)), *Lagena striata* (Plate 4(23)), *G. girardana* (Plate 5(17, 18)), *Anomalinoides aotea* (Plate 5(22)), *Matanzia* sp. (Plate 5(1)), *Praebulimina* sp. (Plate 5(4)), *Neoflabellina* sp. (Plate 5(5)), *Gavelinella danica*, *G. costulata* (Plate 5(16)), *G. beccariiformis* (Plate 5(15)), *Repmanina charoides* (Plate 5(25)), and species of *Aragonia*, *Pullenia* (Plate 4(18)), *Trochammina* (Plate 5(8–10)), *Lobatula* (Plate 4(19, 20)), *Pleurostomella* (Plate 5(29)), *Pullenia* (Plate 5(23, 24)), *Haplophragmoides* (Plate 5(11)), *Osangularia* (Plate 5(21)) and *Nuttallides*.

6.6. Palynology

Sixteen samples were studied for palynology from TDP Site 9. Some samples contain common miospores or dinocysts or both, others have rare miospores or dinocysts or both. Cavate/proximate dinocysts are common, while miospores are generally rare in most of the samples. Samples yielded typical upper Cretaceous (probably Maastrichtian) dinocyst species. The significant diagnostic taxa documented from the samples include: *Dinogymnium deflandrei*, *Deflandrea* spp. (Plate 6(1)) including *D. leptodemata*, *Trichodinium bifurcatum*, *Ceratodynium granulostriata*, *C. granulatum* (Plate 6(13)), *Dinogymnium avellana* (Plate 6(14)), *Paleocystodinium* spp. (Plate 6(2)) including *P. gabonensis*, *P. golzowense* and *P. lidiae*, *Andalusiella polymorpha* and *Alterbidinium montanaense* (Plate 6(20)). Other more long-ranging species include *Callaiosphaeridium asymmetrica*, *Chatangiella ditissima*, *C. senegalensis*, *D. undulosum*, *D. longicornis*, *D. cretaceum* and *Isabelidinium cooksoniae*.

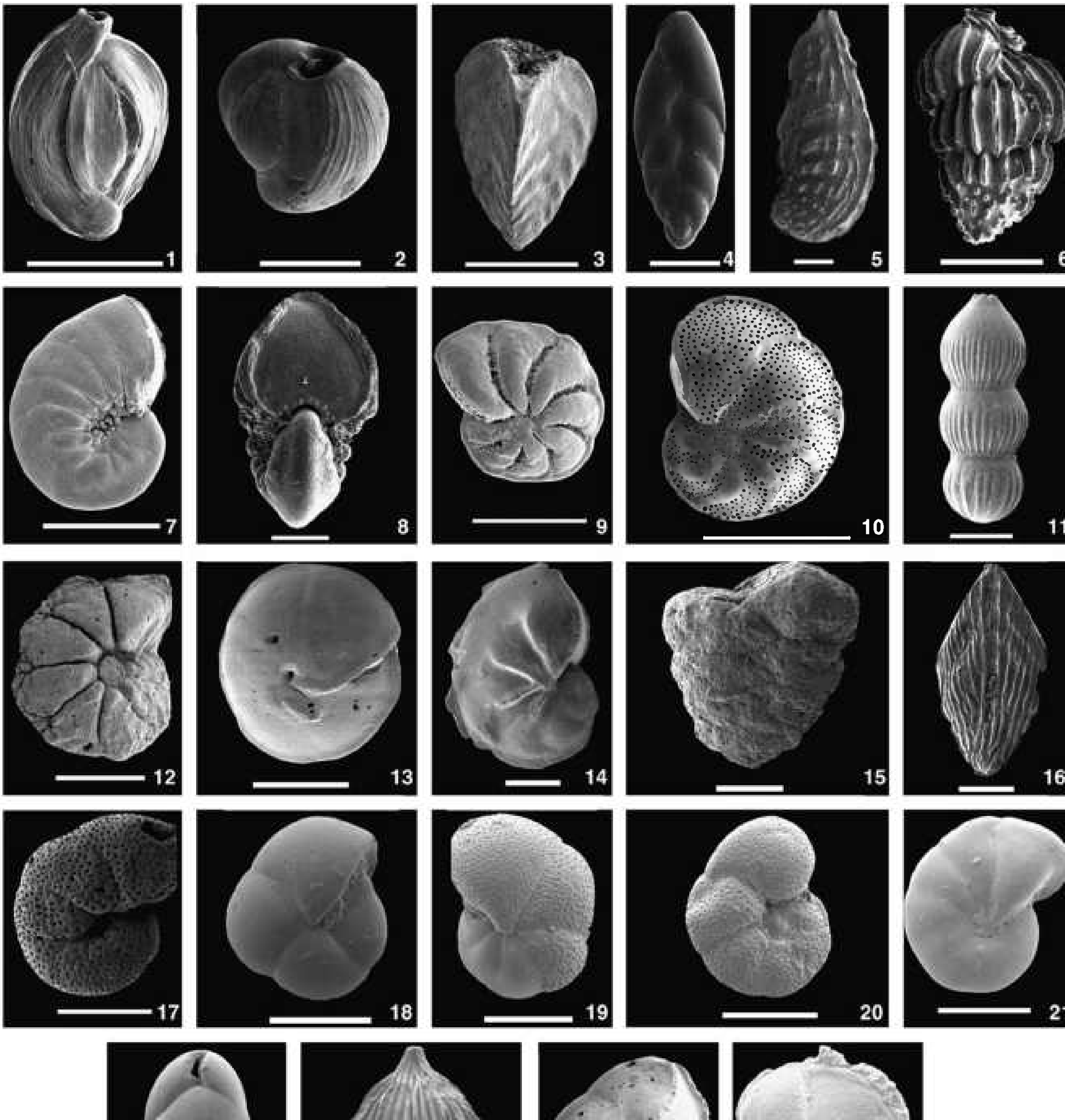

Plate 4. Selected benthic foraminifers from TDP Sites 6–10. Scale bars = 200 μm. (1) *Cycloforina gracilis*, Sample TDP6/7-1, 64–74 cm; (2) *Triloculina austriaca*, Sample TDP6/7-1, 64–74 cm; (3) *Reussella* sp., Sample TDP6/7-1, 64–74 cm; (4) *Fursenkoina schreibersiana*, Sample TDP6/5-1, 40–50 cm; (5) *Vaginulinopsis* sp., Sample TDP6/7-2, 40–50 cm; (6) *Uvigerina* cf. *havanensis*, Sample TDP6/5-1, 40–50 cm; (7) *Nonion* sp., Sample TDP9/36-1, 61–76 cm; (8) *Nonion gulincki*, Sample TDP6/4-1, 40–50 cm; (9) *Toddinella* sp., Sample TDP6/3-1, 32–42 cm; (10) *Hanzawaia isidroensis*, Sample TDP6/7-2, 40–50 cm; (11) *Nodosaria* sp., Sample TDP10/10-2, 10–20 cm; (12) *Pararotalia mexicana*, Sample TDP6/5-1, 40–50 cm; (13) *Oridorsalis* sp., Sample TDP6/5-1, 40–50 cm; (14) *Lenticulina* cf. *pseudomamilligera*, Sample TDP10/10-2, 10–20 cm; (15) *Siphotextularia* sp., Sample TDP10/10-2, 10–20 cm; (16) *Plectofrondicularia* sp., Sample TDP10/10-2, 10–20 cm; (17) *Anomalinoides* sp., Sample TDP10/10-2, 10–20 cm; (18) *Pullenia* sp., Sample TDP9/36-1, 61–76 cm; (19) *Lobatula* sp., Sample TDP9/36-1, 61–76 cm; (20) *Lobatula* sp., Sample TDP9/36-1, 61–76 cm; (21) ? *Valvalabamina* sp., Sample TDP6/5-1, 40–50 vm; (22) *Globulimina* sp., Sample TDP10/10-2, 10–20 cm; (23) *Lagena striata*, Sample TDP9/36-1, 61–76 cm; (24) *Asterigerina* sp. aff. *subacuta*, Sample TDP6/5-1, 40–50 cm; (25) *Oridorsalis lotus*, Sample TDP10/2-1, 10–20 cm.

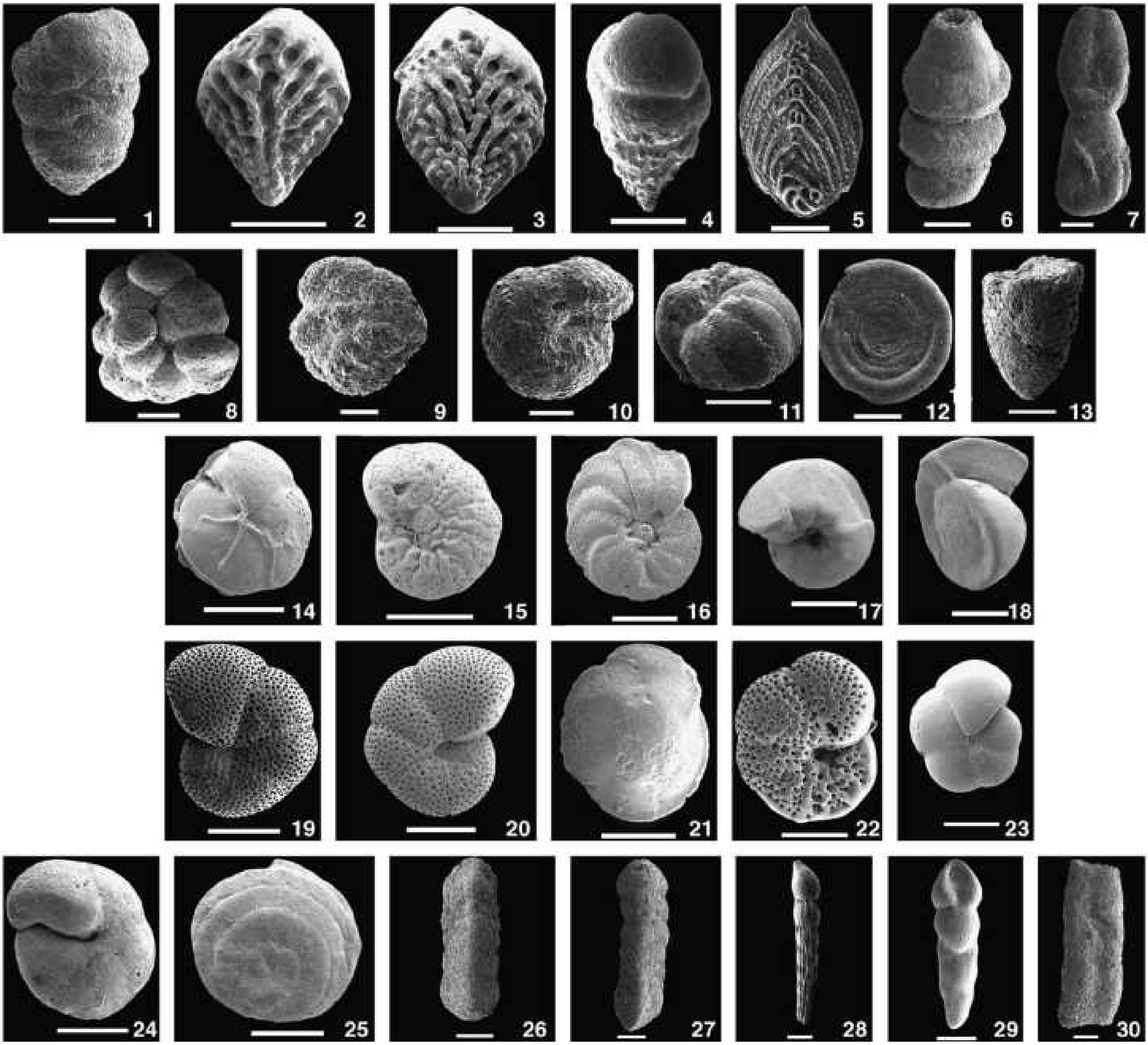

Plate 5. Selected benthic foraminifers from TDP Sites 6–10. Scale bars = 200 μm. (1) *Matanzia* sp., Sample TDP9/36-1, 61–76 cm; (2) *Bolivinoides draco draco*, Sample TDP9/22-1, 75–85 cm; (3) *Bolivinoides draco miliaris*, Sample TDP9/22-1, 75–85 cm; (4) *Praebulimina* sp., Sample TDP9/6-1, 0–6 cm; (5) *Neoflabellina* sp., Sample TDP9/2-1, 25–29 cm; (6) *Hormosina excelsa*, Sample TDP9/36-1, 61–76 cm; (7) *Hormosina velascoensis*, Sample TDP9/59-1, 85–95 cm; (8) *Trochammina* sp., Sample TDP9/6-1, 0–6 cm; (9) *Trochammina* sp., Sample TDP9/36-1, 61–76 cm; (10) *Trochammina* sp., Sample TDP9/36-1, 61–76 cm; (11) *Haplophragmoides* sp., Sample TDP9/22-1, 75–85 cm; (12) *Ammodiscus cretaceus*, Sample TDP9/6-1, 0–6 cm; (13) *Dorothia* sp., Sample TDP7A/20-1, 10–14 cm; (14) *Gyroidinoides* sp., Sample TDP9/59-1, 85–95 cm; (15) *Gavelinella beccariiformis*, Sample TDP9/2-1, 25–29 cm; (16) *Gavelinella costulata*, Sample TDP9/2-1, 25–29 cm; (17, 18) *Gyroidinoides girardana*, Sample TDP9/6-1, 0–6 cm; (19, 20) *Anomalinoides* sp., Sample TDP7B/52-1, 80–85 cm; (21) *Osangularia* sp., Sample TDP9/6-1, 0–6 cm; (22) *Anomalinoides aotea*, Sample TDP9/59-1, 85–95 cm; (23) *Pullenia* sp., Sample TDP7A/20-1, 15–19 cm; (24) *Gyroidinoides* sp., Sample TDP9/4-1, 61–64 cm; (25) *Repmanina charoides*, Sample TDP9/4-1, 61–64 cm; (26) *Tritaxia* sp., Sample TDP9/36-1, 61–79 cm; (27) *Tritaxia gaultina*, Sample TDP9/36-1, 61–79 cm; (28) *Nodosaria* sp., Sample TDP7A/20-1, 20–29 cm; (29) *Pleurostomella* sp., Sample TDP9/36-1, 61–79 cm; (30) *Hyperammina* sp., Sample TDP9/59-1, 85–95 cm.

6.7. Organic geochemistry

One sample (Sample TDP9/28-3, 10–20 cm) was selected for organic geochemical analysis. The saturated hydrocarbon fraction contains predominantly *n*-alkanes (with C_{31} *n*-alkane being the most abundant component) and low abundances of hopenes, hopanes and steranes. However, the saturated hydrocarbon fraction contains neither des-*A*-triterpenes nor des-*E*-hopenes. The aromatic hydrocarbon fraction contains relatively small amounts of aromatic des-*A*-triterpenes and midchain ketones and no aromatic pentacyclic triterpenoids. The polar fraction contains pre-

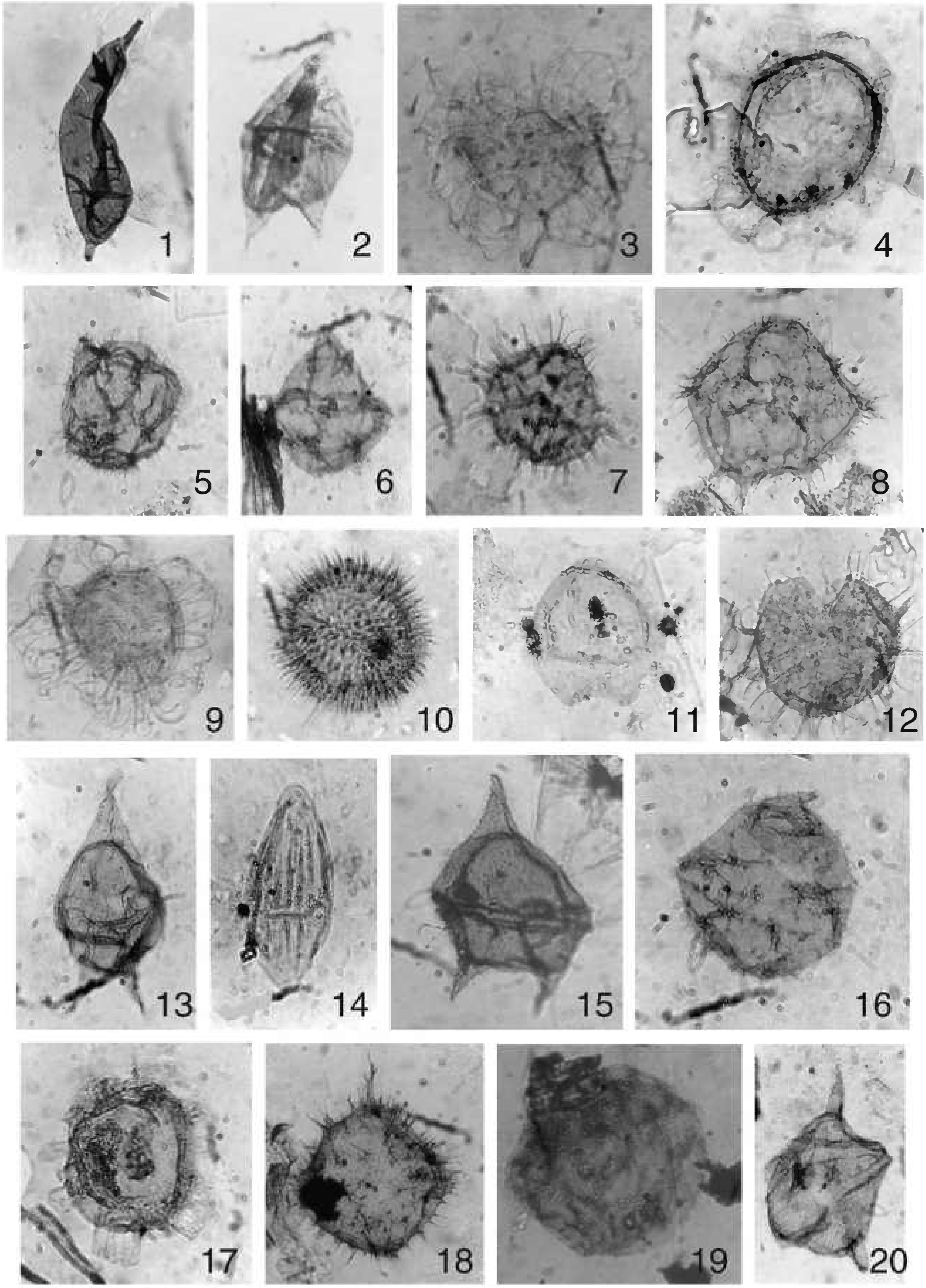
1
2
3
4
5
6
7
8
9
10
11
12
13
14
15
16
17
18
19
20

dominantly *n*-alkanols (Table 1; with C_{28} *n*-alkanol being the most abundant). In addition, the samples contain substantial amounts of hopanoids and minor amounts of steroids but neither the C_{15}/C_{15} diether nor archaeol was detected. The acid distribution of acids in the sample of TDP 9 revealed predominantly hopanoic acids (with 7β(H),21β(H)-bishomohopanoic acid (**XVI**; Fig. 2) being the most abundant) and *n*-alkanoic acids (with the C_{24} *n*-alkanoic acid being the most abundant; Table 1). In addition, the sample contains substantial amounts of ω-hydroxy alkanoic acids (with C_{22} ω-hydroxy alkanoic acid being the most abundant) and lesser amounts of triterpenoic acids.

6.8. Summary

The dominant lithology in TDP Site 9 is dark greenish-grey silty claystone. Preservation of foraminifers is generally affected by diagenetic infilling of the tests by calcite crystals, although the shell walls themselves are often well preserved. The foraminiferal assemblages, including the common agglutinated foraminifers and nodosarids, suggest an outer shelf environment in relatively deep water. This interpretation is supported by the presence of thin sandstones in the lower third of the hole containing *Nererites* ichofacies trace fossils. However, on the narrow Tanzanian shelf the paleo-shoreline may not have been too far distant (Kent et al., 1971) so abundant terrestrial biomarkers are also present.

The nannofossil biostratigraphy, supported by foraminifers and dinocysts, indicates that the site spans the Campanian/Maastrichtian stage boundary, as did TDP Site 5 which was previously drilled near Lindi further to the south of the country (Pearson et al., 2004).

7. TDP Site 10: West of Singino Hill

7.1. Site selection

A series of minor roadside exposures occurs along the road between Nangurukuru junction and Singino Hill. Travelling east from Nangurukuru, they are initially Maastrichtian in age, as at TDP Site 9, but abruptly change to Paleocene in the vicinity of the TDP Site 10 drill site. The Cretaceous/Paleogene boundary along the road is most likely to be faulted as the Paleocene lies topographically lower than the Cretaceous, although both have nearly horizontal dips. Evidence of faulting can be observed in a roadside quarry between the two TDP sites. TDP Site 9 was located in a field beside the main road (UTM 37L 0541243 9028791) to recover Paleocene sediments for the first time from this area, and investigate whether their stratigraphic contact with the uppermost Cretaceous sediments could be established in the drill hole. An integrated stratigraphy is presented in Fig. 9 and a list of core depths in Table 9.

7.2. Lithostratigraphy

The top 4.6 m at this site, consisting of soils and gravel, was drilled without coring. Core TDP10/1 (from 4.6 m to 4.95 m) recovered a medium olive grey (5Y 5/1) claystone with a minor admixture of fine quartz grains, streaked and mottled with greyish-orange to dark yellowish-orange (10YR 7/4 to 10YR 6/6) clays. Although the claystone possesses a waxy lustre, it only reacts sparingly with weak hydrochloric acid. Large benthic foraminifers are occasionally seen dispersed through the claystone. The surface weathering of the claystones persists to a depth of 9.35 m. Below 6.5 m, the color gradually becomes darker, being a mixture of mottled and streaked light olive grey to dark greenish-grey (5Y 6/1 to 5GY 4/1) claystones.

From 9.35 m to 22.95 m the principal lithology is a dark greenish-grey (5GY 4/1 to 5G 4/1) waxy-lustred, crumbly, muddy claystone, similar to that cored in TDP Site 8 and the top 50 m in TDP Site 7. As in these previous holes, the claystone contains occasional, thin, very fine to fine quartz sand partings and horizons. Where present, these produced a light grey (N7) overall color to the cores. In Core TDP10/6, at 10.6 m, a sandy horizon shows clear soft sediment deformation and dislocated ‘sand balls’ from liquefaction. Below this horizon, the laminations are coherent, but inclined at about 30°. Bioturbation is difficult to observe in these disturbed cores, but appears to be rare to uncommon. Small bivalve shell fragments are dispersed through the principal lithology. Beef was observed for the first time in this hole at 12.45 m, and below this depth it is evenly distributed through the remaining lithologies. Between about 18.2 m and 22.95 m, the occurrence of large benthic foraminifers dispersed within the claystones increases markedly and rare echinoid spines were also seen.

From 22.95, to the base of the hole at 100.8 m, the principal lithology is an olive black to olive grey (5Y 2/1 to 5Y 4/1) siltstone to silty claystone. The visible granular component consists of very fine quartz grains, micaceous flakes and occasional small shell fragments. This lithology is sim-

Plate 6. Selected palynomorphs from TDP Sites 6–10. Magnifications are variable. (1) *Cerodinium* sp., Sample TDP9/11-1, 59–64 cm; (2) *Paleocystodinium* sp., Sample TDP9/11-1, 59–64 cm; (3) *Adnatosphaeridium robustum*, Sample TDP7A/64-1, 83–98 cm; (4) *Muratodinium fimbriatum*, Sample TDP7A/65-3, 01–17 cm; (5) *Phthanoperidinium crenulatum*, Sample TDP7A/62-1, 20–30 cm; (6) *Apectodinium parvum*, Sample TDP7A/64-1, 83–98 cm; (7) *Apectodinium homomorphum*, Sample TDP7A/64-1, 83–98 cm; (8) *Apectodinium quinquelatum*, Sample TDP10/30-3, 0–4 cm; (9) *Adnatosphaeridium robustum*, Sample TDP7A/64-1, 83–98 cm; (10) *Operculodinium severinii*, Sample TDP10/10-2, 10–20 cm; (11) *Deflandrea truncata*, Sample TDP8/10-1, 97–100 cm; (12) *Operculodinium* sp., Sample TDP8/9-1, 30–34 cm; (13) *Cerodinium depressum*, Sample TDP9/17-1, 24–34 cm; (14) *Dinogymnium avellana*, Sample TDP9/11-1, 59–64 cm; (15) *Cerodinium speciosum*, Sample TDP10/10-2, 10–20 cm; (16) *Hystrichostrogylon* sp., Sample TDP10/10-2, 10–20 cm; (17) *Hystrichokolpoma* sp., Sample TDP10/10-2, 10–20 cm; (18) *Apectodinium homomorphum*, Sample TDP10/10-2, 10–20 cm; (19) *Thallasiphora reticulata*, Sample TDP6/6-1, 40 cm; (20) *Alterbidinium montanaense* Sample TDP9/11-1, 54–64 cm.

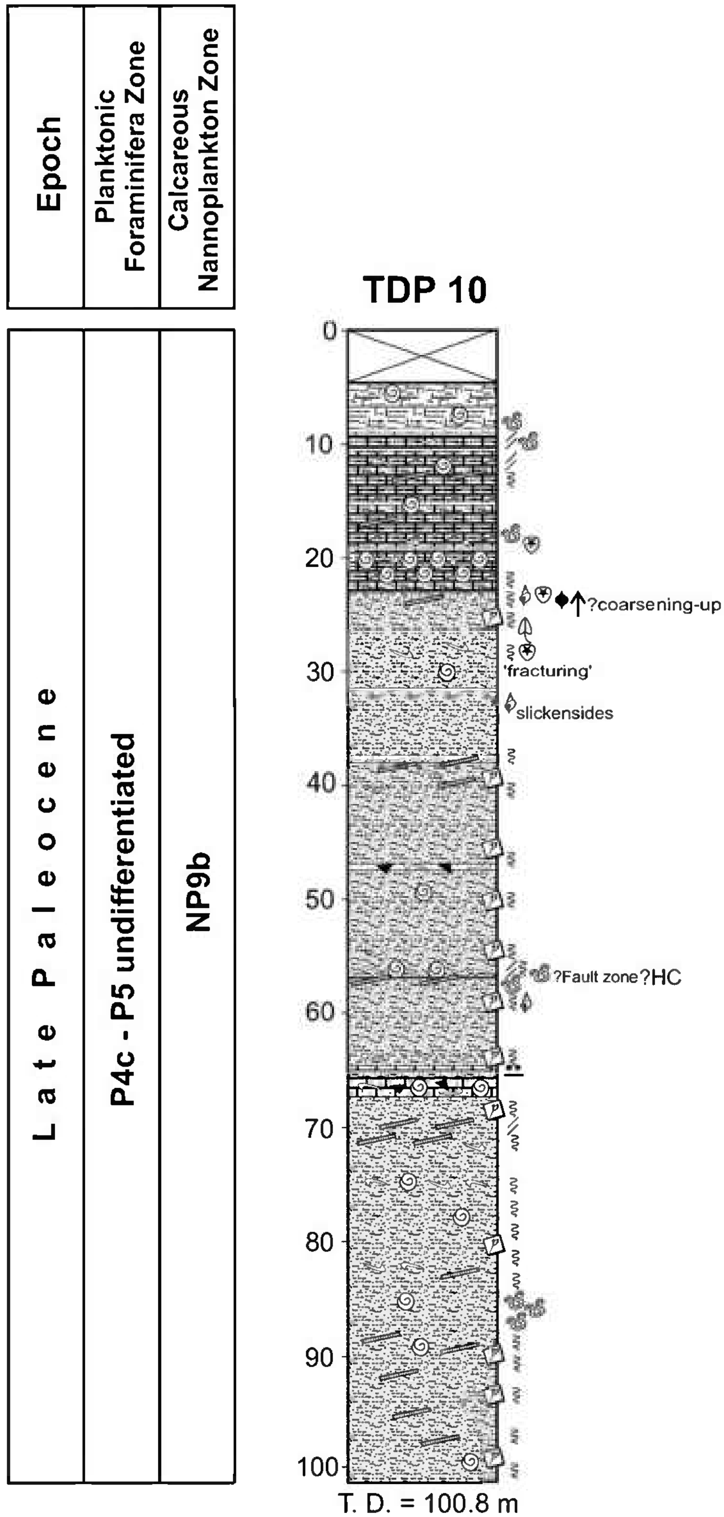

Fig. 9. Integrated litho- and biostratigraphy for TDP Site 10. Symbols as given in Fig. 5.

ilar to that described for the lower units (below 60 m) in TDP Site 7 and which dominates TDP Site 9. However, unlike at those sites, large benthic foraminifers, which are matrix supported and not part of obvious gravity flows, are abundant in some levels. Core TDP10/12 appears to record an overall coarsening-upward trend in the visible grain-size fraction. Bioturbation is common throughout the clayey siltstones in this hole and there is also a common occurrence of pyrite growth in the burrows and trails.

Horizontal laminations are present between 29 m and 30 m. Fractures appear in Core TDP10/15 between 30 m and 30.8 m and slickensides were recorded at 33.8 m. Between 55.8 m and 57.1 m the clayey siltstones are inclined at 45° and again contain a concentration of large

Table 9
Intervals drilled and cored in TDP Site 10 (west Singino Hill, UTM 37L 541243, 9028279)

Site	Core	Top (m)	Bottom (m)	Drilled	Recovered	Recovery (%)	Comment
TDP10/		0.00	4.60	4.60	0.00	0	Interval drilled
	1	4.60	4.95	0.35	0.35	100	1.5 m core barrel; short core
	2	4.95	5.45	0.50	0.50	100	
	3	5.45	6.50	1.05	0.58	55	
	4	6.50	7.45	0.95	0.90	95	
	5	7.45	9.45	2.00	1.80	90	
	6	9.45	10.95	1.50	1.72	115	
	7	10.95	12.45	1.50	1.49	99	
	8	12.45	13.95	1.50	1.80	120	
	9	13.95	16.95	3.00	3.45	115	3 m core barrel deployed
	10	16.95	19.95	3.00	3.20	107	
	11	19.95	22.95	3.00	3.20	107	
	12	22.95	25.95	3.00	2.97	99	
	13	25.95	28.95	3.00	3.07	102	
	14	28.95	30.00	1.05	0.87	83	
	15	30.00	30.80	0.80	0.93	116	
	16	30.80	31.80	1.00	0.98	98	
	17	31.80	34.80	3.00	3.07	102	
	18	34.80	37.80	3.00	2.79	93	
	19	37.80	40.80	3.00	2.89	96	
	20	40.80	43.80	3.00	3.07	102	
	21	43.80	46.80	3.00	2.93	98	
	22	46.80	49.80	3.00	3.12	104	
	23	49.80	52.80	3.00	3.06	102	
	24	52.80	55.80	3.00	2.76	92	
	25	55.80	58.80	3.00	2.83	94	
	26	58.80	61.80	3.00	3.03	101	
	27	61.80	64.80	3.00	2.94	98	
	28	64.80	67.80	3.00	2.63	88	
	29	67.80	70.80	3.00	2.78	93	
	30	70.80	73.80	3.00	2.15	72	Poor recovery
	31	73.80	75.30	1.50	2.38	159	Contains part of previous core
	32	75.30	76.80	1.50	1.68	112	
	33	76.80	79.80	3.00	2.95	98	
	34	79.80	82.80	3.00	2.93	97	
	35	82.80	85.80	3.00	3.08	103	
	36	85.80	88.80	3.00	2.92	97	
	37	88.80	91.80	3.00	3.05	102	
	38	91.80	94.80	3.00	2.57	86	
	39	94.80	97.80	3.00	2.96	99	
	40	97.80	100.80	3.00	2.70	90	
Total drilled: 100.80 m			Total recovered: 95.08 m			Recovery: 94%	

benthic foraminifers. Directly underlying this inclined interval, at 57.1 m, a 15 cm thick, more clay-rich horizontal layer occurs, brownish-black in color (5YR 2/1). This slightly odd coloration may be due in part to the presence of oil in the silty clay. Directly below this clay, a thick beef vein overlies a zone of soft sediment deformation. The close juxtaposition of these structures suggests that the clay represents a fault gouge, as has been postulated in previous holes, and that the claystone deformation is again a consequence of fault drag or localized compression rather than an original syn-sedimentary feature. As at TDP Site 7, small amounts of oil could have migrated along the fault at some time in the past.

Below this apparently disturbed interval, the lamination orientation only becomes visible again briefly at 69.5 m, where it is inclined at 30°. Core TDP10/36 (from 85.8 m to 88.8 m) consists of clayey siltstones with a high degree of soft sediment deformation. Although no single fault zone was observed, it is possible that minor movement could have caused deformation without the development of a clear fracture plane.

At 65 m, a 2.6 m thick interval containing two fossiliferous limestone horizons occurs. These are composed of macrofossil debris including benthic foraminifers, bivalve fragments and shell hash. Interspersed with the fossil debris is a fine quartz sand component and both horizons also contain clay rip-up clasts. At the top of each, the clasts appear to show a crude normal grading, suggesting that this interval was deposited from a double ‘pulse’ of turbulent flows.

Results of geochemical analyses of 11 samples from TDP Site 10 are shown in Table 10. The $CaCO_3$ concentration is generally low, ranging from 0.8% to 10.3%. The variation may represent differing concentrations of calcareous

Table 10
Results of geochemical analyses of sediments from TDP Site 10

Sediments	Depth (m)	$CaCO_3$ (%)	Sulfur (%)	TOC (%)
TDP 10/5-2, 37–47 cm	8.82–8.92	7.3	0.04	0.1
TDP 10/10-1, 90–100 cm	17.85–17.95	0.8	0.3	0.5
TDP 10/13-2, 10–20 cm*	27.05–27.15	5.0	0.3	0.7
TDP 10/17-2, 15–30 cm	32.95–33.10	10.3	0.1	0.7
TDP 10/21-2, 53–68 cm	45.33–45.48	1.3	0.3	0.8
TDP 10/26-1, 92 cm to TDP 10/26-2, 07 cm*	59.72–59.87	3.3	0.4	0.5
TDP 10/29-1, 73–90 cm	68.53–68.70	2.1	0.1	0.2
TDP 10/36-2, 31–47 cm	87.11–87.27	7.5	0.1	0.8
TDP 10/38-2, 73–85 cm	93.53–93.65	3.9	0.2	0.6
TDP 10/40-1, 73–85 cm	98.53–98.65	3.1	0.2	0.4

Sediments highlighted with an asterisk were selected for biomarker study (see Table 1).

microfossils and/or diaganetic calcite. The sulfur content ranges from 0.04% to 04% and TOC from 0.1% to 0.8%.

7.3. Planktonic foraminifers

Planktonic foraminifers are abundant throughout TDP Site 10. Calcite preservation varies considerably within samples and through the sequence, ranging from excellent, with glassy walls and no infilling, to poor, displaying surface dissolution and complete infilling with sparry calcite and or microgranular pyrite. Commonly, specimens exhibit excellent shell surface preservation but are infilled. Assemblages comprise typical late Paleocene low-latitude species, including *Morozovella velascoensis*, *M. acuta*, *M. aequa*, *M. apanthesma*, *G. pseudomenardii*, *S. velascoensis*, *S. patagonica*, *A. soldadoensis* and *A. mckannai*, which are common and consistently present throughout the section. Ancillary species include *I. albeari*, *C. wilcoxensis*, *C. crinita*, *A. nitida*, *G. chapmani* and *G. planoconica*. In addition, *M. conicotruncata* occurs in the stratigraphically lowest sample examined, Sample TDP10/38-2, 76–85 cm. The co-occurrence of *A. soldadoensis* and specimens attributed to *G. pseudomenardii* through the entire site indicates that it might all be assigned to planktonic foraminifer Subzone P4c. However the infra-Paleocene last occurrence of *G. pseudomenardii* has recently been called into question (Orue-Etxebarria et al., 2004), and our own observations at TDP Site 7 suggest that a form similar to *G. pseudomenardii* persists to near the Paleocene–Eocene boundary, suggesting that further work may be needed to reliably distinguish Zones P4c and P5.

Rare but well-developed examples of a form resembling *Pseudohastigerina wilcoxensis,* with a fully rounded periphery and near-planispiral coiling, occur in Samples TDP10/18-1, 90 cm and 10/24-1, 79–94 cm. This is an unusually early occurrence for this morphospecies, which is generally considered restricted to the Eocene, and suggests that its first appearance as a rare component as an extreme variant of *Globanomalina* populations may be geographically and environmentally diachronous.

7.4. Calcareous nannofossils

Seventeen samples were studied for calcareous nannofossils, and all but three yielded rare to common, diverse nannofossil assemblages of moderate or moderate to good preservation. *C. dela* is present throughout and, in the absence of age-diagnostic discoasters and *Rhomboaster* species, this would appear to indicate an age corresponding to upper Zone NP9 (Subzone CP8b); the marker species for Zone NP9, *D. multiradiatus*, is absent. Unfortunately, the reliability of the *C. dela* (Plate 2(18)) (or *C. eodela*; Plate 2(17)) datum has been questioned, both because the differentiation between the two species is poorly constrained, and also because the origination of the genus/species has been recorded earlier than the position indicated by the established zonation schemes. Bralower and Mutterlose (1995) recorded the FO of *C. eodela* in Zone NP7 (Zone CP6), and Perch-Nielsen (1981) infers the origin of the genus in upper Zone NP5 (Zone CP3). However, a series of additional occurrences strongly support the Zone NP9 assignation, including the FO of *Lophodolithus nascens* (Plate 2(14)) and presence of *Z. bijugatus* (Plate 2(34)), and *Pontosphaera* (Perch-Nielsen, 1981; Bybell and Self-Trail, 1995; Bralower and Mutterlose, 1995); other notable occurrences include *C. frequens*, *Ericosonia subpertusa* and *E. robusta*.

Additonal species illustrated from this site are *C. aperta* (Plate 2(1)), *Pontosphaera plana* (Plate 2(4)), *P. rimosa* (Plate 2(5)), *N. chiastus* (Plate 2(8)), *Zygodiscus plectopons* (Plate 2(15)), *C. frequens* (Plate 2(23)), *Ericsonia robusta* (Plate 2(24)), *E. subpertusa* (Plate 2(25)), *T. eminens* (Plate 2(26)), *Micrantholithus disculus* (Plate 3(2)), and *F. tympaniformis* (Plate 3(18)). Five species were described as new from this site by Bown (2005), namely *Z. sheldoniae* (Bown, 2005, p. 33), *N. substricus* (Bown, 2005, p. 33), *Lanternithus simplex* (Bown, 2005, p. 39), *Semihololithus dimidius* (Bown, 2005, p. 41) and *S. tentorium* (Bown, 2005, p. 41).

7.5. Benthic foraminifers

Forty-eight samples were examined for benthic foraminifers, with substantial variation in abundance and preservation. Some samples display excellent preservation while others vary from moderate to poor. Eighty-one genera of benthic foraminifers have been identified from this site.

Long- as well as short-ranging taxa present include *Nummulites*, *Asterocyclina*, *Lepidocyclina*, *Plectofrondicularia* sp. (Plate 4(16)), *Siphotextularia* sp. (Plate 4(15)), *Operculina* sp., *Oridorsalis lotus* (Plate 4(25)), *G. girardanus*, *G. subangulatus*, *Amphistegina* sp., *B. trinitatensis*, *N. truempyi*, *B. eocenicus*, *P. incrassata*, *Haplophragmoides kirki*, *H. concavus*, *Pseudonodosaria aequalis*, *Kalamopsis grysbowskii*, *D. communis*, *D. leguminiformis*, *Lenticulina rotulata*, *Spiroplectammina laevis*, *S. dentata*, *A. velascoensis*, *Nodosaria* sp. (Plate 4(11)), *Lagena costata*, *L. globulosa*, *Anomalinoides* sp. (Plate 4(17)), *Anomalinoides rubiginosus*, *A. fasciatus*, *M. barleeanum*, *Hoeglundina elegans*, *Glandulina laevigata*, *C. dayi*, *C. velascoensis*, *Lagenaglandulina laevigata*, *M. longiforma*, *Globobulimina* sp. (Plate 4(22)), *Trochammina globigerineformis*, *T. deformis*, *Subreophax pseudoscalaris*, *M. wetherellii*, *G. altiformis*, *Clavulinoides subparisiensis*, *N. laevigata*, *Marssonella oxycona*, *Spiroplectammina* sp., *R. linearis*, *Bathysiphon annulatus*, *B. eocenicus*, *Ammodiscus cretaceus*, *Marssonella oxycona*, *N. longiscata*, *Matanzia velascoensis*, *Textularia plummerae* and *Stilostomella verneuillina*. Most of the species described above range from the Late Cretaceous to Late Paleocene.

Short-ranging species of Paleocene age include *B. midwayensis*, *B. velascoensis*, *B. trigonalis*, *Coryphostoma (Bolivina) midwayensis*, *Spiroplectammina thanetensis*, *Svratkina toulmini*, *Globulina ampulla*, *Gyroidina florealis*, *Matanzia varians*, *Anomalinoides danicus*, *Cibicides cantii*, *Astacolus platypleura*, *Cibicidoides succedens* and *Lenticulina pseudomamilligera* (Plate 4(14)).

The benthic foraminifer biofacies is that of a deep outer shelf to upper bathyal paleoenvironment, as indicated by benthic foraminifers such as *Neoflabellina jarvisi*, *Angulogavelinella avnimelechi*, *Coryphostoma midwayensis*, *A. danicus*, *A. rubiginosus*, *Aragonia velascoensis*, *C. velascoensis*, *N. truempyi* and *B. trinitatensis*.

7.6. Palynology

Eight samples were studied for dinocysts and miospores. Samples TDP/10-2, 0–10 cm, TDP10/15-1, 25–40 cm and TDP10/20-2, 0–15 cm contain common dinocysts and rare miospores. Stratigraphically significant taxa include *M. fimbriatum*, *Adnatosphaeridium robustum*, *Achomosphaera danica*, *Cerodinium speciosum* (Plate 6(15)), *Alterbidinium pentaradiatun*, *Apectodinium quinquelatum*, *A. homomorphus* (Plate 6(18)), *Spiniferites septatus* and *Deflandrea foveolata* and *Hystrichokolopoma* sp. (Plate 6(16)), *Hystrichostrogylon* sp. (Plate 6(16) and *Operculodinium* sp. (Plate 6(10)). These indicate a late Paleocene age.

7.7. Organic geochemistry

Two samples (Samples TDP10/13-2, 10–20 cm and TDP10/26-1, 92 cm – 26-2, 7 cm) were selected for organic geochemical analysis. The saturated hydrocarbon fractions contain predominantly *n*-alkanes (with the C_{31} *n*-alkane being most abundant in Sample TDP 10/13-2, 10–20 cm and C_{29} *n*-alkane being most abundant in Sample TDP10/26-1, 92 cm – 26-2, 7 cm), hopenes and hopanes and lesser amounts of steranes. However, the saturated hydrocarbon fraction contains only trace abundances of des-*A*-triterpenes and des-*E*-hopenes. The TDP Site 10 aromatic hydrocarbon fractions contain relatively small amounts of aromatic des-*A*-triterpenes and, in the case of Sample TDP10/26-1, 92 cm – 26-2, 7 cm, also small amounts of aromatic pentacyclic triterpenoids (Table 1). The polar fractions are dominated by triterpenoids (Table 1). In addition, the samples contain substantial amounts of *n*-alkanols (with C_{28} *n*-alkanol being the most abundant), hopanoids and minor amounts of steroids; however neither C_{15}/C_{15} diether nor archaeol was detected. The distribution of acids in the samples revealed predominantly *n*-alkanoic acids (with the C_{24} *n*-alkanoic acid being most dominant in the case of Sample TDP 10/13-2, 10–20 cm and the C_{28} *n*-alkanoic acid being most abundant in Sample TDP10/26-1, 92 cm – 26/2, 7 cm; Table 1). Hopanoic acids are also abundantly present in the case of Sample TDP 10/13-2, 10–20 cm. In addition, it also contains substantial amounts of ω-hydroxy alkanoic acids (with C_{22} ω -hydroxy alkanoic acid being the most abundant) and triterpenoic acids. In the case of Sample TDP10/26-1, 92 cm – 26-2, 07 cm, hopanoic acids and triterpenoic acids and ω-hydroxy alkanoic acids are also present but in substantially lower amounts compared to Sample TDP 10/13-2, 10–20 cm.

7.8. Summary

The sediments at TDP Site 10 consist of predominantly dark greenish-grey claystones similar to those cored at other sites around Singino Hill. Biostratigraphic age assignment (based on calcareous nannofossils and planktonic foraminifers, with supporting information from dinoflagellates and benthic foaminifers), indicates an upper Paleocene age. The sediments are slightly older than the deepest sediments cored at TDP Site 7, which were lowermost Eocene. Unfortunately, neither site contains an unequivocal record across the Paleocene/Eocene boundary, but taken together they indicate that an expanded Paleocene/Eocene boundary probably occurs in the area.

The inferred environment of deposition is a deep outer shelf to slope setting, and the facies is closely similar to that observed at TDP Sites 3 and 7.

The fact that at least 100 m of Paleocene claystones occurs in TDP Site 10 indicates that the local boundary with the uppermost Cretaceous formation, as inferred from roadside outcrops, is a fault. This information helps constrain the geological structure of the Singino Hill area (Nicholas et al., in press).

8. Conclusions

The Tanzania Drilling Project cored five sites in 2003, ranging in age from Campanian to Oligocene. The new sites supplement previous drilling results from the area, as summarized by Pearson et al. (2004). In particular, the new sites help constrain the geological structure around Singino Hill to the north end of the Kilwa peninsula and indicate that an expanded Paleocene/Eocene boundary can very likely be found in the area, with excellent microfossil preservation. The nature of the Cretaceous/Tertiary and Eocene/Oligocene boundaries remain unresolved by this year's drilling.

All of the sites are dominated by silty claystones. Their low permeability and shallow burial depths probably explains the excellent microfossil preservation that is commonly encountered, and which drew us to the area. However, diagenetic infilling of foraminiferal shells is also frequently encountered, so future geochemical investigations need to be focused on the best preserved and non-infilled parts of the record so far obtained.

The cores provide valuable paleoenvironmental and taxonomic information, which helps reconstruct the depositional environment, the species present, and how they changed through time. For most of the sediments from Late Cretaceous to Eocene age, the benthic foraminiferal assemblages and lithofacies indicates a deep outer shelf environment, with water depths of at least several hundred meters. This is supported by the relatively high planktonic:benthic foraminiferal ratios and the fully diverse planktonic foraminiferal assemblages that are commonly encountered, also the development of 'flysch'-type trace fossils of the *Nereites* ichnofacies in the Campanian of TDP Site 9. The nannofossil assemblages, however, show strong shelf affinities, as do the dinoflagellates, which are more often typical of shallow-water conditions. The organic geochemistry is dominated by terrestrially derived biomarkers, although some marine compounds are also present. These observations can be resolved through the observation that the East African shelf is very narrow, hence material from the continent and shallow marine environments is easily delivered in large quantities to the outer shelf and slope. The Oligocene sediments recovered in TDP Site 6 seem to represent a much shallower environment, although it is still offshore, as evidenced by the observation that occasional calcareous debris flows were introduced down-slope into an otherwise clay-dominated environment. The Oligocene sediments may have been deposited in a large but semi-restricted embayment with dysaerobic bottom waters and fluctuating salinity in the surface.

The organic geochemistry supports the investigations made on TDP Sites 1–5, namely that the sediments are dominated by terrestrial organic matter and are all of unusually low thermal maturity, indicating that they have never been deeply buried. Traces of migrated oil were found in TDP Sites 7 and 10, to supplement that already reported from TDP Site 3 (Pearson et al., 2004). We have also found a small seep at Kilwa Masoko. This new information, when combined with the new structural interpretation that is emerging from our work (Nicholas et al., in press), may aid future hydrocarbon exploration in the area.

Acknowledgements

The drilling was funded by the UK Natural Environment Research Council through Grant NE/X509345/1 to P.N. Pearson. Enterprise Ireland Basic Research Grant SC/2002/255 funded the participation of C.J. Nicholas and M. Pearson. We are grateful for the Tanzania Petroleum Development Corporation for scientific and logistic support and for archiving the cores. We thank the Tanzania Commission for Science and Technology (COSTECH) for permission to conduct our researches. We thank the District Commisioner, District Administrative Officer and the District Executive Director in Kilwa for facilitating our research, including permission to drill, and also for their generous hospitality. Ephrem Mchana, Michael Mkereme and Doreen Mkuu provided expert technical assistance in the field and in the core lab.

References

Angori, E., Monechi, S., 1995. High resolution calcareous nannofossil biostratigraphy across the Paleocene/Eocene boundary at Carava (southern Spain). Isr. J. Earth Sci. 44, 197–206.

Aubry, M.-P., 1995. Towards an upper Paleocene–lower Eocene high resolution stratigraphy based on calcareous nannofossil stratigraphy. Isr. J. Earth Sci. 44, 239–253.

Aubry, M.-P., 1999. Handbook of Cenozoic calcareous nannoplankton, Book 5: Heliolithae (Zygoliths and Rhabdoliths). Micropaleontology Press, American Museum of Natural History, New York.

Aubry, M.-P., Berggren, W.A., Stott, L., Sinha, A., 1996. The upper Paleocene–lower Eocene stratigraphic record and the Paleocene–Eocene boundary carbon isotope excursion: implications for geochronology. Geological Society Special Publication 101, 353–380.

Berggren, W.A., Pearson, P.N., 2005. A revised tropical to subtropical Paleogene planktonic foraminifer zonation. J. Foram. Res. 35, 279–298.

Berggren, W.A., Kent, D.V., Swisher, C.C. III, Aubry, M.-P., 1995. A revised Cenozoic geochronology and chronostratigraphy. In: Berggren, W.A., Kent, D.V., Aubry, M.P., Hardenbol, J. (Eds.), Geocheonology, Time Scales and Global Stratigraphic Correlation. SEPM Spec. Publ., No 54, pp. 129–212.

Bown, P.R., 2005. Palaeogene calcareous nannofossils from the Kilwa and Lindi areas of coastal Tanzania (Tanzania Drilling Project 2003-4). J. Nannoplankton Res. 27, 21–95.

Bown, P.R., Young, J.R., 1998. Techniques. In: Bown, P.R. (Ed.), Calcareous Nannofossil Biostratigraphy. Kluwer Academic, pp. 16–28.

Bralower, T.J., Mutterlose, J., 1995. Calcareous nannofossil biostratigraphy of Site 865, Allison Guyot, Central Pacific Ocean: a tropical Paleogene reference section. Proc. ODP, Sci. Res. 143, 31–74.

Burnett, J.A. (with contributions from Gallagher, L.T., Hampton, M.J.), 1998. Upper Cretaceous. In: Bown, P.R. (Ed.), Calcareous Nannofossil Biostratigraphy. British Micropaleontological Society Series. Chapman & Hall, Kluwer Academic Press, pp. 132–199.

Bybell, L.M., Self-Trail, J.M., 1995. Evolutionary, biostratigraphic, and taxonomic study of calcareous nannofossils from the continuous Paleocene–Eocene boundary section in New Jersey. US Geological Survey Professional Paper 1554, p. 36.

Carbonnel, G., de Klasz, I., de Klasz, S., Horvath, M., Lang, J., Oyede, M., 1996. Microfaunas and depositional environments of the

Oligocene levels overlying the so-called "Oligocene unconformity" on the on-shore part of the coastal sedimentary basin of the Benin Republic (West Africa). Journal de l'Afrique et de l'Atlantique Sud; Actes Colloques Angers 1994, 235–273, 3 Figs., 1 tab., 10 Pl.; pau, June 29, 1996.

de Kaenel, E., Villa, G., 1996. Oligocene–Miocene calcareous nannofossil biostratigraphy and paleoecology from the Iberia Abyssal Plain. Proc. ODP, Sci. Res. 149, 79–145.

Eglinton, G., Hamilton, R.J., 1963. The distribution of *n*-alkanes. In: Swain, T. (Ed.), Chemical Plant Taxonomy. Academic Press, pp. 187–217.

Eglinton, G., Hamilton, R.J., 1967. Leaf epicuticular waxes. Science 156, 1322–1335.

Ernst, G., Zander, J., 1993. Stratigraphy, facies development, and trace fossils of the Upper Cretaceous of southern Tanzania (Kilwa District). In: Geology and Mineral Resources of Somalia and Surrounding Areas. Inst. Agron. Oltremare Firenze, Relaz. E Monogr. 113, Firenze, pp. 259–278.

Frank, T.D., Thomas, D.J., Leckie, R.M., Arthur, M.A., Bown, P.R., Jones, K., Lees, J., 2005. The Maastrichtian record from Shatsky Rise (northwest Pacific): a tropical perspective on global ecological and oceanographic changes. Paleoceanography 20, PA1008. doi:10.1029/2004PA001052.

Freeman, K., Boreham, C.J., Summons, R.E., Hayes, J.M., 1994. The effect of aromatisation on the isotopic compositions of hydrocarbons during early diagenesis. Org. Geochem. 21, 1037–1049.

Gardin, S., Odin, G.S., Bonnemaison, M., Melinte, M., Monechi, S., von Salis, K., 2001. Results of the cooperative study on the calcareous nannofossils across the Campanian–Maastrichtian boundary at Tercis les Bains (Landes, France). In: Odin, G.S. (Ed.), The Campanian–Maastrichtian Stage Boundary. Characterisation at Tercis les Bains (France) and Correlation with Europe and other Continents, Developments in Paleontology and Stratigraphy, 19. Elsevier, Amsterdam, pp. 293–309.

Gierlowski-Kordesch, E., Ernst, G., 1987. A flysch trace assemblage from the Upper Cretaceous shelf of Tanzania. In: Matheis, G., Schandelmeier, H. (Eds.), Current Res. African Earth Sci., Rotterdam, pp. 217–222.

Gough, M.A., Rowland, S.J., 1990. Characterization of unresolved complex mixtures of hydrocarbons in petroleum. Nature 344, 759–761.

Gough, M.A., Rowland, S.J., 1991. Characterization of unresolved complex mixtures of hydrocarbons from lubricating oil feedstocks. Energy Fuels 5, 648–650.

Gough, M.A., Rhead, M.M., Rowland, S.J., 1992. Biodegradation studies of unresolved complex mixtures of hydrocarbons: model UCM hydrocarbons and the aliphatic UCM. Org. Geochem. 18, 17–22.

Greiner, A.Ch., Spyckerelle, C., Albrecht, P., 1976. Aromatic hydrocarbons from geological sources—I. New naturally occurring phenanthrene and chrysene derivatives. Tetrahedron 32, 257–260.

Hauke, V., Graff, P., Wehrung, P., Hussler, G., Trendel, J.M., Albrecht, P., Riva, A., Connan, J., 1993. Rearranged des-*E*-hopanoid hydrocarbons in sediments and petroleum. Org. Geochem. 20, 415–423.

Holloway, P.J., 1982. The chemical constitution of plant cutins. In: Cutler, D.F., Alvin, K.T., Price, C.E. (Eds.), The Plant Cuticle. Linnean Soc. Lond. Academic Press, London, pp. 45–85.

Kates, M., Kushner, D.J., Matheson, A.T., 1993. The Biochemistry of Archaea (Archaebacteria). Elsevier, Amsterdam, 582 pp.

Kent, P.E., Hunt, J.A., Johnstone, D.W., 1971. The Geology and Geophysics of Coastal Tanzania. Institute of Geological Sciences Geophysical Paper No. 6, HMSO, London.

Koga, Y., Morii, H., Akagawa-Matsushita, M., Ohga, M., 1993. Ether lipids of methanogenic bacteria: structures, comparative aspects, and biosyntheses. Microbiol. Res. 57, 164–182.

Lees, J.A., Bown, P.R., 2005. Upper Cretaceous calcareous nannofossil biostratigraphy, ODP Leg 198 (Shatsky Rise, northwest Pacific Ocean). In: Bralower, T.J., Premoli Silva, I., Malone, M., et al. (Eds.), Proc. ODP, Sci. Res., p. 198.

MacLeod, K.G., Huber, B.T., Ward, P.D., 1996, The biostratigraphy and paleogeography of Maastrichtian inoceramids. In: Ryder, G., Fastovsky, D., Gartner, S. (Eds.), The Cretaceous-Tertiary Event and Other Catastrophes in Earth History. Boulder, CO, Geological Society of America Special Paper 307, pp. 361–373.

Magoon, L.B., Claypool, C.E., 1985. Alaska North Slope Oil Rock Correlation Study. The American Association of Petroleum Geologists, Tulsa.

Martini, E., 1971. Standard Tertiary and Quaternary calcareous nannoplankton zonation. In: Farinacci, A. (Ed.), Proceedings of the Second Planktonic Conference Roma 1970, vol. 2. Edizioni Tecnoscienza, Rome, pp. 739–785.

Moore, W.R., McBeath, D.M., Linton, R.E., Terris, A.P., Stoneley, R., 1963. Geological Survey of Tanganyika Quarter Degree Sheet 256 & 256E. 1:125 000, Kilwa, first ed. Geological Survey Division, Dodoma.

Nederbragt, A.J., 1991. Late Cretaceous biostratigraphy and development of Heterohelicidae (planktic foraminifera). Micropaleontology 37, 329–372.

Nicholas, C.J., Pearson, P.N., Bown, P.R., Dunkley-Jones, T., Huber, B.T., Karega, A., Lees, J.A., McMillan, I.K., O'Halloran, A., Singano, J.M., Wade, B.S., in press. Stratigraphy of the Upper Cretaceous and Paleogene Kilwa Group, southern coastal Tanzania. J. Afr. Earth Sci.

Okada, H., Bukry, D., 1980. Supplementary modification and introduction of code numbers to the low-latitude coccolith biostratigraphic zonation (Bukry, 1973; 1975). Marine Micropaleontol. 5, 321–325.

Olsson, R.K., Hemleben, C., in press. Taxonomy, biostratigraphy and phylogeny of Eocene *Globanomalina*, *Planoglobanomalina* n. gen. and *Pseudohastigerina*. In: Pearson, P.N. et al. (Eds.), Atlas of Eocene Planktonic Foraminifera. Cushman Foundation Special Publication.

Orue-Etxebarria, X., Bernaola, G., Baceta, J.I., Angori, E., Caballero, F., Monechi, S., Pujalte, V., Dinares-Turell, J., Apellaniz, E., Payros, A., 2004. New constraints on the evolution of planktic foraminifers and calcareous nannofossils across the Paleocene–Eocene boundary interval: the Zumaia section revisited. Neues Jarbuch für Geologie und Paläontolgie-Abhandlungen 234, 223–259.

Ourisson, O., Albrecht, P., Rohmer, M., 1979. The hopanoids. Pure Appl. Chem. 51, 709–729.

Pancost, R.D., Boulaoubassi, I., Aloisi, G., Sinninghe Damsté, J.S., Medinaut Shipboard Scientific Party, 2001. Three series of non-isoprenoidal dialkyl glycerol diethers in cold-seep carbonate crusts. Org. Geochem. 32, 695–707.

Pant, P., Rastogi, R.P., 1979. The triterpenoids. Phytochemistry 18, 1095–1108.

Pearson, P.N., Ditchfield, P.W., Singano, J., Harcourt-Brown, K.G., Nicholas, C.J., Olsson, R.K., Shackleton, N.J., Hall, M.A., 2001. Warm tropical sea surface temperatures in the Late Cretaceous and Eocene epochs. Nature 413, 481–487.

Pearson, P.N., Nicholas, C.J., Singano, J.M., Bown, P.R., Coxall, H.K., van Dongen, B.E., Huber, B.T., Karega, A., Lees, J.A., Msaky, E., Pancost, R.D., Pearson, M., Roberts, A.P., 2004. Paleogene and Cretaceous sediment cores from the Kilwa and Lindi areas of coastal Tanzania: Tanzania Drilling Project Sites 1-5. J. Afr. Earth Sci. 39, 25–62.

Pearson, P.N., Olsson, R.K., Huber, B.T., Hemleben, C., Berggren, W.A. (Eds.), in press. Atlas of Eocene Planktonic Foraminifera. Cushman Foundation Special Publication.

Perch-Nielsen, K., 1981. Nouvelles observations sur les nannofossiles calcaires á la limite Crétacé/Tertiaire prés de El Kef, Tunisie. Cah. Micropaléontol. 3, 25–36.

Perch-Nielsen, K., 1985. Mesozoic calcareous nannofossils. In: Bolli, H.M., Saunders, J.B., Perch-Nielsen, K. (Eds.), Plankton Stratigraphy. Cambridge University Press, Cambridge, pp. 329–426.

Premoli Silva, I., Sliter, W.V., 1994. Cretaceous planktonic foraminiferal biostratigraphy and evolutionary trends from the Bottaccione section, Gubbio, Italy. Palaeontographica Italica 82, 1–89.

Robaszynski, F., Caron, M., 1995. Foraminifères planktoniques du Crétacé: commentaire de la zonation Europe-Mediterranée. Société géologique de France 166, 681–692.

Schlüter, T., 1997. Geology of East Africa. Borntraeger, Stuttgart, 512 pp.

Schmitz, B., Asaro, F., Molina, E., Monechi, S., von Salis, K., Speijer, R.P., 1997. High-resolution iridium $\delta^{13}C$, $\delta^{18}O$, foraminifera and nannofossil profiles across the latest Paleocene benthic extinction event at Zumaya, Spain. Palaeogeogr. Palaeoclimatol. Palaeoecol. 133, 49–68.

Sissingh, W., 1977. Biostratigraphy of Cretaceous calcareous nannoplankton. Geologie en Mijnbouw 56, 37–65.

Speijer, R.P., Samir, A.M., 1997. *Globanomalina luxorensis*, a tethyan biostratigraphic marker of Paleocene global events. Microplaeontology 43, 51–62.

Stewart, D.R.M., Pearson, P.N., Ditchfield, P.W., Singano, J.M., 2004. Miocene tropical Indian Ocean temperatures: evidence from three exceptionally preserved foraminiferal assemblages in Tanzania. J. Afr. Earth Sci. 40, 173–190.

ten Haven, H.L., Peakman, T.M., Rullkötter, J., 1992. Early diagenetic transformation of higher-plant triterpenoids in deep-sea sediments from Baffin Bay. Chim. Cosmochim. Acta. 56, 2001–2024.

Trendel, J.M., Lohmann, F., Kintzinger, J.P., Albrecht, P., Chiaroni, A., Riche, C., Cesario, M., Guilhem, J., Pascard, C., 1989. Identification of des-*A*-triterpenoid hydrocarbons occurring in surface sediments. Tetrahedron 45, 4457–4470.

van Dongen, B.E., Schouten, S., Sinninghe Damsté, J.S., 2003. Sulfurization of carbohydrates results in a S-rich, unresolved complex mixture in kerogen pyrolysates. Energy Fuels 17, 1109–1118.

Volkman, J.K., 1986. A review of sterols markers for marine and terrigenous organic matter. Org. Geochem. 9, 83–99.

Volkman, J.K., Kearney, P., Jeffrey, S.W., 1990. A new source of 4-methyl sterols and 5a(H)-stanols in sediments: prymnesiophyte microalgea of the genus *Pavlova*. Org. Geochem. 15, 489–497.

Volkman, J.K., Barrett, S.M., Dunstan, G.A., Jeffrey, S.W., 1993. Geochemical significance of the occurrence of dinosterol and other 4-methyl sterols in a marine diatom. Org. Geochem. 20, 7–15.

Volkman, J.K., Rijpstra, W.I.C., de Leeuw, J.W., Mansour, M.P., Jackson, A.E., Blackburn, S.I., 1999. Sterols of four dinoflagellates from the genus *Prorocentrum*. Phytochemistry 52, 659–668.

Withers, N.W., Tuttle, R.C., Holz, G.G., Beach, D.H., Goad, L.J., Goodwin, T.W., 1978. Dehydrodinosterol, dinosterone and related sterols of a non-photosynthetic dinoflagellate, *Crypthecodinium cohnii*. Phytochemistry 17, 1987–1989.

Wolff, G.A., Trendel, J.M., Albrecht, P., 1989. Novel monoaromatic triterpenoid hydrocarbons occurring in sediments. Tetrahedron 21, 6721–6728.